INFORMATION TO USERS

This manuscript has been reproduced from the microfilm master. UMI films the text directly from the original or copy submitted. Thus, some thesis and dissertation copies are in typewriter face, while others may be from any type of computer printer.

The quality of this reproduction is dependent upon the quality of the copy submitted. Broken or indistinct print, colored or poor quality illustrations and photographs, print bleedthrough, substandard margins, and improper alignment can adversely affect reproduction.

In the unlikely event that the author did not send UMI a complete manuscript and there are missing pages, these will be noted. Also, if unauthorized copyright material had to be removed, a note will indicate the deletion.

Oversize materials (e.g., maps, drawings, charts) are reproduced by sectioning the original, beginning at the upper left-hand corner and continuing from left to right in equal sections with small overlaps. Each original is also photographed in one exposure and is included in reduced form at the back of the book.

Photographs included in the original manuscript have been reproduced xerographically in this copy. Higher quality 6" x 9" black and white photographic prints are available for any photographs or illustrations appearing in this copy for an additional charge. Contact UMI directly to order.

UMI

A Bell & Howell Information Company
300 North Zeeb Road, Ann Arbor MI 48106-1346 USA
313/761-4700 800/521-0600

Structure and Mobility of Lignin in Relation to Pulp Washing and Bleaching

By

Lianyun He

A thesis submitted in partial fulfillment of the requirements for the degree of Master of Science

Chemistry Department
Lakehead University
Thunder Bay, Ontario
December 30 1996

ACKNOWLEDGMENTS

I would like to thank Miss Karen Joy Maa and Bill Morgan for their help in answering some experimental questions and supplying glassware and chemical reagents I required.

A special thank you to my family for their encouragement and support during my study in Canada.

Finally, thank you to Dr. Ted Garver for his patience, understanding and guidance throughout this project.

Funding for this project was provided by NSERC, Mechanical and Chemimechanical Wood-Pulps Network and Lakehead University.

Abstract

The roles of molecular size and structure were investigated in relation to the extent of peroxide bleaching and lignin adsorption on pulp. Structural analysis of components from effluents generated by peroxide bleaching was accomplished using UV-visible spectrophotometry and ^{1}H and ^{13}C NMR spectroscopy. These results provide evidence for a 1:1 sugar:aromatic ratio of components in the effluent mixture. Results are consistent with the presence of both hydroquinone and benzylic acid aromatic structures. Both ^{13}C NMR and UV analysis support the hypothesis that about 12% of the aromatic structures are of a benzylic acid form. During peroxide brightening, low-mass components with a higher fraction of phenolic structures are released into solution most rapidly while carbohydrate degradation appears to be more important over extended periods. Changes in the UV spectra of the effluent during bleaching appear to be dominated by changes resulting from a reduction of pH arising from carbohydrate degradation. The principle pK_a values, determined by titration with UV spectrophotometry, for effluents generated from alkaline hydrogen peroxide bleaching are at 4.64, 8.01 and 10.01. These pK_a values correspond to the dissociation of carboxylic acid, p-hydroxybenzylic acid (phenolic proton), and phenolic hydroxyl groups. In contrast, the pK_a of kraft lignin was estimated at ~7.5 and 10.3 corresponding to the ionization of phenolic groups with and without conjugated a-carbonyl structures. The acid dissociation constants decrease between 0.2 and 0.7 pK_a units with increasing ionic strength as do model compounds. The combined effects of decreasing the pK_a and ionic strength screening of ion-ion interactions leads to increased adsorption of lignin on cellulose with increasing ionic strength. Around the effective pK_a values the protonation of phenolic groups dominates the extent of interaction of lignin with cellulose. Pulsed Field Gradient NMR (PFGNMR) was utilized to evaluate the structure-size relationships for lignin preparations. Difficulties with the PFGNMR technique, including interaction of the gradient with r.f. and the superconducting magnet are discussed in detail. Results from PFGNMR indicate that high molecular weight kraft lignin has a lower frequency of ionizable phenolic groups. PFGNMR is compared to other NMR relaxation methods as a means to investigate size-structure relationships.

Contents

List of Figures

Chapter One

Introduction

Lignin is the second most abundant natural polymer next to cellulose[1.1]. It is found in conjunction with hemicellulose components between cellulose microfibrils, in the cell wall of vascular plants, such as hardwood and softwood trees, non-woody grasses. Its functions in the plant cell wall are primarily for structural stability and defense against attack by microorganisms [1.1,1.2,1.3,1.4].

The structure of lignin has not been clearly understood. This is in part because carbohydrates are always bound to lignin in situ[1.3], it is very hard to prepare a lignin sample identical to the lignin in situ. Furthermore, it would be impossible to determine a 'universal' lignin structure as lignin is different from each tree species and even between locations in a single tree[1.4]. Chemically, lignin is a phenylpropanoid macromolecule formed by an enzymic dehydrogenative polymerization of lignin precursors: p-coumaryl, coniferyl and sinapyl alcohols(Figure 1.1). These monomers are joined by various linkages such as ether or carbon-carbon bonds to form the lignin macromolecule[1.3]. Lignin biosynthesis is currently perceived to occur by random coupling of free-radical intermediates derived from phenylpropanoid alcohols, the 'polymerization' steps of lignin biosynthesis are poorly understood.

Lignin in softwood, such as spruce, consists mainly of

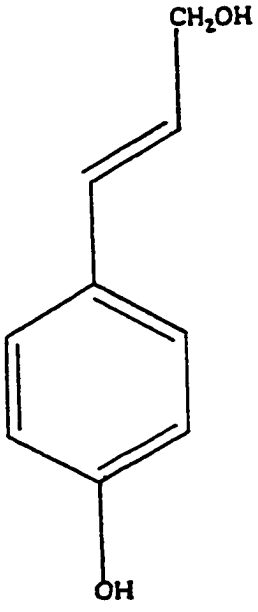

p-coumaryl alcohol

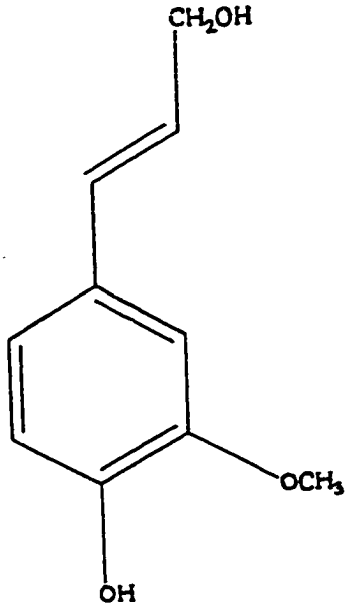

coniferyl alcohol

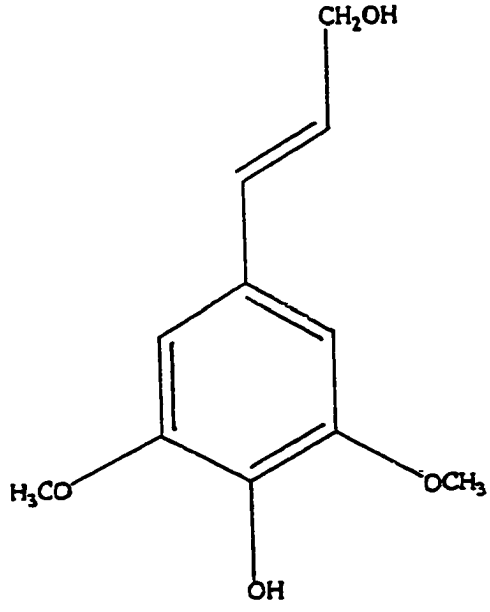

sinapyl alcohol

Figure 1.1 Lignin precursors

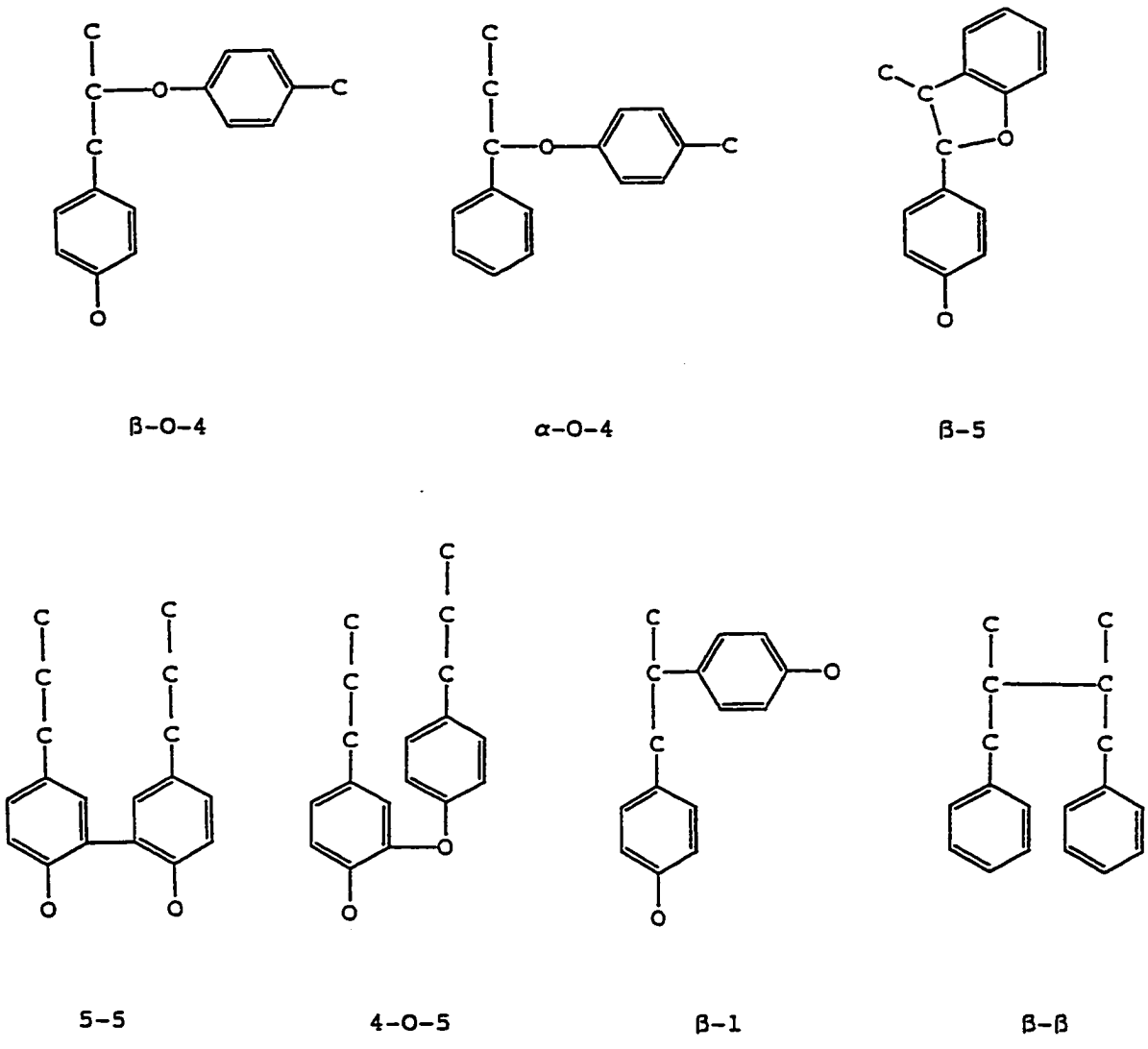

Figure 1.2 The linkages between lignin structural units

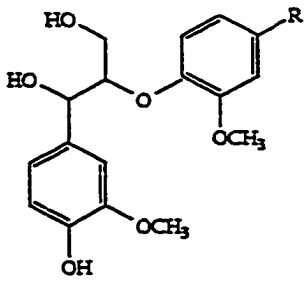

1a R = CHO
1b R = CH=CHCHO
1c R = $CHCH_2OH$

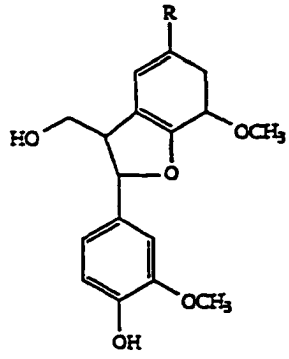

2a R = CH=CHCHO
2b R = $CH=CHCH_2OH$

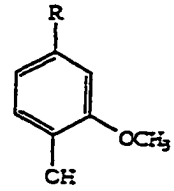

3a R = CHO
3b R = $CH_2CH_2CH_2OH$
3c R = CH=CHCHO
3d R = $CH=CHCH_2OH$

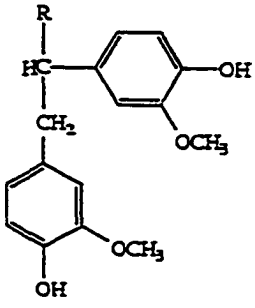

4a R = H
4b R = CH_2OH

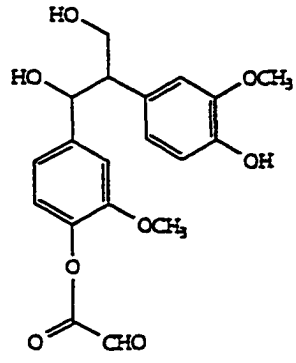

5

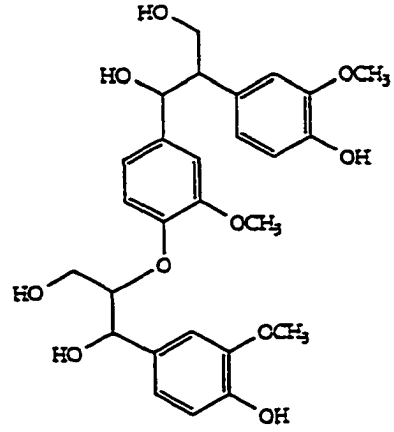

6

Figure 1.3 Lignin structural units

4-hydroxy substituted phenylpropane units(guaiacyl-type). About 65% of these units are joined by ether type linkages and the rest by carbon-carbon bonds. The linkages between the units are β-O-4, α-O-4, β-5, 5-5, 4-O-5,β-1 and β-β(Figure 1.2). Types of structural units in lignin are shown in Figure 1.3. The 'guaiacyl-syringyal' lignin, which occurs typically in hardwoods, such as aspen, is a copolymer of coniferyl and sinapyl alcohols, the ratio varying from 4:1 to 1:2 for the two monomeric units[1.3]. The lignin concentration is high in the middle lamella and low in the secondary wall. Because of its thickness, at least 70% of the lignin is located in the secondary wall.

Lignin functionality is dominated by oxygen containing groups such as methoxyl groups, hydroxyl groups and carbonyl groups. Lignin is one of the main components of paper from mechanical pulps. The colour of paper is believed to be resulted from the lignin. In order to remove the colour from paper and pulp, lignin can be bleached by chemicals or leached from pulp. With the environmental concerns, more and more researchers are investigating to lignin leaching from pulp. Both molecular size and structure of lignin are important considerations in developing methods for removing and leaching lignin from pulp, and processing effluents. The leaching of lignin from pulp is controlled by diffusion.

Diffusion is the net result of the thermal motion-induced random-walk process experienced by particles or molecules in solution. The theory of diffusion is highly

developed and extensive and can be found in many presentations[1.5,1.6, 1.7]. The diffusion data provide uniquely information on molecular organization and phase structure. Diffusion coefficients(D_0) are quite sensitive to structural changes and to binding and association phenomena. Furthermore, the values of diffusion coefficients(D_0) are directly related to molecular size and shape without any more interprations.

The powerful PFGNMR has been applied widely in determination of the diffusion coefficients. In this study, our main purpose is to employ PFGNMR to measure lignin diffusion coefficients(D_0) and to obtain size-resolved spectra.

The mechanism of hydrogen peroxide bleaching of machanical pulps was been studied by analysis of the structure of bleaching effluent components using UV-VIS and NMR spectrometry. The UV-VIS titration method has been used to measure the pK_as of model compounds and lignins. The titration curves of lignin and its model compounds were used to study their hydrodynamics properties and to deduct their molecular structure information.

References

[1.1] K.V.Sarkanen; C.H. Ludwig eds Lignins ; John Wiley & Sons : New York, (1971)

[1.2]. S.Y. Lin; C.W. Dence eds Methods in Lignin Chemistry ; Springer-Verlag :Berlin (1992)

[1.3]. E. Sjostrom, Wood Chemistry, Academic Press: New

York,(1981)

[1.4]. D. Fengel; G. Wegener; WOOD, Walter de Gruyter: Berlin,(1984)

[1.5]. J. Crank; The Mathematics of Diffusion 2nd edtion, Clarendon Press, Oxford (1975)

[1.6].R.B.Bird., W.E.Steward., and E.N Lighfoot; Transport Phenomina, Wiley, New York (1960)

[1.7]. Einstein,A. Investigations in the Theory of Brownian Movement, Dover, New York, (1956)

Chapter Two
NMR and UV-VIS Study of Alkaline Hydrogen Peroxide Bleaching Process

Introduction

The colour of paper and pulp is believed to result from some highly conjugated structures such as orthoquinone, α-carbonyl phenolic, stilbene and coniferaldehyde structures (Figure 2.1). Bleaching agents are used to destroy the conjugated structures and to remove light absorption in 400-500 nm range. Alkaline hydrogen peroxide has proved effective in environmentally bleaching mechanical and chemimechanical pulps[2.1]. Although lignin rich mechanical pulps can be bleached to rather high brightness without any substantial dissolution of lignin components (lignin retaining bleaching), it is found that alkaline hydrogen peroxide treatment of chemimechanical pulps results in some lignin removal[2.1].

It is very important to know the structures of the wood components before and after peroxide bleaching to gain an understanding of bleaching mechanism. A systematic approach to study these changes can be employed to improve the efficiency of the bleaching process. For this purpose, a series of effluent obtained from successive bleaching treatments was characterised using UV-VIS, ^{1}H and ^{13}C NMR spectroscopy.

Chapter 2 Alkaline Hydrogen Peroxide Bleaching Studies

Lignin Chromophores and Leucochromophores in Pulps

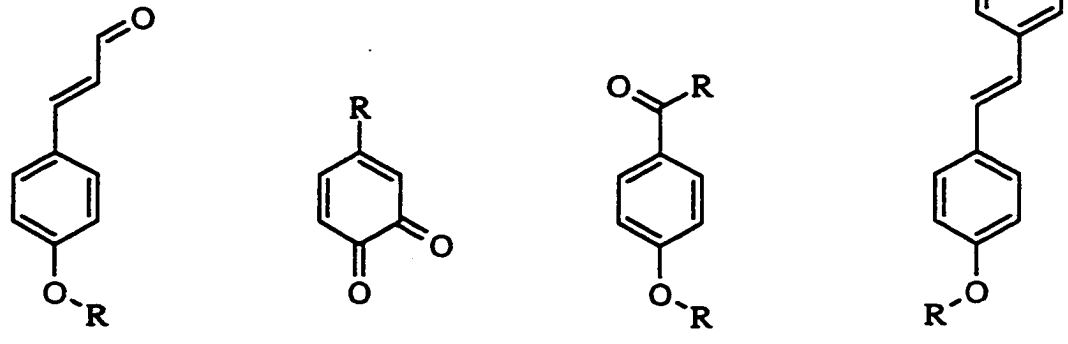

coniferaldehyde type **quinone type** **α-carbonyl type** **stilbene type**

R=H, another lignin structural unit or a hemicellulose chain.

2.1 The structures that cause colour in paper

Chapter 2 Alkaline Hydrogen Peroxide Bleaching Studies

Hydrogen Peroxide(H_2O_2)

The bleaching action of hydrogen peroxide is primarily attributed to the hydroperoxyl anion (HOO^-). The pK_a of hydrogen peroxide is 11.6 at 20°C. High pH increases its reactivity but decreases its stability[2.1].

$$H_2O_2 + OH^- \Leftrightarrow H_2O + HOO^-$$

Under alkaline conditions, hydrogen peroxide dissociates to form hydroperoxyl anion(HOO^-). The hydroperoxyl anion (HOO^-) will promote degradation reactions leading the formation of hydroxyl radicals($OH\cdot$) and hydroperoxyl anion (HOO^-). These ions may degrade to superoxide(O_2-) and singlet oxygen($^1O_2$) which then may lead to the formation of chromophoric groups by the reaction with lignin to decrease the brightness of pulp[2.2]. The decomposition of hydrogen peroxide depends mainly on pH and metal ions such as Fe^{3+}, Cu^{2+}, Mn^{2+} and Zn^{2+}, which catalyse the decomposition[2.2]. The strongest bleaching ability of hydrogen peroxide occurs at pH values near the pK_a (11.6)[2.3]. The stability of the hydrogen peroxide is at a minimum at this pH. Under standard conditions, pH buffers were added to control pH, and sodium metasalicate, magnesium sulphate and Na_2DTPA (sodium diethylenetriaminepenta-acetate) are added to compete with or chelate unwanted metal ions[2.2].

The Bleaching Reactions

Investigations into the reactions between the components of peroxide bleaching liquors and the organic substrates are intrinsically complex because of the variable properties of pulps. For this reason, most studies have involved model compounds and milled wood lignin rather than the chemical components of pulp and bleached effluent. Within these limits, the identification of the specific

reactions in the bleaching process is a difficult matter. The following is a summary of the study of the reactions of hydrogen peroxide with model compounds and lignin.

The Dakin Reaction

In organic chemistry, the Dakin reaction[2.4] is used to obtain a predictable variety of hydroxylated aromatic nuclei from appropriate ortho- or para- hydroxylated aldehydes or ketones by reaction with alkaline hydrogen peroxide[2.5]. There are several versions of the mechanism of the Dakin reaction. The simplest one is shown in Figure 2.2[2.5]. In this mechanism, the initial step in the degradation of these structures is the nucleophilic addition of the hydroperoxide anion (OOH^-) to the electron deficient centre. The second step is the rearrangement of the carbon to ester, this is a slow step, which may involve a spirocyclic transition state or intermediate. The final step is the migration of RCOO- group. A very strong electron-donating substitutents (X, or Y) such as OH ($-O^-$) on the aromatic nucleus is required in order to make the Dakin reaction occur. The Dakin reaction is the single most important reaction in alkaline hydrogen peroxide bleaching of pulp.

α-Ketone and α, β-Unsaturated Aldehydes

Phenolic α-ketone structures are oxidized by alkaline peroxide hydrogen via the Dakin reaction to the corresponding hydroquinone [2.6] (Figure 2.3). α, β-unsaturated aldehyde type structures are oxidized by alkaline hydrogen peroxide to produce aryl-α-carbonyl structures. The proposed mechanism was shown in Figure 2.4 [2.6, 2.7].

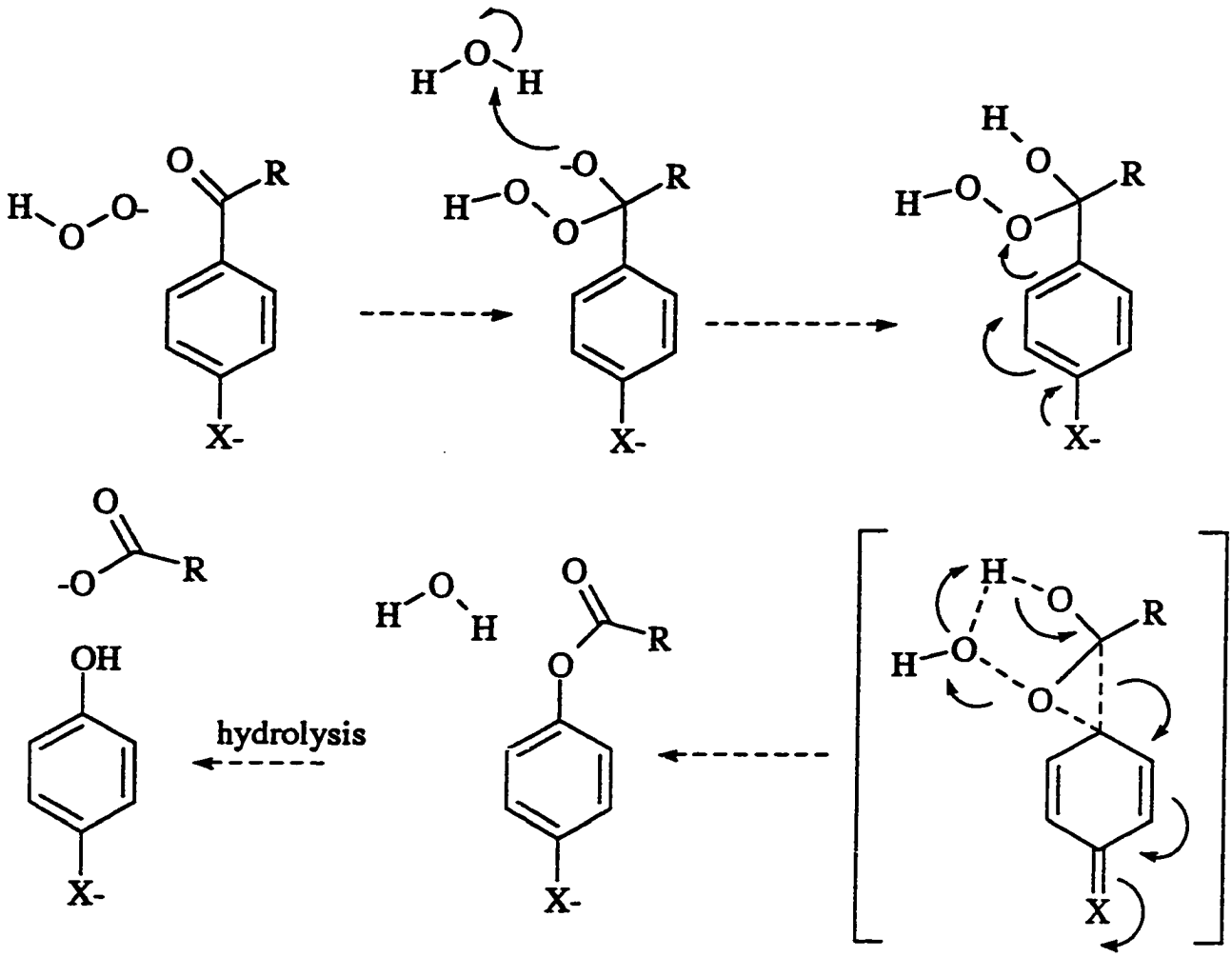

Figure 2.2 The mechanism of Dakin reactions[2.5]

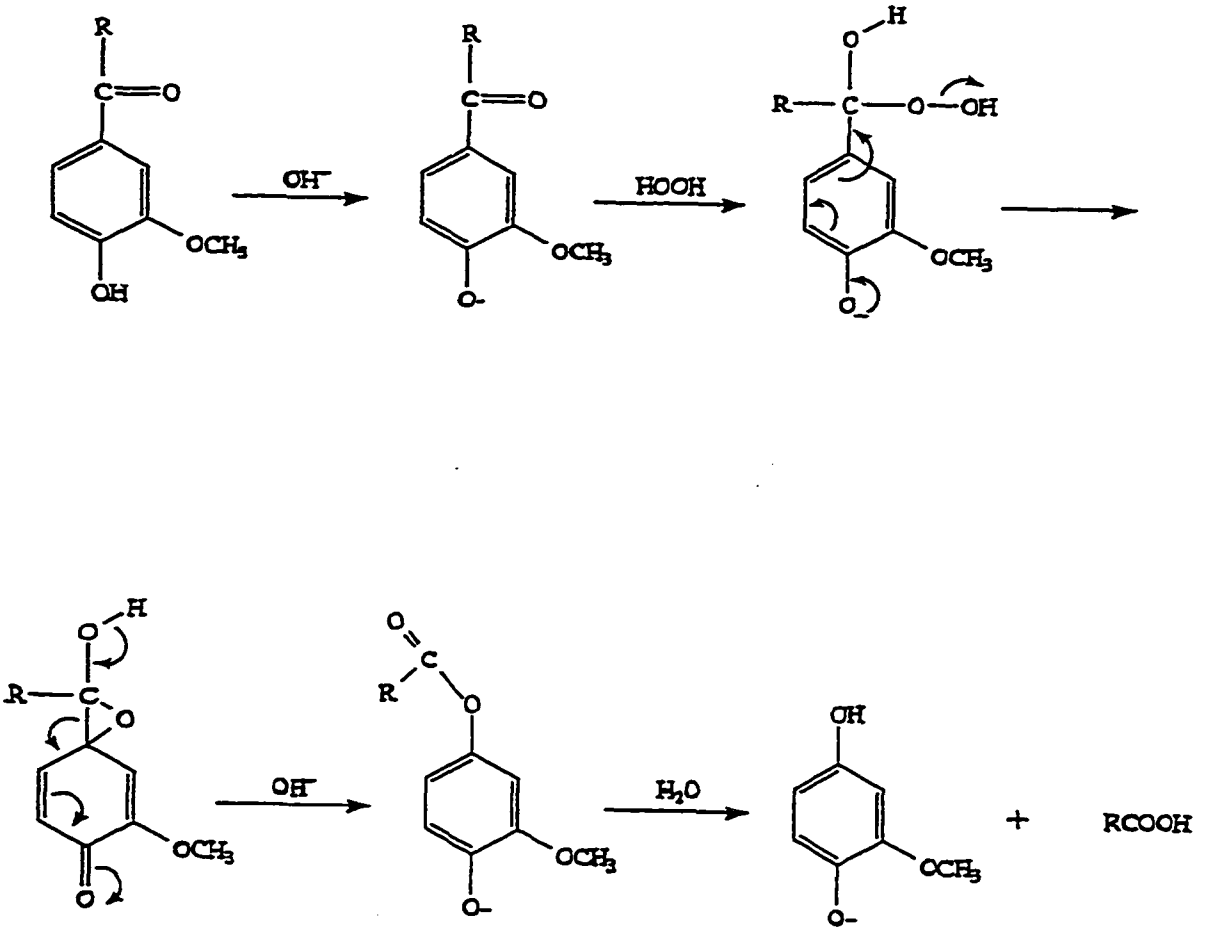

Figure 2.3 The mechanism of the oxidation of α-ketones by alkaline hydrogen peroxide[2.6]

Chapter 2 Alkaline Hydrogen Peroxide Bleaching Studies

Reaction of Phenolic Structures

Non-carbonyl phenolic structures may be degraded by unstablized hydrogen peroxide but it has been reported that stabilized peroxide has no effect on phenolic structures. α-Hydroxyl phenolic groups may be degraded by Dakin like reactions if the α-hydroxyl group is first oxidizied to a carbonyl. The opening of an aromatic ring is possible if the methoxyl is oxidized to an o-quinone that may readily react with a peroxide. Some proposed reactions for phenolic structures are shown in Figure 2.5[2.8].

The literature suggests that β-O-4 units in the model compound and lignin were virtually unreactive toward peroxide stabilized by Na_3DTPA or silicate[2.9]. These components may react under condition in which the peroxide is unstabilized.

Reactions of β-1 structures

The main reactions of 1,2-diarylpropane models with stabilized alkaline hydrogen peroxide at pH=10.5 have been shown to be nucleophilic attack of hydroperoxide anion on a quinonemethide structure(Figure 2.6)[2.10]. Oxidation of stilbene structures by reactions with alkali may occur. Both of these reactions are not kinetically favoured and require higher temperature. The β-1 diol model was more reactive toward unstabilized peroxide than toward stabilized peroxide with Na_2DTPA [2.11].

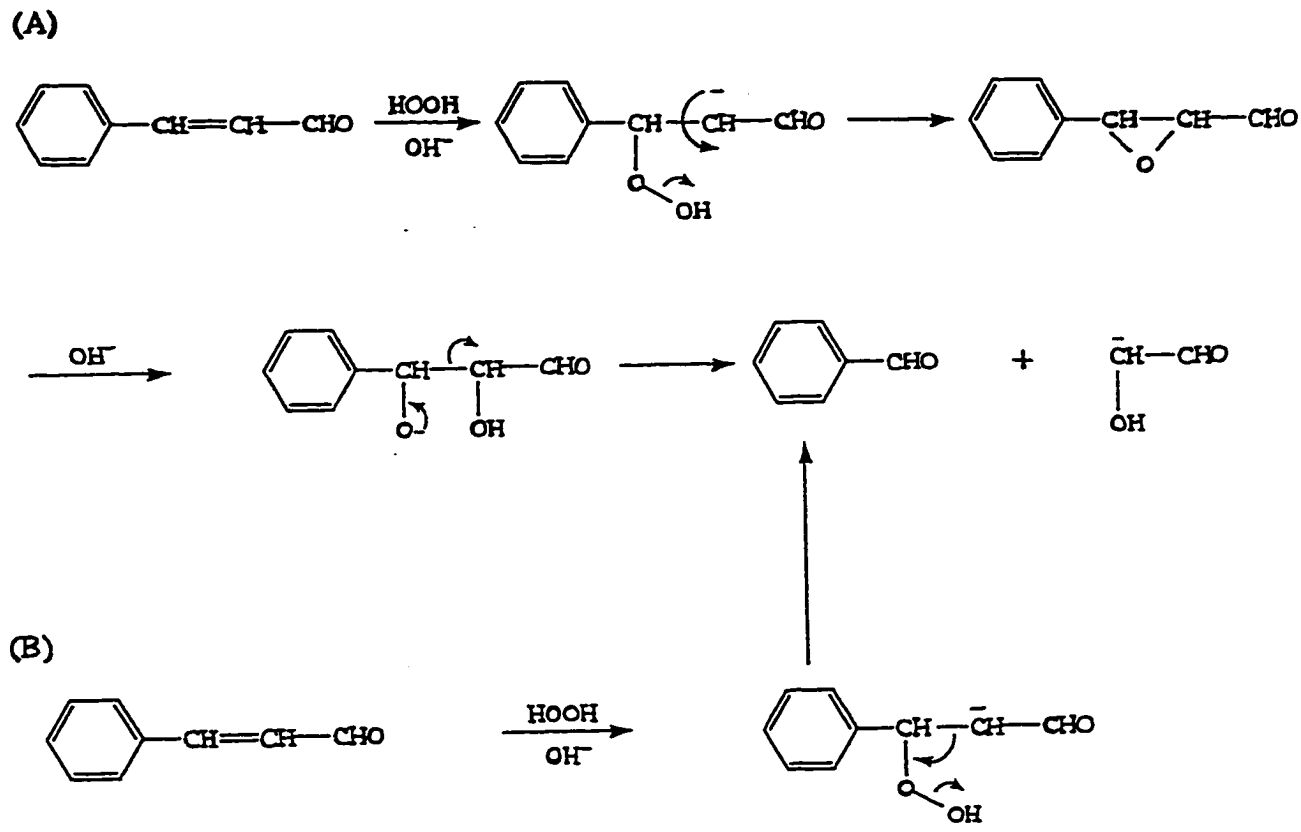

Figure 2.4 The mechanism of the oxidation of α,β-unsaturated aldehydes by alkaline hydrogen peroxide[2.6].

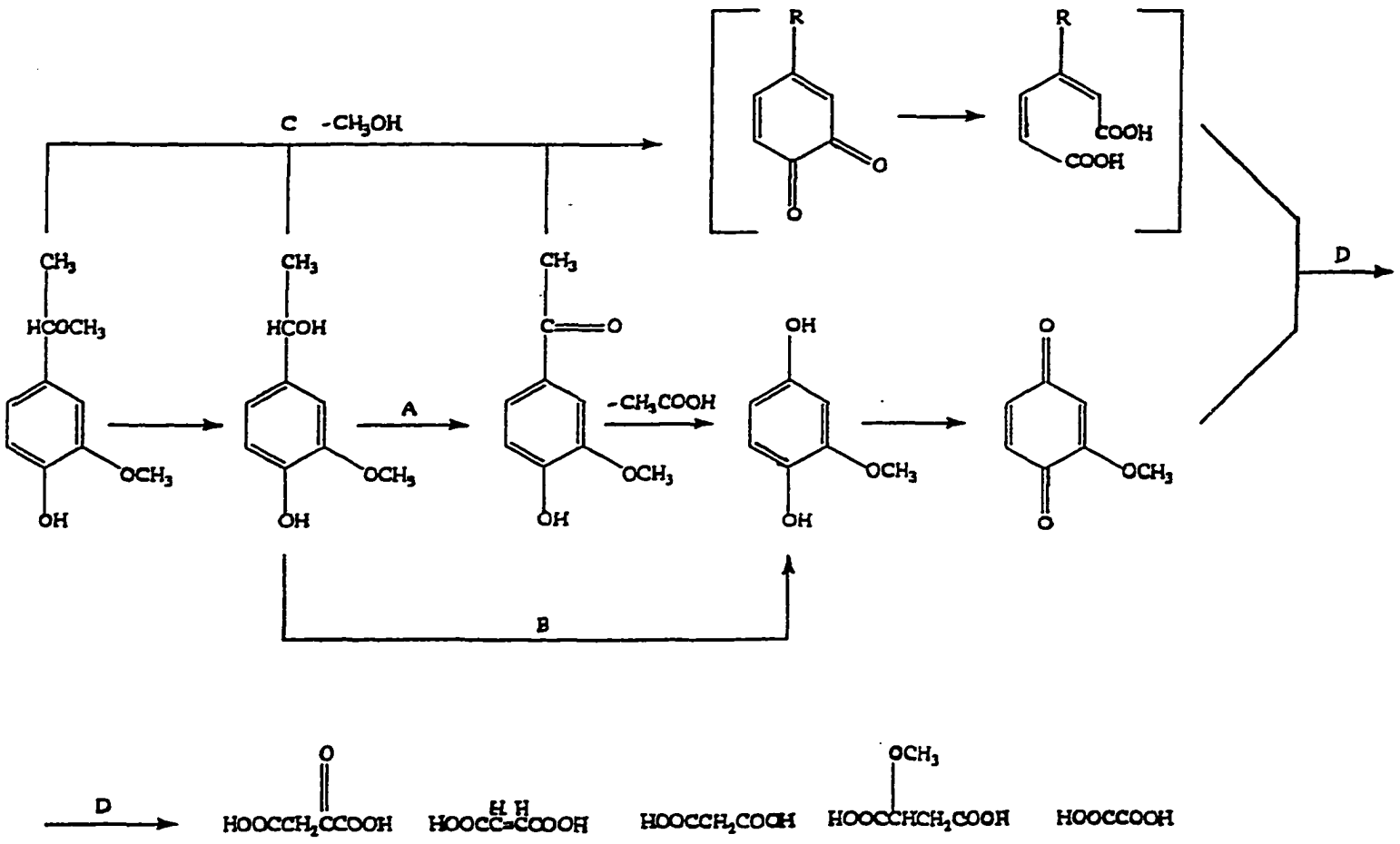

Figure 2.5 The reactions of phenolic structures [2.9].

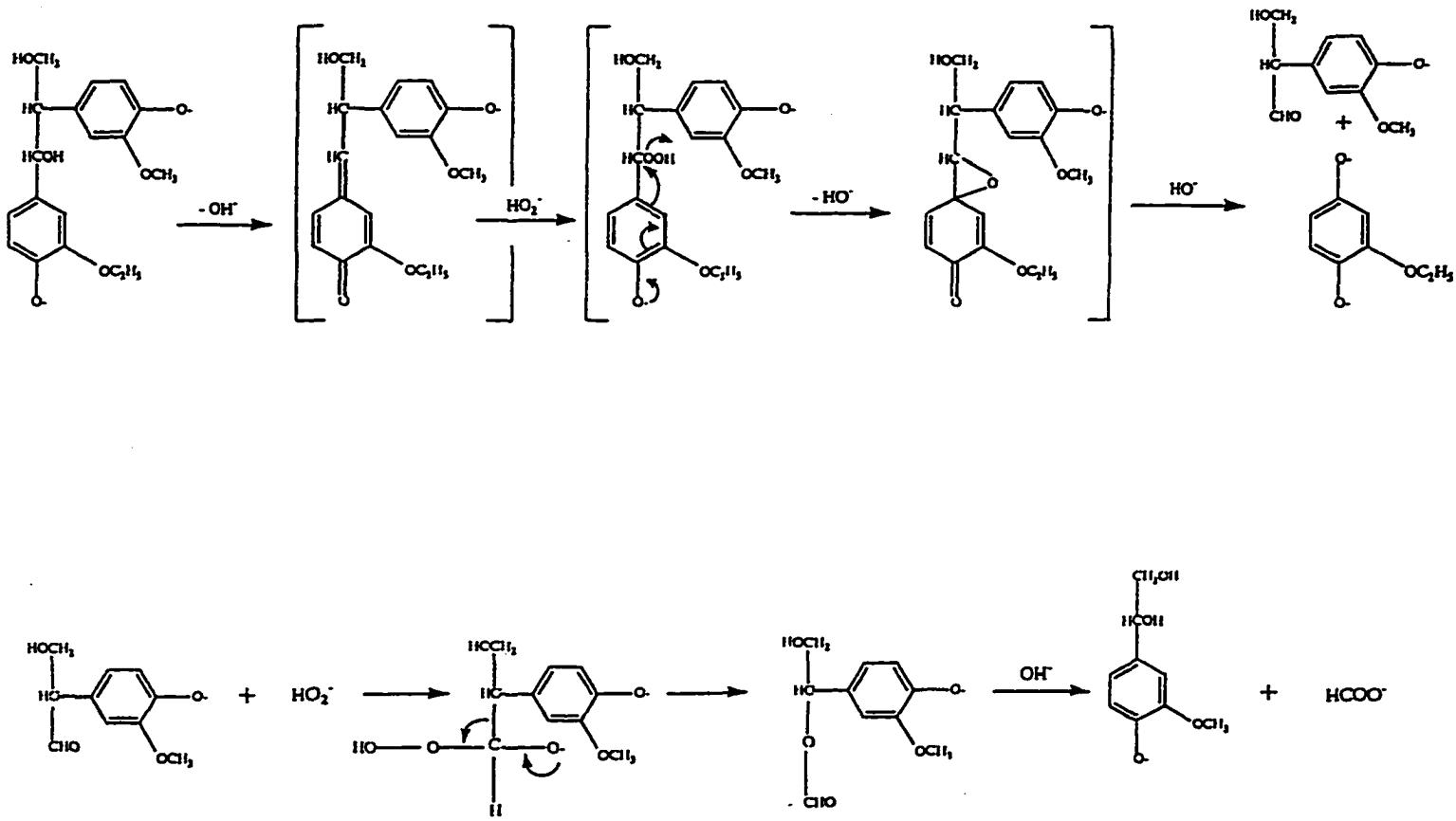

Figure 2.6 Reaction of β-1 structures.

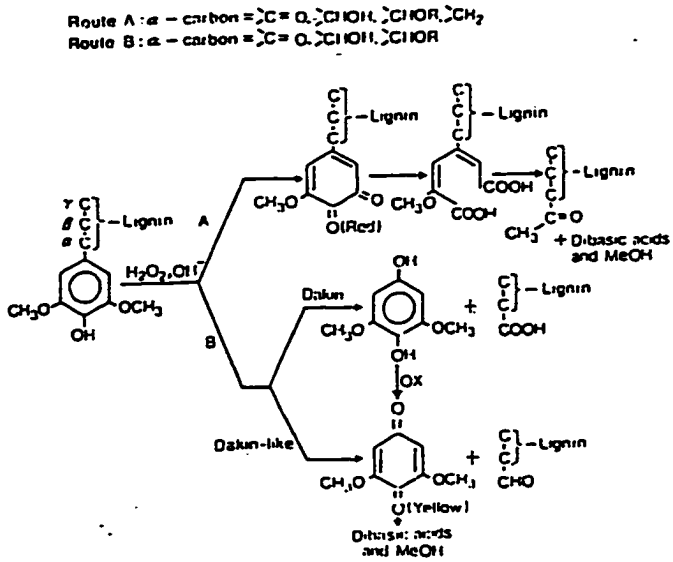

Figure 2.7 The proposed reactions for spruce groundwood bleaching, according to Bailey and Dence[2.8].

Chapter 2 Alkaline Hydrogen Peroxide Bleaching Studies

Reactions of Lignin

Despite the variable properties of pulp, there are some proposed lignin bleaching reactions based on the experimental observations and model compound studies. One of the most important observations is that the yields of groundwood bleached with peroxide commonly lie in the range of 98-100%[2.6]. This suggests that very little of the lignin is degraded to the point of solubilization. Bailey and Dence [2.8] proposed reactions for spruce groundwood, as shown in Figure 2.7. Kempf and Dence proposed a reaction sequence for oxidative breakdown of hardwood lignin reacted with alkaline hydrogen peroxide[2.12]. A wider bleaching reaction concept of lignin structure by alkaline peroxide, which was based on the nucleophilic addition of hydroperoxide anions to carbonyl and conjugated carbonyl structures, was published[2.13]. But these proposed reactions and reaction sequence have not confirmed yet.

In this chapter, UV-VIS, ^{1}H and ^{13}C NMR spectra techniques are applied to the analysis of effluent compositions generated from lignin bleaching process. The results provide evidence for the proposed lignin bleaching reactions.

UV-VIS Spectrum

A UV-VIS spectrum is a plot of the wavelength or frequency of absorption against the absorption intensity (absorbance in our experiments). The principal characteristics of an absorption are its position and intensity. The position of the absorption corresponds to the wavelength of radiation whose energy is equal to that required for an electronic transition. The intensity of absorption is related to two factors: (1) the probability of interaction

between the radiation energy and the electronic system raising the ground level to an excited state and the polarity of the excited state. (2) the concentration of the substance in the solution.

Gunhild Aulin-Erdtman et al studied the UV-VIS absorption of lignin and its model compounds. They found that UV-VIS spectra of lignin model compounds and lignin can be divided into 4 areas (2.14).

(1). long-wave benzenoid π-π^* bands (= L.E bands of the $^1Arg \rightarrow {}^1B_{2u}$ type). These bands occur at about 270-280 nm in the absorption curves of phenol and non-methoxylated p-alkylphenols.

(2). Short-wave bands, with maxima up to approximately 250 nm. These bands may be either displaced benzoic primary L.E bands(the $^1Arg \rightarrow {}^1B_{2u}$ type) or p-p^* bands resulting from the transfer of p electron from oxygen substitutes (in -OH or $-OCH_3$) to the benzene ring, or combinations of these band types. With some model compounds studies, it is found that these short wave bands, which are often called 'first primary bands', partially overlap with stronger bands having maxima at shorter wavelengths, presumably 'second primary bands'(the $^1Arg \rightarrow {}^1E_{2u}$ type).

(3). E. T. Bands (k-bands), largely result from electron transfer from a p orbital of one unsaturated group to a p^* orbital of a conjugated unsaturated group, which occurred at around 350nm.

(4). Complex long wave bands, these bands occur at more than 400 nm, which are contributed from more than one kind of electron excitations.

2.2 Experiments

Chapter 2 Alkaline Hydrogen Peroxide Bleaching Studies

The alkaline hydrogen peroxide bleaching

The standard conditions for brightening consist of 4% H_2O_2, 0.05% $MgSO_4$, 0.15% DTPA(diethylenetriaminepentaacetic acid), 3% Na_2SiO_3 (sodium metasilicate) on O.D. aspen pulp at 60°C, 10% consistency and an initial pH as required(typically 11.0). The pulp was mixed in a Hobart mixer with water, DTPA and H_2O_2, then the magnesium sulphate and sodium silicate were added. Finally, the pulp was brought up to pH 11 by addition of NaOH solution, mixed and rapidly placed in a controlled temperature heater bath for the duration of the bleaching reaction.

A 250 ml syringe with a layer of glass wool in the bottom was used to squeeze the effluents from pulp. About 200 ml pulp was used to obtain the effluent. About 50 ml effluent was squeezed from the pulp at different time (0, 5, 10...50, 60 minutes) and frozen by immersion in liquid nitrogen. The iced samples were freeze dried immediately. The dry bleached effluent was acetylated according to the procedure described in Chapter 4. NMR spectrometer and its parameters can be found in Chapter 4.

UV-VIS spectrometer and procedure

UV-VIS spectrometer used in this experiment is a Varian CARY® 1E. The parameters used were as following,

Method Name: Bleaching Study
Photometric Mode: ABS
Abscissa Mode: NM
Ordinate(y) Min/Max: -0.2000/2.000
Abscissa(x) Min/Max: 230.00/500.00 nm
SBW(nm): 1.000
Energy level: 1.000
Signal Averaging time(sec): 0.500

Data Interval: 0.5000
Scan Rate(nm/min): 60.00
Lamp On: UV-VIS
Baseline Correct: On
Auto Scale: NO
Auto Store Data: Yes
Auto Store report: NO

The solution was taken from the squeezed effluent described as above. A special 1 mm flow through UV cell was used and a 0.45 μm syringe filter was put at the head in order to remove any colloidal components. The UV-VIS spectra are obtained using the parameter described as above.

2.3 Results and Discussion

2.3.1 ^{1}H NMR Spectra of Bleaching Effluents

^{1}H NMR spectra of the acetylated effluent components from peroxide bleaching of aspen hardwoods are shown in Figure 2.8. The effluents were taken at 1.75 minutes, (spectrum A), 10.5 minutes (spectrum B), 20 minutes (spectrum C) and 30.75 minutes (spectrum D). Assignments are shown in Table 2.1. The presence of peaks related to carbohydrate structures and the variation in the phenolic acetoxyl (~2.2 ppm) with time is noteworthy. These samples were prepared by acetylation of freeze dried effluents. The acetylation and purification process will remove significant portion of the acidic structure and for this reason we must consider these results as relating primarily to the neutral compounds.

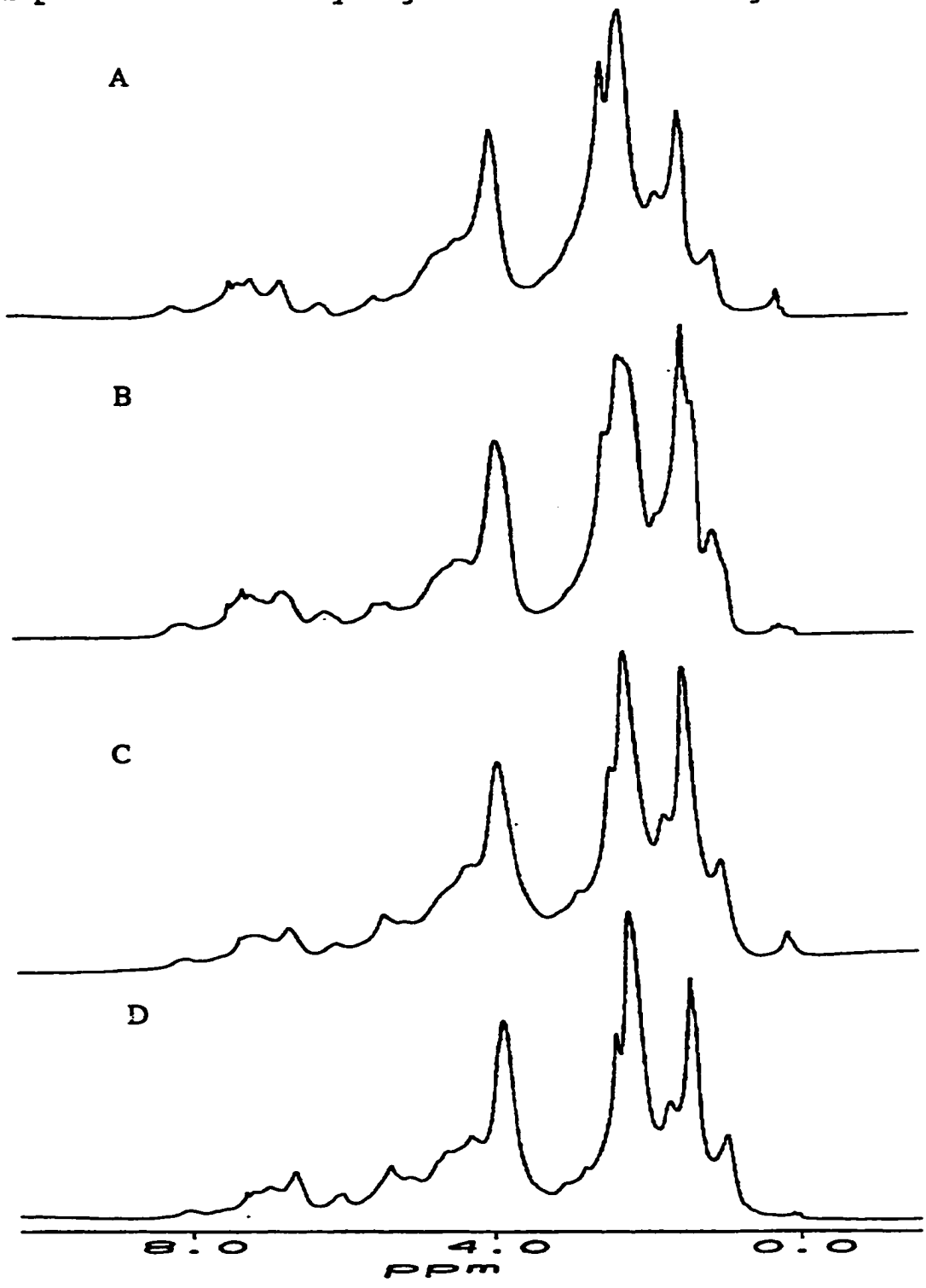

Figure 2.8 ^{1}H NMR spectra of the bleaching effluents at 1.75(A), 10.5(B), 20(C) and 30.5(D) minutes.

Table 2.1 Assignments for Proton NMR of Acetylated H_2O_2 Bleaching Effluents

7.99	aromatic protons adjacent to α-carbonyl groups
7.40	aromatic protons adjacent to α-carbonyl groups
6.88	aromatic protons
6.51	aromatic protons
5.96	H_α in β-O-4 and β-β groups
5.04	xylan (C3 proton)
4.60	H_β in β-O-4
3.67	methoxyl protons
2.23	aromatic acetate (lignin, phenolic extractives)
1.97	aliphatic acetate (carbohydrates, lignin side chains)
1.52	water
1.25	γ-methyl structures and aliphatic extractives
0.80	aliphatic extractives

β-O-4 Structures

^1H NMR spectra of the effluents have peaks at ~6.0 and ~4.6 (Figure 2.8) that indicate the presence of α and β protons in β-O-4 structures. Peaks on ^1H NMR spectra of effluents from bleaching process were integrated using a Lorentzian fit program(in FELIX package) and various ratios were calculated using the measured integral of the different groups. Plots of the normalized integral of β-O-4 units (5.97 ppm) and methoxyl groups(3.67 ppm) is shown in Figure 2.9. There is a decrease in the relative frequency of β-O-4 structures (5.97 ppm) with increasing bleaching time. Methoxyl group frequency appears to first increase, then decrease as do the aromatic protons (Figure 2.10). β-O-4 structures were present in the effluent from early in

the bleaching sequence, suggesting that deligninfication plays a role in the initial brightening reactions. More than 80% of the decrease occurs in the first 20 minutes, indicating that most of the reaction contributing to the quantity of components in solution occurs in the first 20 minutes. This result, indicates the stability of β-O-4 structures to peroxide bleaching, and agrees with a bleaching mechanism in which lignin leaching from pulp plays a significant role in determining the brightening rate[2.18]. Although dissolved components are known to decompose during peroxide bleaching [2.19], it appears that this decomposition does not involve destruction of β-O-4 structures.

Phenolic Structures

The relative frequency of phenolic structures was measured by the normalized integration of the aromatic acetoxyl peak (2.23 ppm) on the ^1H NMR spectra. Integration of the aromatic acetoxyl groups indicates the relative proportion of phenolic hydroxyls decreased with bleaching time in the first 30 minutes of bleaching(Figure 2.10). This may suggest that phenolic units that were more susceptible to peroxide were removed in the earlier bleaching time. Later hydroquinone type structures may be destroyed by further reactions. The addition of carbohydrate structures or degradation of phenolic structures (evidenced by the increase in the peak at 1.97 ppm) by ring opening reactions will also lower the relative amount of phenolic OH as a function of bleaching time.

Aromatic Structures

Most aromatic protons in lignin structures have chemical shifts between 6.6 and 7.2 ppm. These have been integrated as one broad peak at 6.9 ppm which increase,

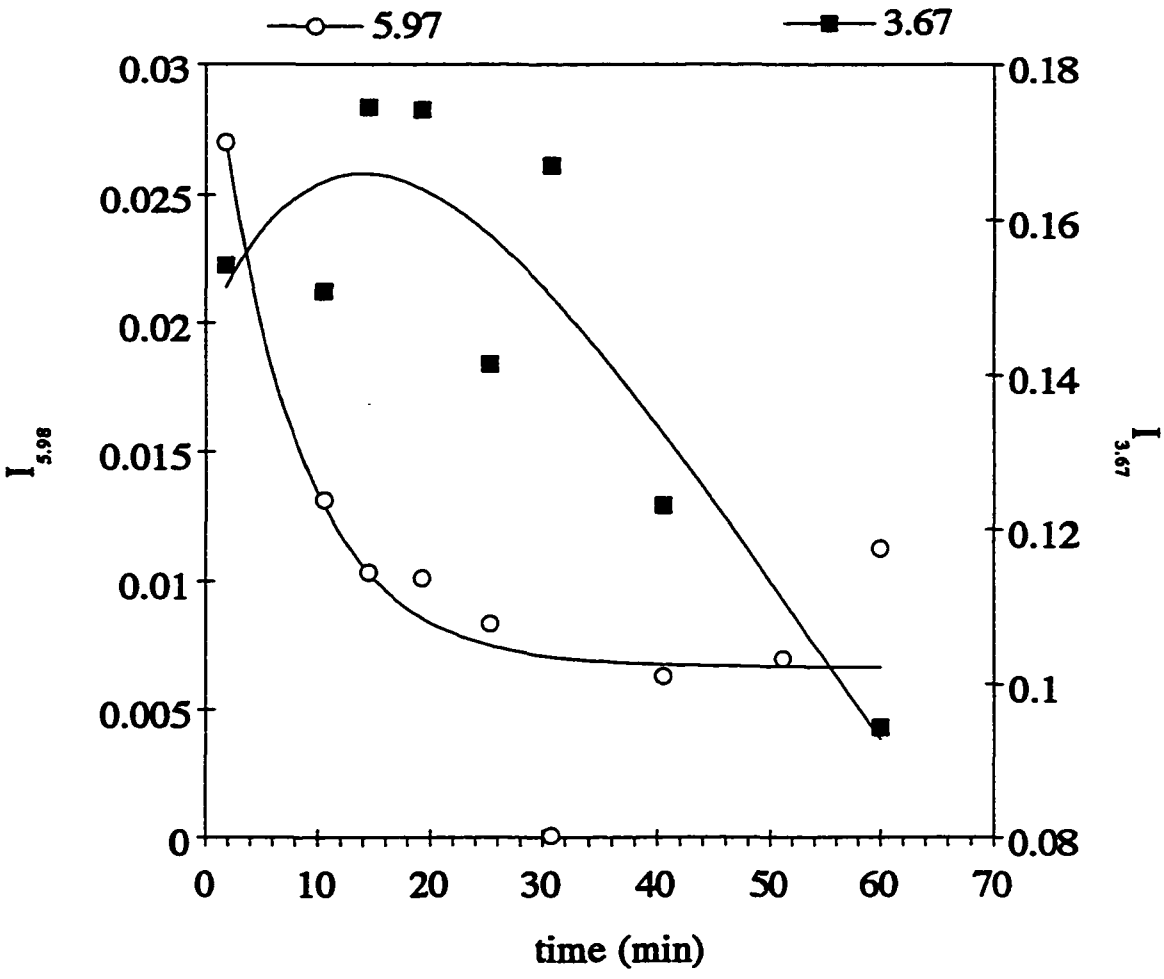

Figure 2.9 Plot of the frequency of β-O-4 units (5.97ppm) and methoxyl groups(3.7 ppm).

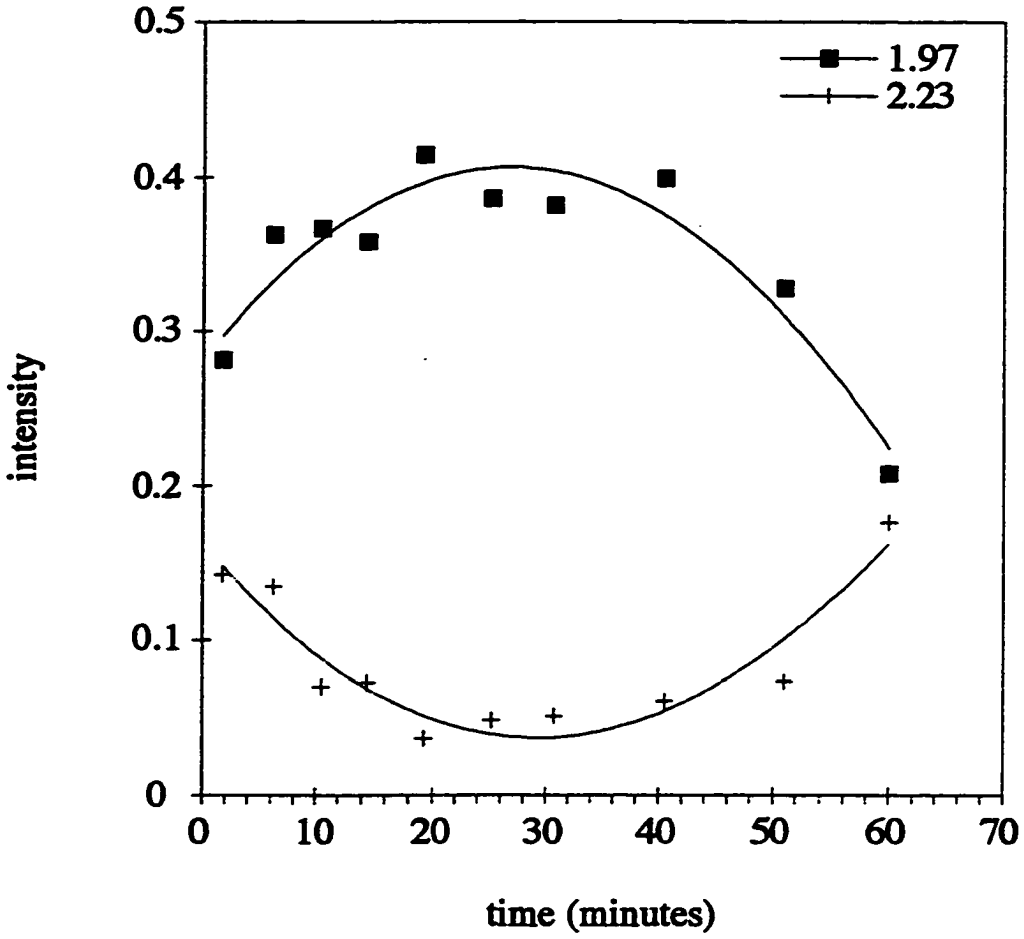

Figure 2.10 Plot of the frequency of aromatic acetoxyl (2.23ppm) and aliphatic acetoxyl(1.97 ppm) groups.

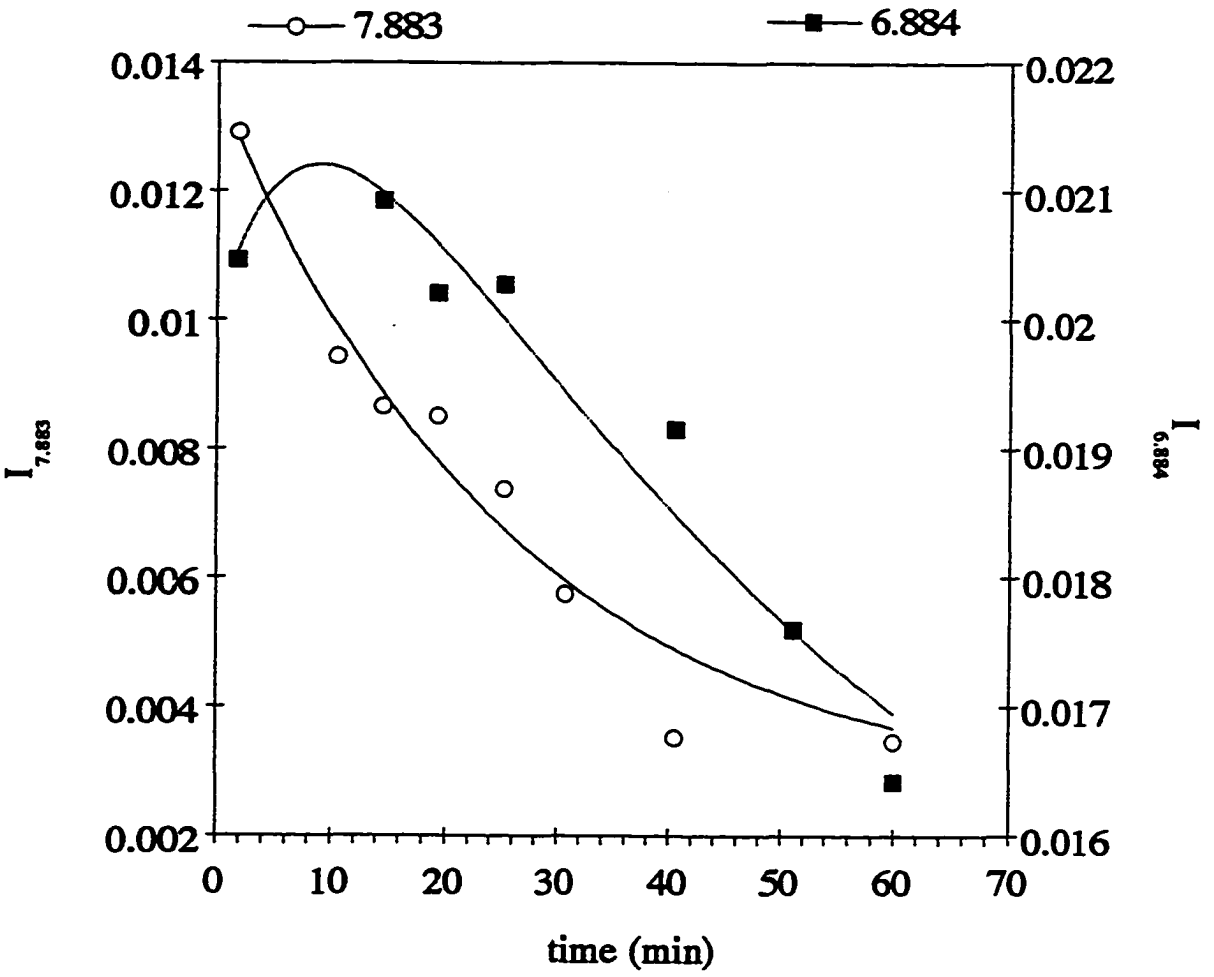

Figure 2.11 Plot of the downfiled aromatic protons (7.883ppm) and aromatic protons (6.884 ppm)

then decrease in intensity as shown in Figure 2.11. This result is similar to the result for methoxyl groups. Aromatic structures with α-carbonyl groups have protons at the C_2 and C_6 with peaks in the 7.2 - 7.8 ppm region [2.15]. Initially there are two aromatic protons corresponding to α-carbonyl structures for every three protons on noncarbonyl substituted aromatic structures. The peak at 7.8 ppm decreases exponentially with a rate constant of 0.037 Min^{-1} as shown in Figure 2.11. The steady decrease in these structures is a expected result of peroxide brightening.

Carbohydrates

^1H NMR spectra of the effluent indicated the presence of carbohydrates at 5.25, 5.04 and 4.69 ppm [2.16]. These peaks were difficult to integrate. The aliphatic acetoxyl group , however, showed a remarkable increase in intensity in the first 20 minutes before decreasing as shown in Figure 2.10.

Other Structures and Conclusion

There are two peak changing patterns in the effluent. One relates the peaks at 6.8, 6.5, 3.67 and 1.94 ppm which appear to increase for 20 minutes then decrease. This suggests that there are some accumulations of these structures in the effluents at the first 20 minutes. These reactions may involve rate limiting removal of lignin and carbohydrates. The peaks at 7.883, 5.97, 0.79 ppm form the other pattern which decreases exponentially.

2.3.2 The ^{13}C NMR spectra of bleached lignin

^{13}C NMR spectroscopy was first used to study kraft lignin structure by Lüdemann and Nimz [2.17]. ^{13}C NMR spectrometry has proved to be a valuable tool for the direct observation of structural changes in polymeric

lignin resulting from chemical reactions. The ^{13}C NMR spectrum of lignin can be divided into three main parts: the first(175 to 165ppm) contains signals assignable carbonyl carbons including carboxylic acid structures; the second(165 to 108 ppm) is ascribable to aromatic and olefinic carbons; and the third (108 to 10 ppm) is attributed to aliphatic carbon atoms. We have further separated the aliphatic region into aliphatic carbon with hydroxyl substitution (108-56 ppm) and non-substituted carbon (90-10 ppm).

Our ^{13}C NMR spectrum was obtained by dissolving bleached lignin in DMSO, the sample was obtained by freeze drying the effluents from the standard bleaching condition. The parameters of ^{13}C NMR spectrometer are as following: SW=20,000Hz, SF= 50.3MHz. The ^{13}C NMR spectrum of bleached lignin is shown in Figure 2.12. The integrals and assignments are given in Table 2.2.

There are several major conclusions we can draw from the ^{13}C spectrum upon examination of Table 2.2. First, comparison of the total signal between 150 and 110 ppm, with the signal for the C_1 sugar 90-105 ppm indicates that the ratio of sugar units to aromatic groups is approximately one to one. Second, comparison of the aromatic region with the aliphatic OH substituted region (108-60 ppm) yields a 2:1 ratio. This ratio accounts for aliphatic hydroxyl substituted groups on lignin side chains. The number of methoxyl groups (57-55.5 ppm) is about 2 for each aromatic residual which is about 2 for each aromatic residue which is consistent with the product containing mostly syringyl type aromatic structures. The frequency of carboxylic groups (166-176 ppm) is high at about 2 for each aromatic moiety. Of these carboxylic acid structures, the frequency of acids directly bonded to the

aromatic group (166-168 ppm) is about 0.12(12%) for each aromatic group. Aliphatic carboxylic structures (~173.4 ppm) possibly related to β-substituted aromatic acids

Table 2.2 Integrals and ^{13}C chemical shifts values for Peroxide Bleached Effluents (DMSO-d6 solvent).

Chemical Shift	Relative Integral	Sum of Integral for Region	Assignment
193.2			
191.3	0.001224		aldehyde
186.9	0.000457		
183.2	0.000401	0.00214 (182-191 ppm)	
179.1	0.00097		
176.3	0.0088		carboxylic acid
173.1	0.850		carboxylic acid
167.7	0.0526		carboxylic acid
166.1	0.185	1.088 (166-176 ppm)	carboxylic acid
161.9	0.0903		
152	1.00		
147.7	0.283		
138.1	0.514		
134.2	0.694		
130.5	0.00881		
127.2	0.0409		
123.4	0.0338		
118.4	0.139		
114.8	0.183		
110.9	0.0199	3.007 (110-162 ppm) aromatic	
105.8	0.226		c1 sugar
103.6	0.897		c1 sugar
99.8	0.00656	1.129 (99-107 ppm)	c1 sugar
96.9	0.0199		
92.3	0.0441		
85.7	0.490		
82.4	0.462		
80.3	0.0691		
78.5	0.401		
73.9	0.294		
71.9	1.114		
69.2	0.481		
62.5	0.123		
60	1.378	6.00 (60-106 ppm)	
57	0.418		methoxyl
55.5	1.158	1.56 (55-57 ppm)	methoxyl

(179.5 ppm) constitute the dominate 166 ppm acid type structure. These structures are present at a frequency of 0.85 groups per sugar residue [2.14].

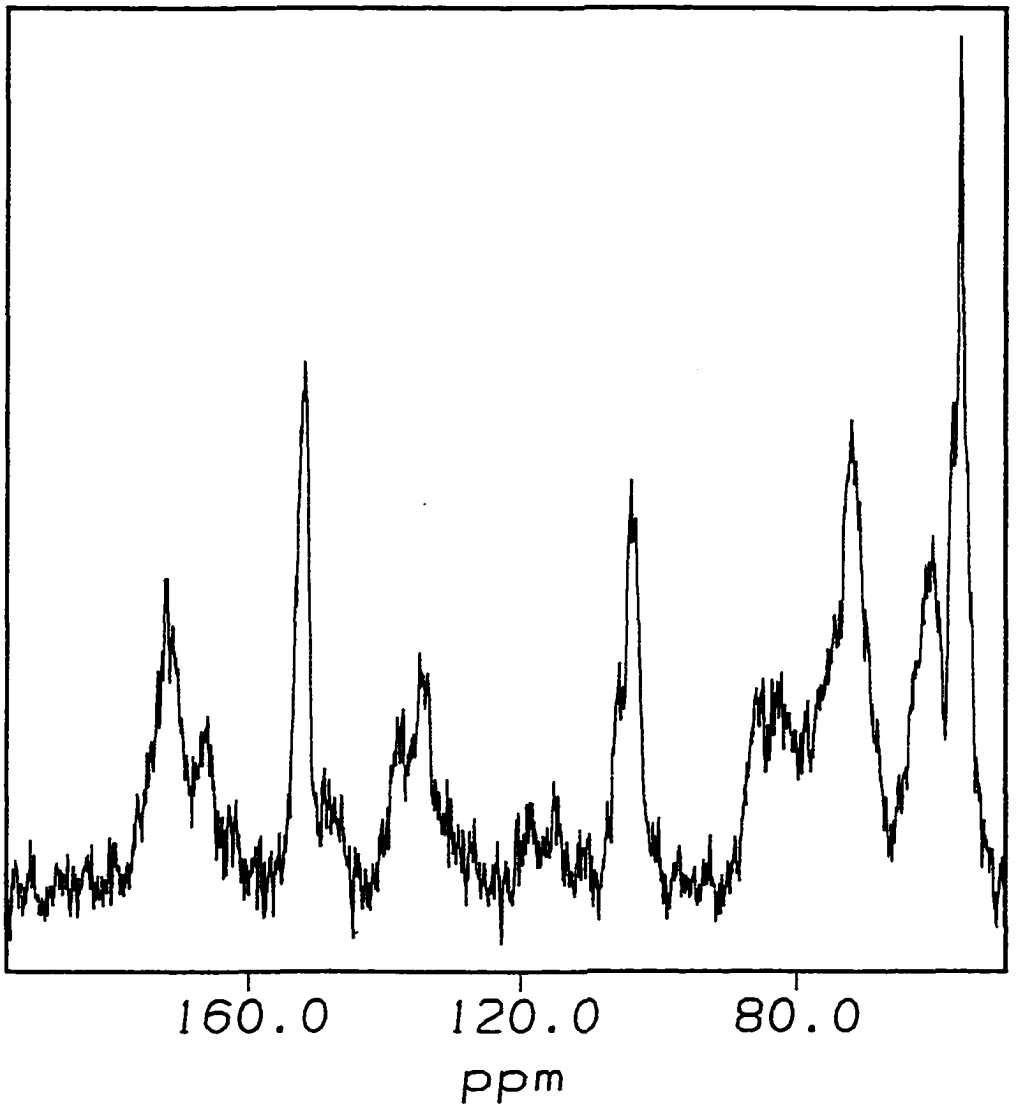

Figure 2.12 ^{13}C NMR spectrum of Bleaching Effluent

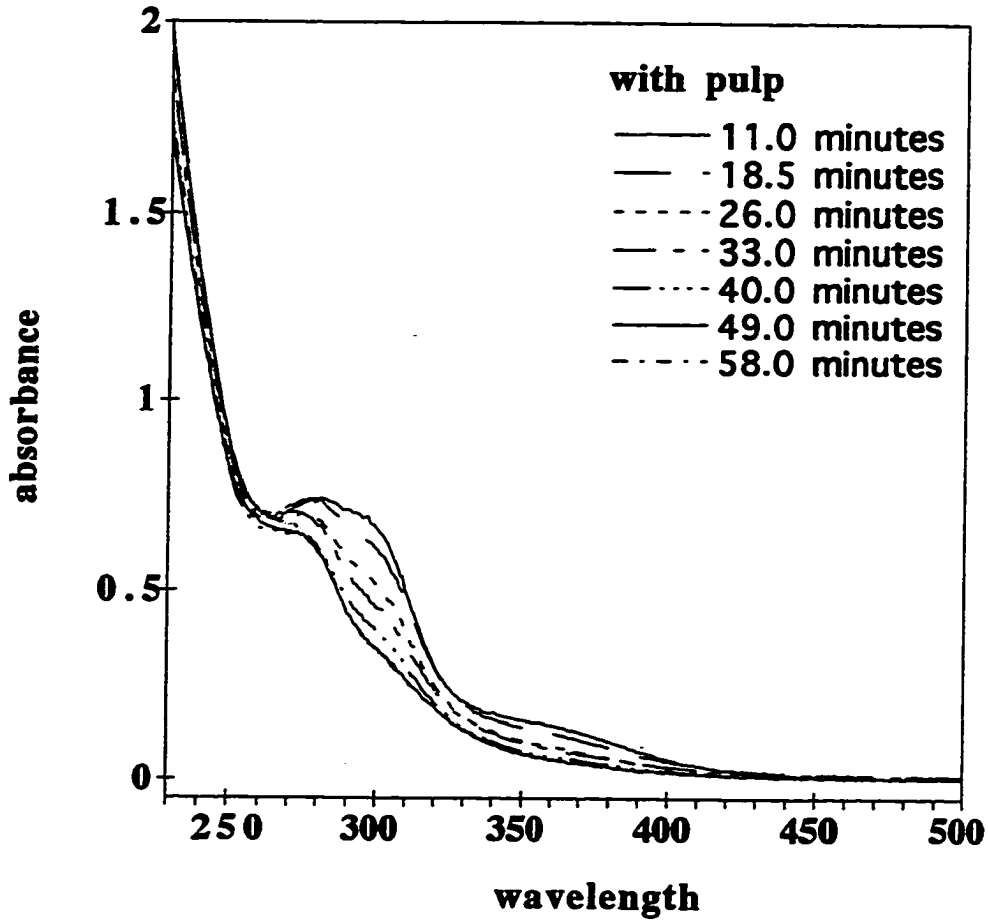

Figure 2.13 UV spectra during the reaction of alkaline hydrogen peroxide with pulp.

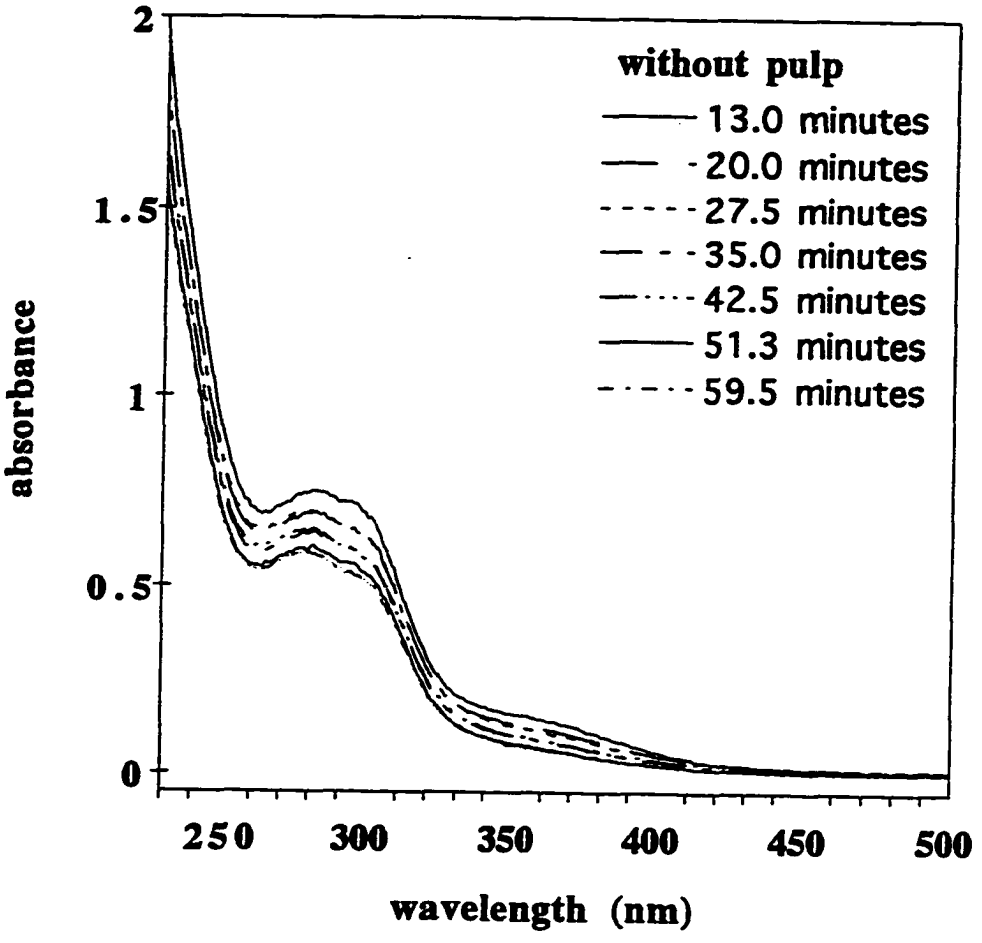

Figure 2.14 UV spectra as a function of time during the reaction of alkaline hydrogen peroxide without pulp.

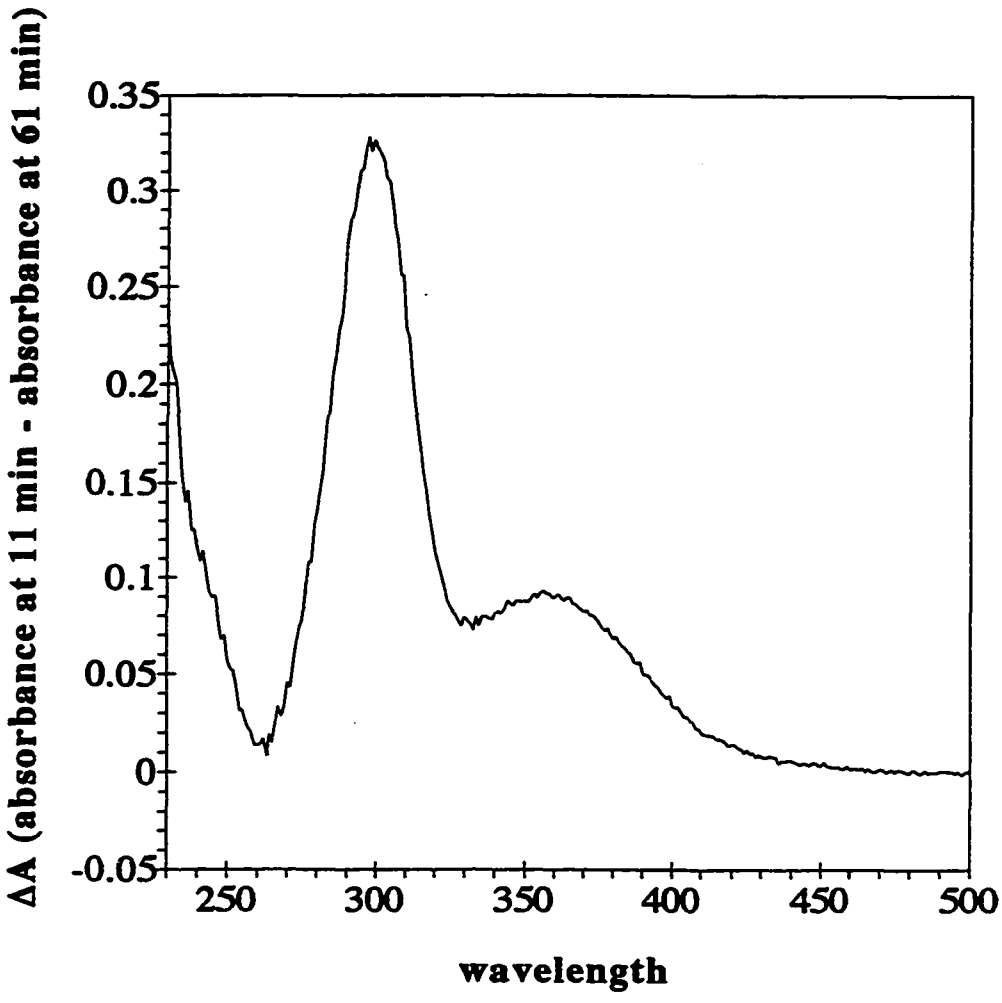

Figure 2.15 UV (time) difference spectra for effluents from hydrogen peroxide bleaching of pulp.

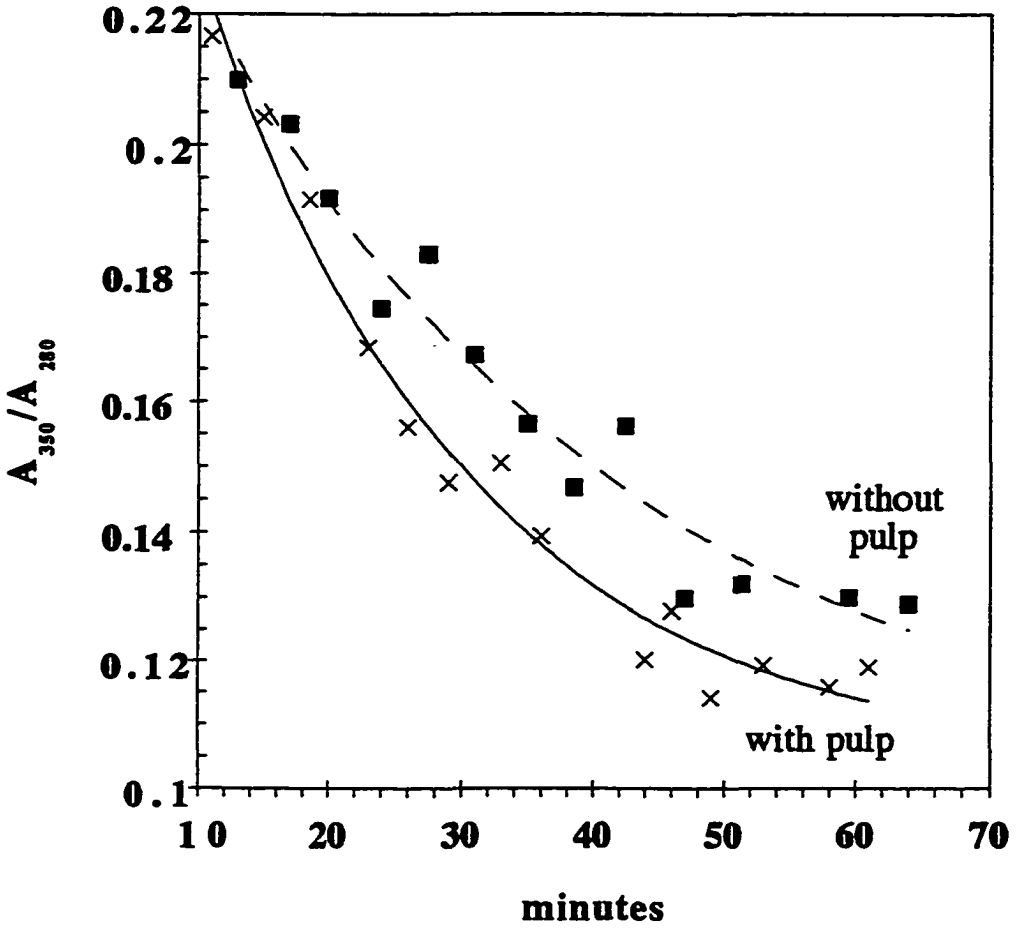

Figure 2.16 The ratio of A_{350}/A_{280} in the solution with and without pulp showing the loss of carbonyl structures.

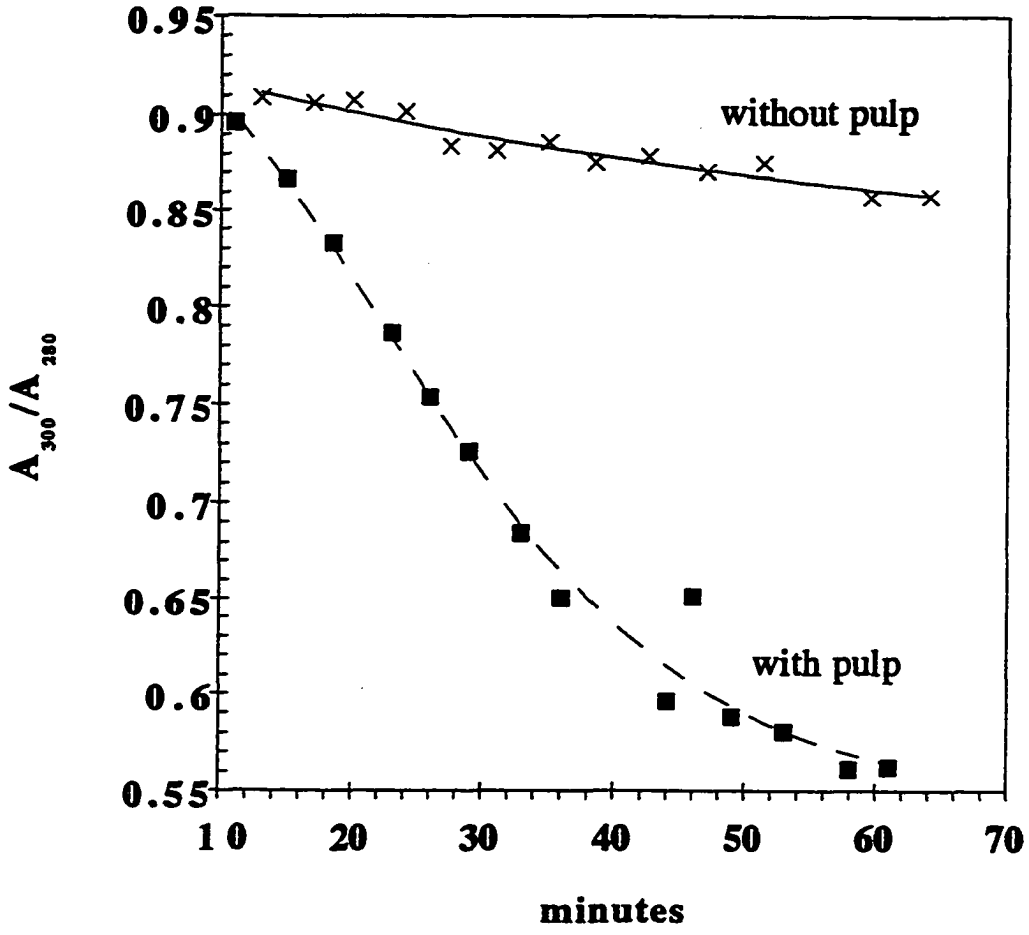

Figure 2.17 The ratio of A_{300}/A_{280} in the solution with and without pulp.

2.3.3 UV-VIS study of bleaching effluent

UV spectrum of H_2O_2 bleaching effluents from stoneground aspen pulp were taken as a function of time during pulp brightening. The difference between the absorbance changes when the effluent was removed from the pulp (Figure 2.13) and when it was not(Figure 2.14) is examined here. Further analysis of the titration of H_2O_2 generated bleaching effluents will be examined in Chapter 3. The overall changes in the absorbance with time are shown by the difference spectra (as a function of bleaching time) in Figure 2.15. These difference spectra, taken as the difference in absorbance between 11 minutes and 60 minutes are very much like pH difference spectra (cf. Figure 3.15).

During the brightening reaction, α-carbonyl groups are generated and destroyed, phenolic hydroxyl groups are generated and protonated as the pH drops. Evidence of loss of colour occurs, is provided by the decrease in the absorbance at 350 nm from as shown Figure 2.16. The rates of change are similar to the solution with pulp (0.037 min^{-1}) and without pulp (0.048 min^{-1}).

The relative amount of phenolic groups may be examined from the absorbance ratio of A_{300nm} /A_{280nm} (larger ionizied). This is due to the bathochromic shift upon ionization. Examination of this ratio, in Figure 2.17 shows that the extent of ionizied groups and phenolic structures decreases much more rapidly with pulp than without pulp. It appears that the primary difference between the UV of the effluents with and without pulp is the substantial decline in pH occurring with the presence of pulp. It is expected that the decomposition and solubilization of carbohydrates

contributes to the decline in pH.

References

[2.1] R. P. Singh Ed. The Bleaching of Pulp Third Edition.; Tappi Press, pp.211-212(1979).

[2.2] R. Agnemo; G. Gellerstedt; E.L. Lindfors; Acta Chem. Scand., B33. 154.(1979).

[2.3] R. Agnemo; G. Gellerstedt; Acta Chem. Scand., B33. 337 (979).

[2.4] H. D. Dakin Am. Chem. J. 42, 477,(1909).

[2.5] M. B. Hocking; and J.H. Ong; Can. J. Chem., 55, 102,(1977).

[2.6] R.H. Reeves; I.A. Pearl TAPPI, 48, 121,(1965).

[2.7] G. Gellerstedt; R. Angemo; Acta Chem.Scand, B34, 275 (1980).

[2.8] C.W. Bailey; C.W. Dence; TAPPI, 52, 491, (1969).

[2.9] S. Omori; Dence, C.W. Wood Sci.Technol. 15, 113,(1969).

[2.10] A.J. Nonni; C. W. Dence Holzforschung, 42, 37,(1969).

[2.11] R. Agnemo; G. Gellerstedt; Acta Chem. Scand., B34. 461,(1980).

[2.12] A. W. Kempf and C. W. Dence, TAPPI, 58(6),104-108,(1975).

[2.13] J. Gierer and F. Imsgard, Svensk Papperstidn., 80(14) 510-518 (1977).

[2.14] Aulin-Erdtman, Gunhild and R. Sandén. Acta Chem. Scand. 22: 1187-1209 (1968).

[2.15] K. J. Maa. Master's Thesis. Lakehead University, (1995).

[2.16] K. Lundquist; R. Simonson; K Tingswick. Svensk

Papperstid 9 272 (1979).
[2.17] H.D. Lûdemann and H. Nimz Biochem. Biophys.Res.Comm., 52(4),1162-1169,(1973).
[2.18]. B.D. Favis, P. M. K. Choi, P. M. Adler and D.A.I. Goring.Transactions, Technical Section, Canadian Pulp and Paper Association, 7, TR35 (1981).
[2.19] Garver, T. M. Jr.; Maa, K. J.; Xu, E. C. and D. G. Holah. Res. Chem. Intermed. 21(3-5) 503-519 (1995).

Chapter Three
Lignin Ionization and Adsorption

3.1 Introduction

Lignin derived compounds may contain methoxyl substituted phenolic structures and unsaturated propyl side chains that may be substituted with carbonyl, hydroxyl and carbonyl groups, conjugation of phenolic structure with olefinic and carbonyl moieties in the side chains is common. The ionization of phenolic hydroxyl and carboxylic moieties determines the pK_a of lignin, which in turn dominates features contributing to the hydrodynamic properties and solubility of lignin. Among the physical properties related to the ionization of lignin are solubility, adsorption on cellulose, conformation, hydrodynamic size and the extent of association. An understanding of the extent of ionization of lignin is critical to the study of lignin adsorption and removal on/from pulp. For example, in the following adsorption/desorption experiments, we found that the adsorption of lignin on pulp had a sudden increase at the dominated pK_a of the lignin.

Some useful techniques, such as light scattering, chromatography, viscosimetry, and tracer analysis, have been implemented to study lignin hydrodynamics. The problems of fractionation and purification due to association and adsorption on chromatographic media, the ubiquitous absorbence and fluorescence bands in light scattering [3.1] have been impeded their application. The deficiency of information of lignin hydrodynamics has led to the confusion about lignin's branching and conformation [3.2, 3.3]. In this study, two techniques, PFGNMR(Chapter 4) and UV-VIS titration have been employed to investigate lignin's

hydrodynamics.

There are many titration methods used in lignin studies. Because high pK_a phenolic OH-groups occur on lignin, direct titration with base needs nonaqueous solvents with a base character[3.4]. All these methods, including direct titration[3.4], potentiometric titration [3.5, 3.6, 3.7], conductometric titration [3.8, 3.9 3.10] and UV-VIS spectrometric titration, were first developed to determine phenol and carboxyl groups in lignin. Later, Mikawa et al performed the systematic studies of lignin model compounds' pK_a by conductometric titration [3.11, 3.12, 3.13, 3.14]. The drawback of potentiometric and conductometric titration is that a large amount of lignin (0.5-1.5 g)[3.15] and high concentration titrant(1.4 N-1.5 N LiOH) must be used [3.16]. Even the high frequency conductometry(HFC) method[3.17] is not practical in our experiment because some of our lignin preparations are only about 80 mg. On the contrary, the UV-VIS titration utilises a very small amount (0.5 mg) or very low concentration of lignin preparations (0.02 mg/ml). Because a very small amount of titrant(HCl) was used in the UV-VIS titration, the constant ionic strength during the titration can be maintained using ionic strength buffer solution(NaCl solution in our experiment).

From UV-VIS titration studies, we found that pK_as of model compounds and lignins depend on ionic strength greatly (Figure 3.4). Potentially, the measured pK_as of vanillin have different values when examined by different titration methods because the experiments were done at different, or varying, The high concentrations required for direct potentiometric and conductometric titrations would lead to lower pK_a values. Obviously, the UV-VIS titration doesn't have this problem. With the development of computer hardware and software, it makes it possible to extract the molecular

structure information, such as pK_a and absorption coefficients(ε) of every component of lignins and its model compounds in solution through fitting the titration curve. Furthermore, the molecular photon absorption cross section(σ) and molecular structure information of lignin and its model compounds may be deduced according to its absorption coefficient(ε) variation with ionic strengths(I). Because spectrometric titration is based on a bathochrome shift of the UV spectral band of phenol structure of lignin after ionization, only the pK_as and the absorption coefficients(ε) of phenol hydroxide can be determined by this method. This is the shortcoming of UV titration study.

3.2 Experiments

Stock solution was made by dissolving 50 mg lignin (kraft softwood, kraft hardwood or H_2O_2 bleached mechanical lignin or model compounds), which was weighted by an analytical balance (Metter® AE100 0.0001 g), into a 25 ml flask and then adding 0.1M NaOH solution to 25 ml. 0.25 ml the stock solution was put into a 25 ml flask using a 0.25ml syringe. Because the syringe is not accurate enough, the stock solution was weighted by an analytical balance to improve the accuracy. Different volumes (0, 0.1, 0.2,0.25, etc.) of 0.1 M HCl was added into the flask to adjust pH. 0.1 M NaCl was added to the volume for the purpose of keeping ionic strength in the solution constant.

The blank was made by adding 0.25ml 0.1M NaOH(without lignin) and the same amount of 0.1M HCl and 0.1M NaCl as that in the sample. In order to remove any possible errors, only two flasks (one used for the sample, one used for

blank) were used in the whole titration experiment. Because lignin and lignin model compound solutions are extremely sensitive to air and light, the one by one titration method was found to reduce the errors caused by exposure to air and light.

UV-VIS spectrum was obtained using CARY® 44 UV-VIS spectrometer, its measurement parameters were described in Chapter 2.

An ORION® Model 920 pH meter with an 8103 ROSS® combination pH electrode was used to measure pH of the solution. This pH meter was calibrated by three standard pH buffers, pH=12.604 ($Ca(OH)_2$ saturated at 20°C), pH=6.874 (0.025m KH_2PO_4 and 0.025 m Na_2HPO_4 at 20°C) and pH=4.645 (0.1m acetic acid and 0.1 m Na acetate at 20°C). The preparation and pH values of standard buffer are described in the following section. All titrations are conducted at room temperature(about 20 °C).

3.3 Results and Discussions

Hardwood, softwood and bleached mechanical lignins and some model compounds were titrated by UV-VIS spectrometry in our experiments.

pK_a of lignin model compounds

In order to explain lignin titration curves and pK_a measurements, two model compounds, 4-hydroxy-3-methoxybenz-aldehyde (vanillin), and 4- hydroxy - 3-methoxybenzyl alcohol (vanillyl alcohol) were titrated by UV-VIS spectrometry. Figure 3.1 is UV-VIS spectrum of vanillin at different pH values. Figure 3.1 shows the bathochrome shift

of vanillin's UV spectrum upon ionization. The isosbestic point is where all UV-VIS meet and the isosbestic point of vanillin is 317 nm. The isosbestic point is a necessary condition to prove that there are only two absorbing substances in the equilibrium. Figure 3.2 is the UV-VIS difference spectrum of vanillin. Figure 3.3 is vanillin's titration curves at 0.1M, 1M and 3M NaCl solution. From Figure 3.3, we can find that different titration curves have different curve rates.

pK_a can be calculated according to following equations from fitting titration curves.

According to the Beer-Lambert's Law:

$$A=\varepsilon bc \qquad \text{(Equ. 3.1)}$$

Where

A is absorbence.

ε is the extinction coefficient.

C is the concentration.

b is the length of the cell.

Because the absorbence (A) of vanillin at any wavelength contains two components, one is from vanillin (HA) and the other is from its salt(A^-), so

$$A = \varepsilon_{[HA]}bc_{[HA]} + \varepsilon_{[A^-]}bc_{[A^-]} \qquad \text{(Equ. 3.2)}$$

Where $c_{[HA]}=f[HA]*c$

$c_{[A^-]}= f[A^-]*c$

$f[HA], f[A^-]$ ($f[HA]+f[A^-]=1$) are distribution factors of HA and A^- in the solution.

$$f[HA]=[HA]/([HA]+[A^-])=K_a/([H^+]+K_a) \quad \text{(Equ.3.3)}$$

$$f[A^-]=[A^-]/([HA]+[A^-])=1-K_a/([H^+]+K_a) \quad \text{(Equ. 3.4)}$$

Because we always use an isosbestic point to divide the absorbance(A), which only depends on the concentration of the sample, after substituting all the equations into Equation 3.2, we can get

$$A/A_{isos} = m_1*f[HA] + m_2*f[A^-]$$

$$=m_1*K_a/([H^+]+K_a) +m_2*[1-K_a/([H^+]+K_a)] \quad \text{(Equ. 3.5)}$$

Where $m_1 =(c*\varepsilon_{[HA]})/A_{isos}$

$m_2 =(c*\varepsilon_{[A-]})/A_{isos}$

Through titration curve fitting, we can calculate m_1, m_2 and pK_a, while m_1 and m_2 are directly related to the extinction factors ($\varepsilon_{[HA]}$ and $\varepsilon_{[A-]}$). Linda et al [3.14] proved that the extincton coefficient (ε) is related directly to its absorption cross section(σ). From Table 3.1, the change of vanillin's cross section from 0.1M NaCl solution to 1M NaCl solution is very small, it shows that vanillin has a sphere shape and it has the smallest surface area, so it is hard to change its shape when ionic strength varies.

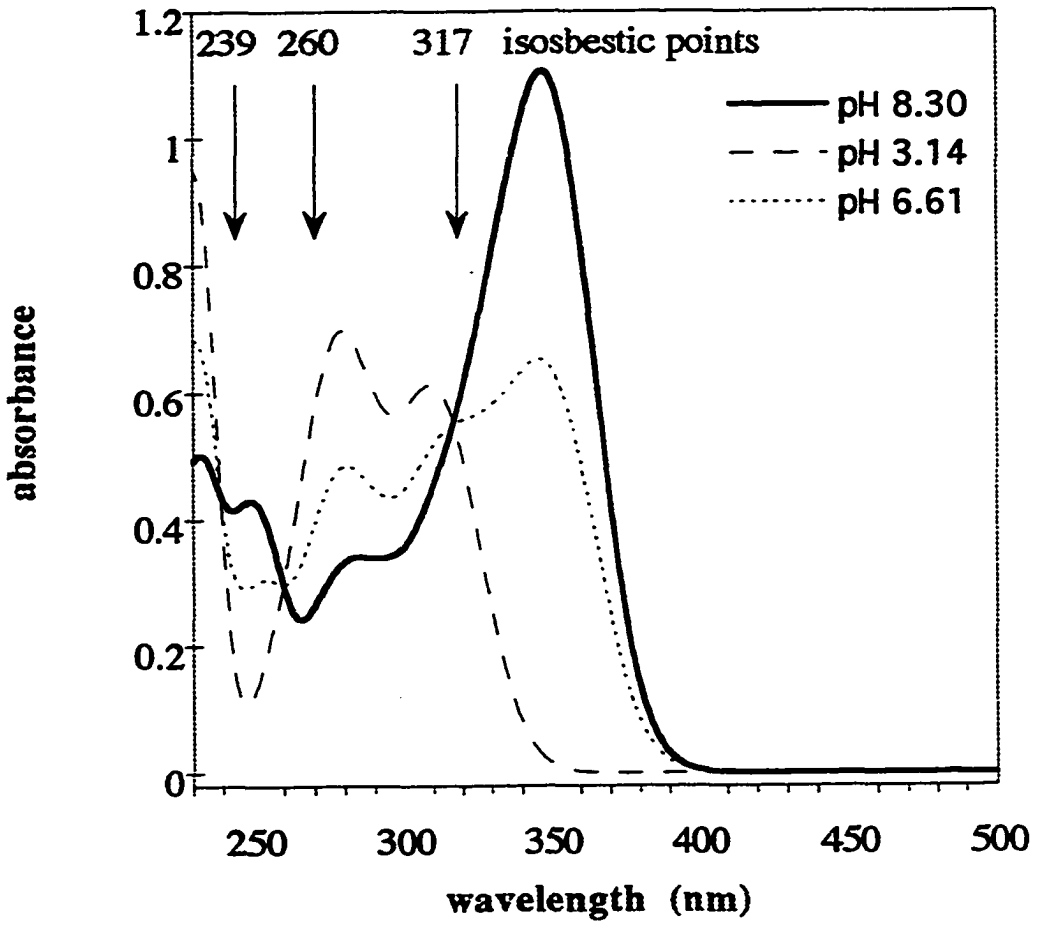

Figure 3.1 UV-VIS spectra of vanillin at different pH values.

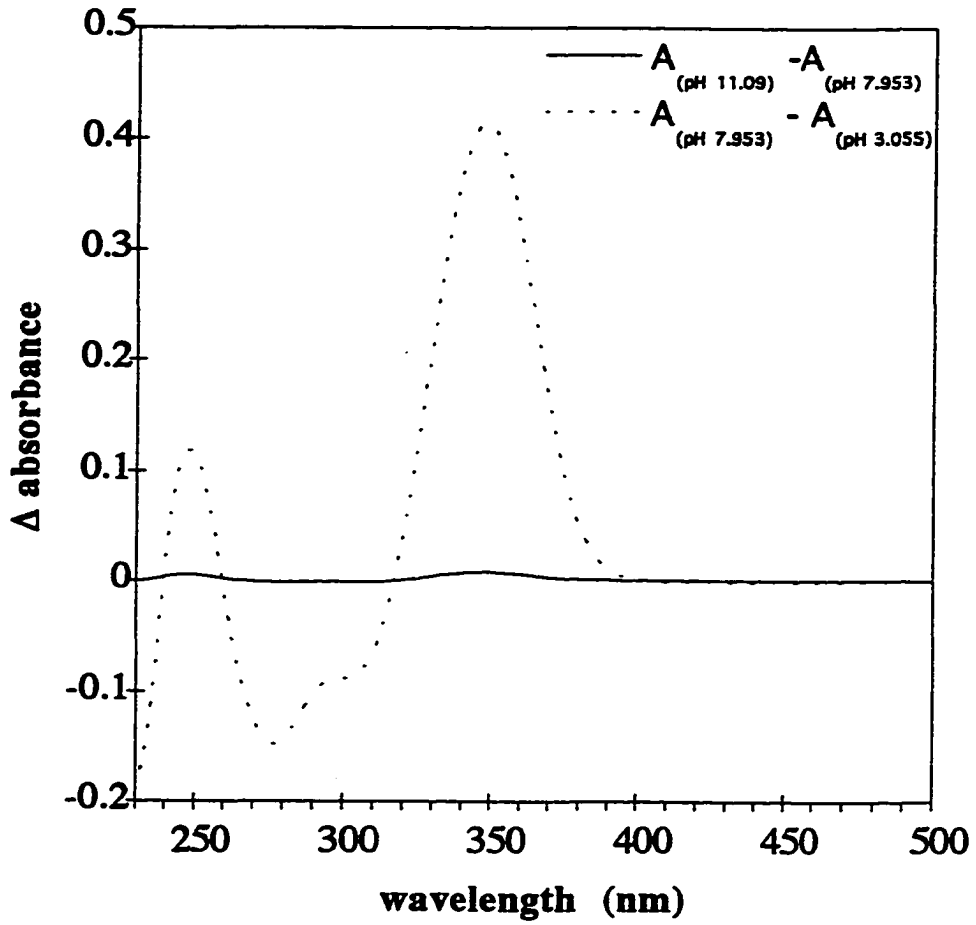

Figure 3.2 UV-VIS difference spectra of vanillin.

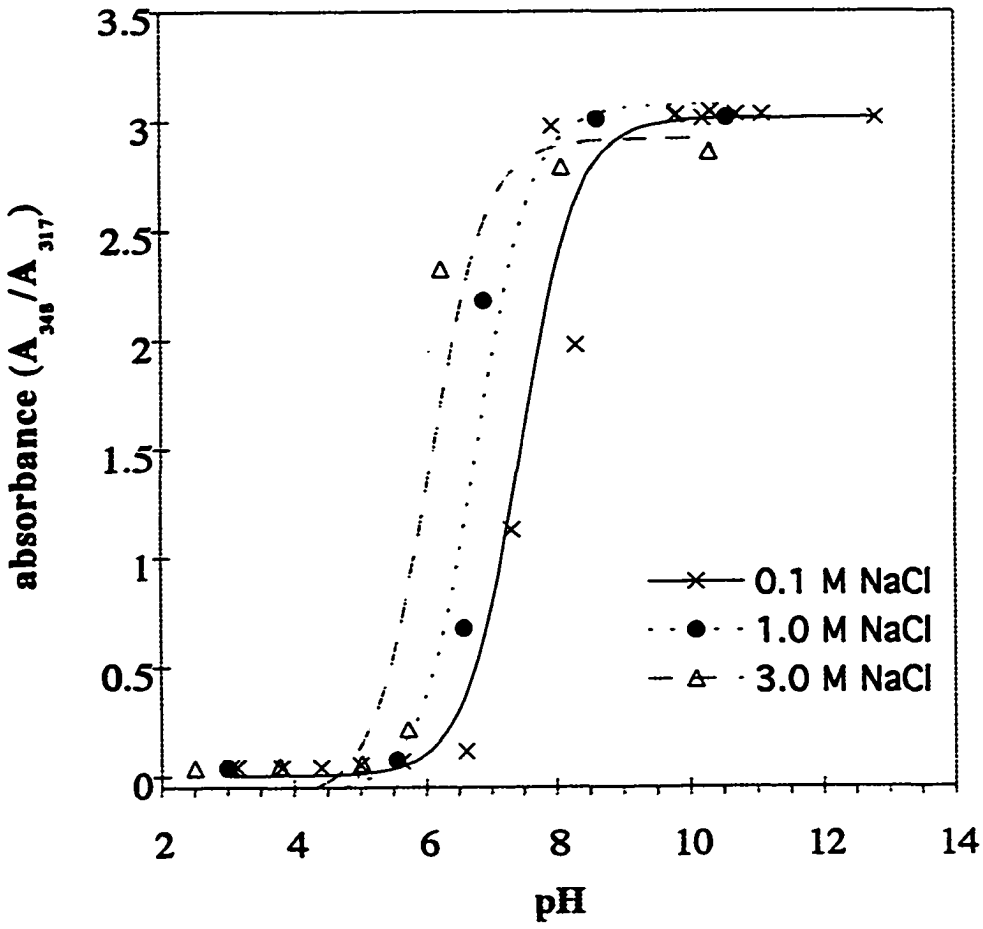

Figure 3.3 Vanillin's titration curve in 0.1 M NaCl solution by UV-VIS.

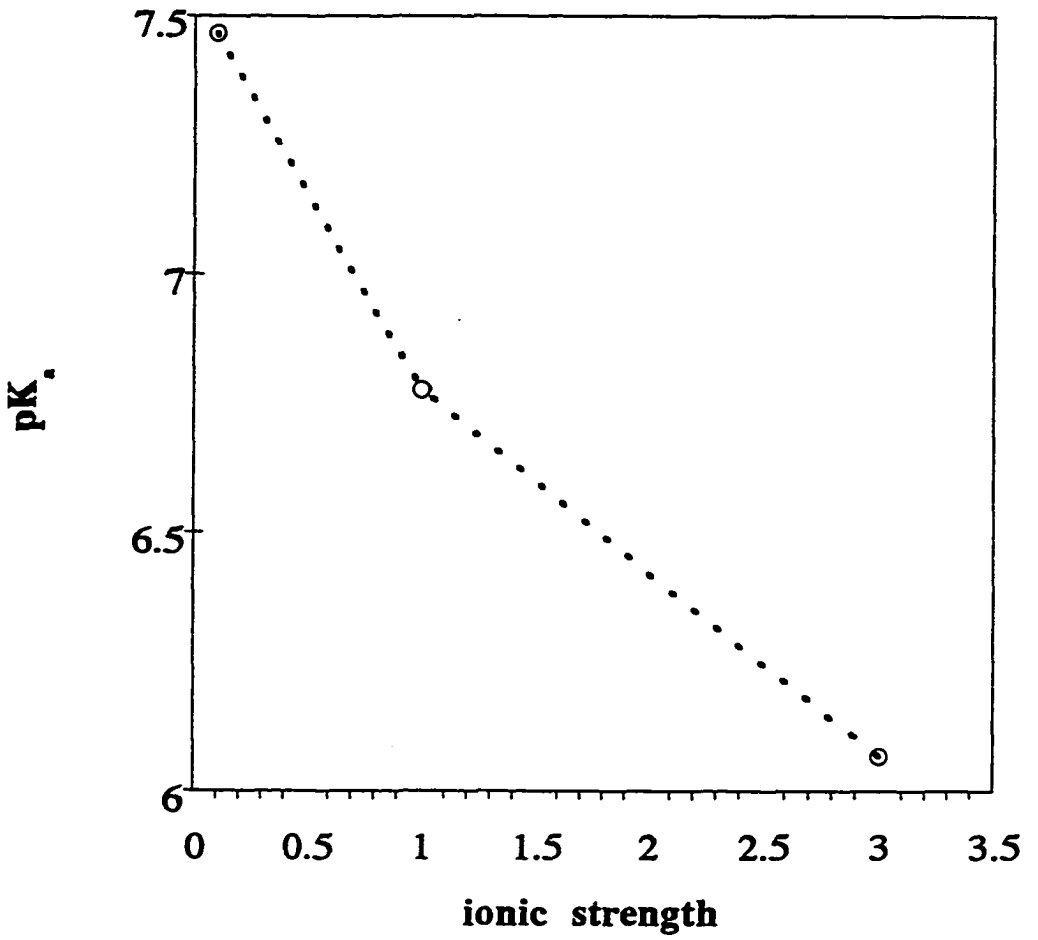

Figure 3.4 Vanillin's pKa value vs. ionic strength.

Table 3.1 Calculation Results of Vanillin

A/A_{isos}	m1	m2	pK_a
348nm/317nm 0.1MNaCl	3.0138	.0046283	7.466
1MNaCl	3.0735	-.075667	6.7772
3MNaCl	2.917	-0.1035	6.0677
297nm/317nm 0.1MNaCl	.39549	1.0271	7.3019
1MNaCl	.39547	1.0276	6.7651
3MNaCl	.55984	1.0757	6.0549
277nm/317nm 0.1MNaCl	.21058	1.2454	7.3114
1MNaCl	.18732	1.2679	6.7683
3MNaCl	.1538	1.3443	6.056
247nm/317nm 0.1MNaCl	1.0496	.2145	7.332
1MNaCl	1.104	.15563	6.7792
3MNaCl	1.0743	.16259	6.058

As pointed out above, the ionic strength in the solution is hard to control in the direct titration, or any other method which employed a titrant. We found that pK_a of vanillin change from 7.46 in 0.1M NaCl to 6.0677 in 3M NaCl solution (Figure 3.4). Vanillin's pK_a has about 1.4 decrease when ionic strength increases from 0.1M NaCl to 3M NaCl. If the curve in Figure 3.4 were extrapolated to zero M NaCl, vanillin's pKa would be about 7.55. It is predictable that the measured pKa varies according to its titration method. In literature, vanillin's pKa has been measured as 7.30 ± 0.03[3.4], 7.40[3.18] and 7.45[3.19]. Most likely, the variation of pKa is resulting from the variation of solution's ionic strength variations.

Figure 3.6 shows the UV-VIS spectra of 4-hydroxy -3-methoxybenzyl alcohol or vanillyl alcohol II. The isosbestic

point of 4-hydroxy -3-methoxybenzyl alcohol is 233.5nm. Figure 3.5 is UV-VIS spectra of 4-hydroxy-3-methoxybenzyl alcohol at different pH values. Figure 3.6 is the difference spectra rusulting from the subtraction of the absorbance for 4-hydroxy-3-methoxybenzyl alcohol at 4.5 from that of an identical concentration of the compound at pH 13.0. Figure 3.7 is the titration curve of 4-hydroxy-3-methoxy-benzyl alcohol in 0.1 M NaCl solution. Literature values for the pK_a of 4-hydroxy-3-methoxybenzyl alcohol has been measured as 9.76 ± 0.03 [3.1] and 10.19[3.20].

Table 3.2 Calculation results for vanillyl alcohol at different ionic strengths.

nm/nm	NaCl	pK_a	m1	m2
295/	0.1M	9.7953	0.77917	0.031758
233.5	1.0M	9.5032	0.76667	0.074706
249/	0.1M	9.7373	1.8362	0.11959
233.5	1.0M	9.5015	1.8844	0.21334

Titration of Softwood and Hardwood Kraft Lignin

Softwood kraft lignin in 0.1M, 0.5M, 0.8M, 1M, 1.2M and 2.0M NaCl solution has been titrated by UV-VIS spectrometry. Figure 3.8 is UV-VIS spectrum of softwood kraft lignin at different pH values. There is no true isosbestic point for lignin because lignin has more than one kind of titratable group. Figure 3.9 is UV-VIS difference spectra of softwood lignin at different pH. Figure 3.10 is the titration curves for softwood kraft lignin at different pH values.

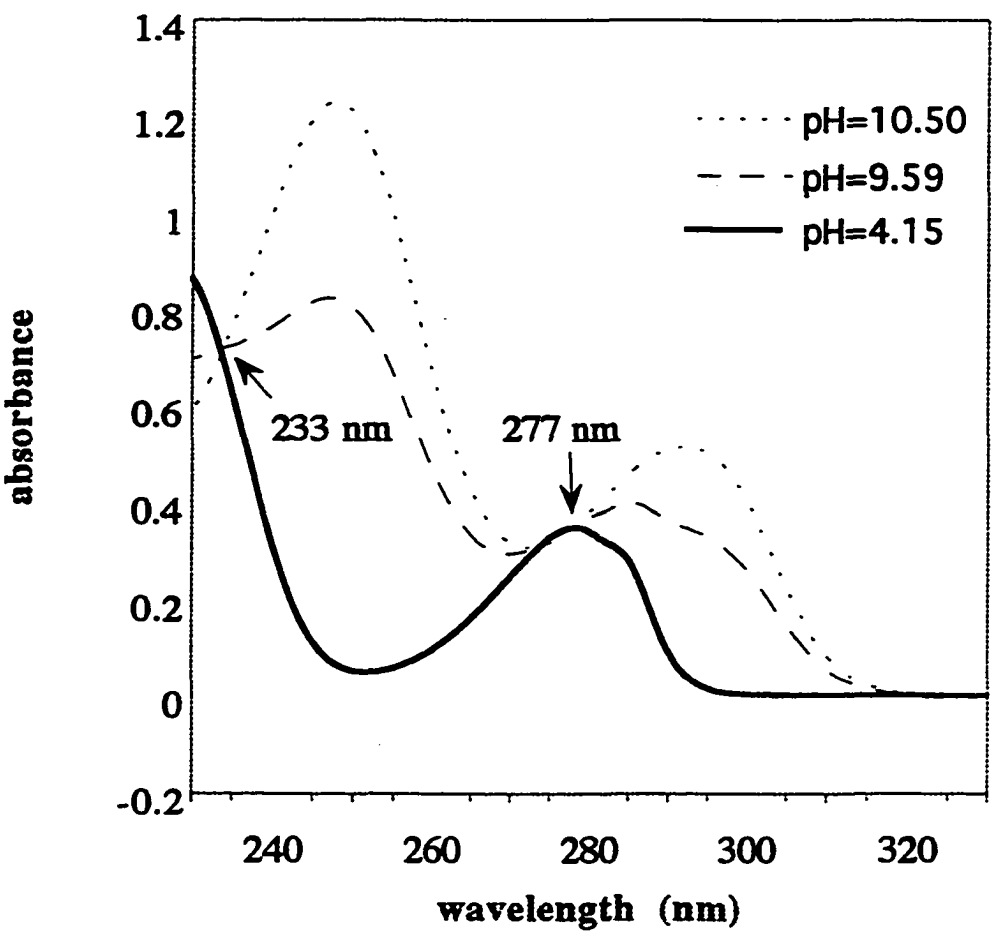

Figure 3.5 UV-VIS spectra of 4-hydroxy-3-methoxybenzyl alcohol.

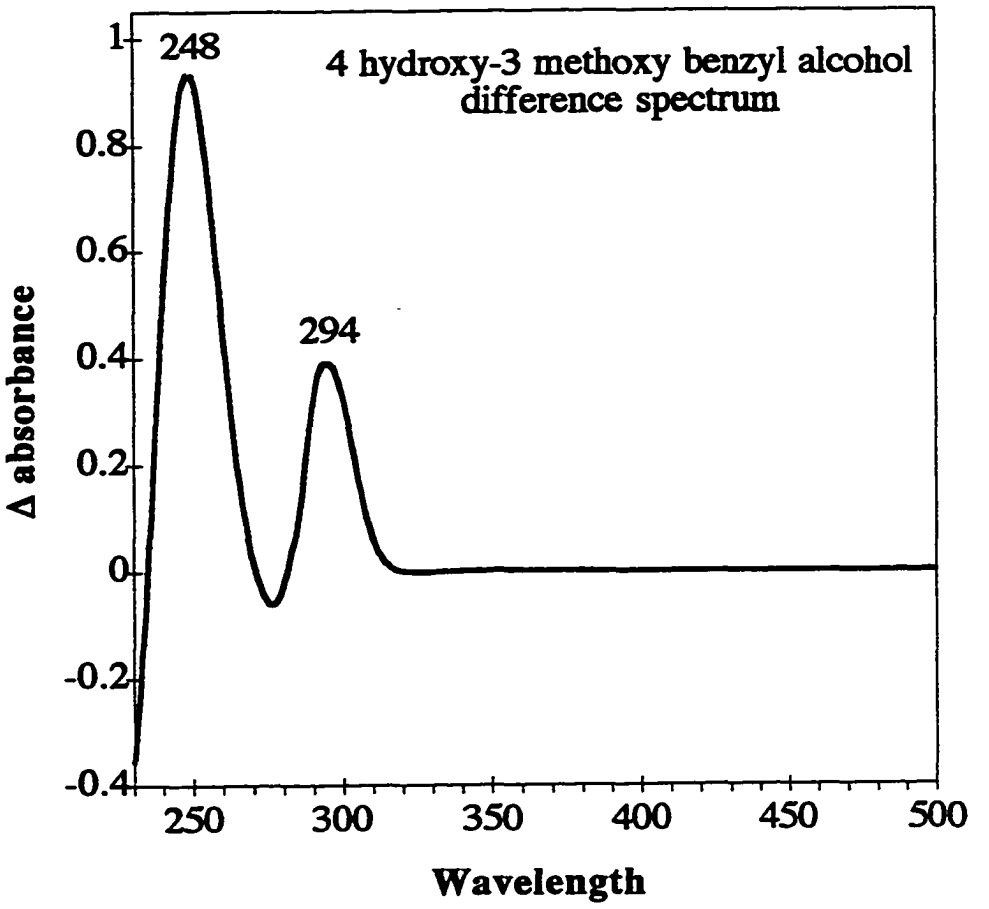

Figure 3.6 UV-VIS difference spectra of 4-hydroxy-3-methoxybenzyl alcohol

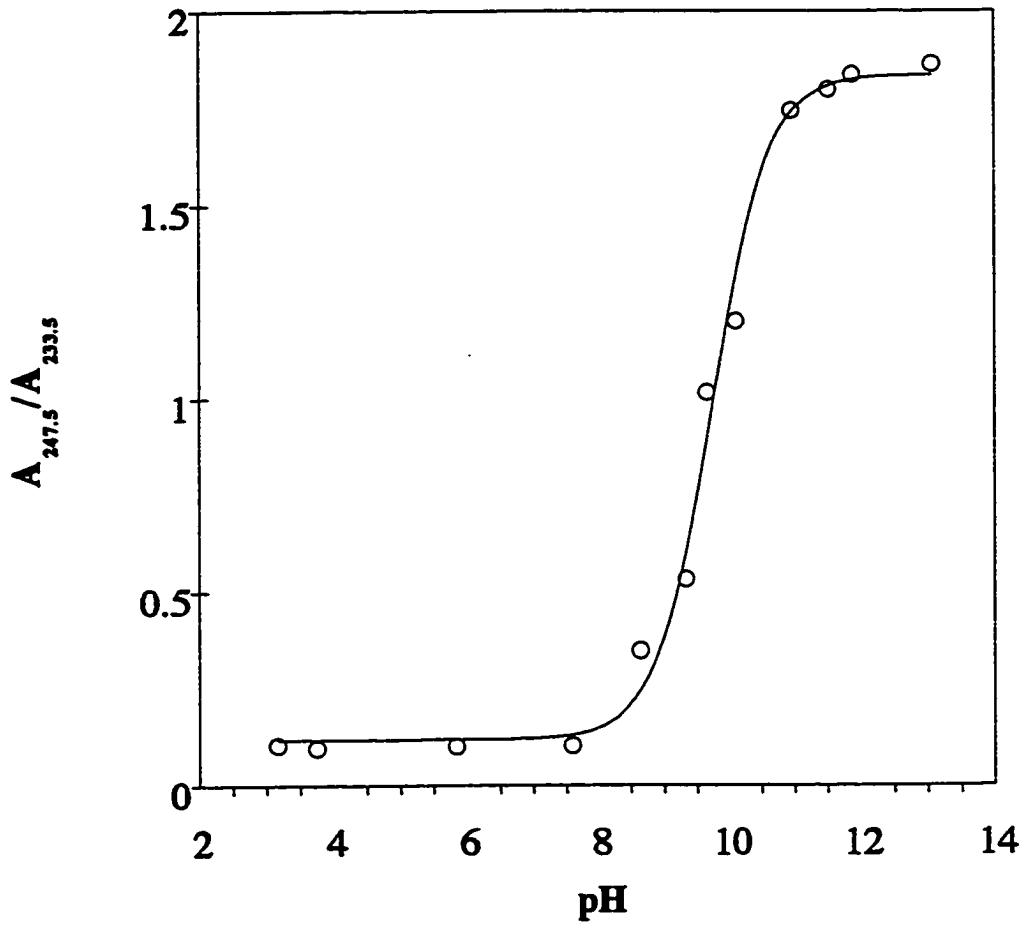

Figure 3.7 The titration curve of 4-hydroxy-3-methoxybenzyl alcohol in 0.1M NaCl solution by UV-VIS

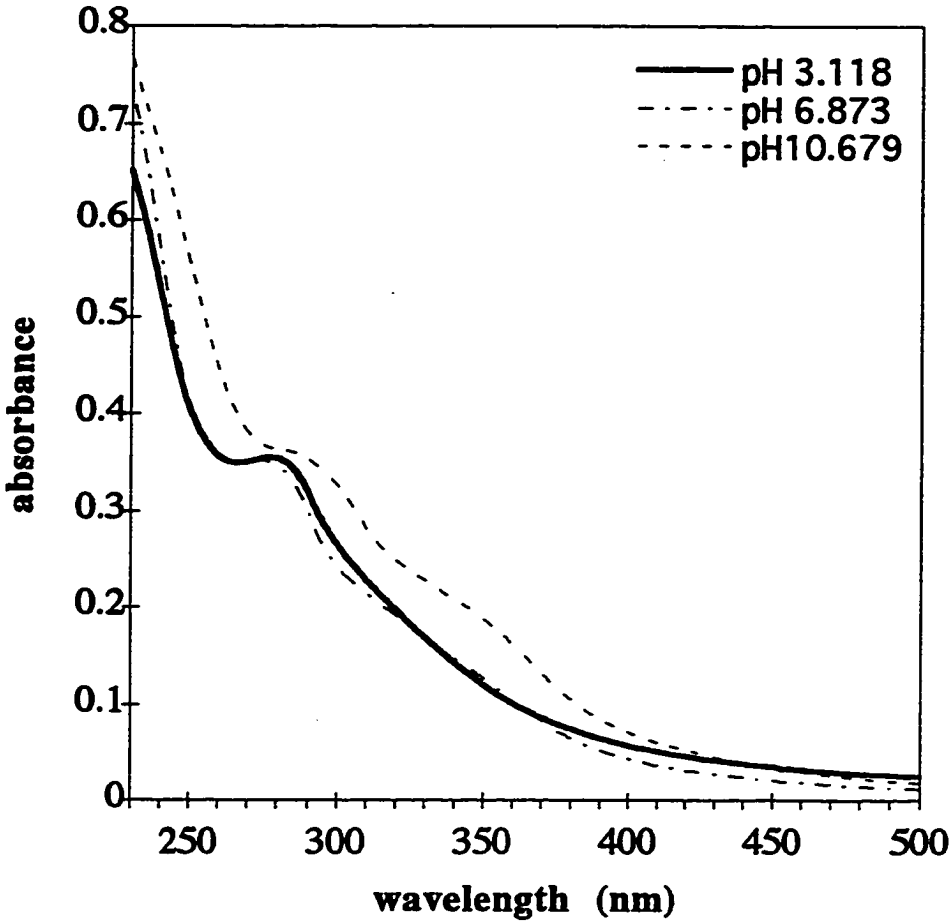

Figure 3.8 UV-VIS spectra of softwood lignin at different pH

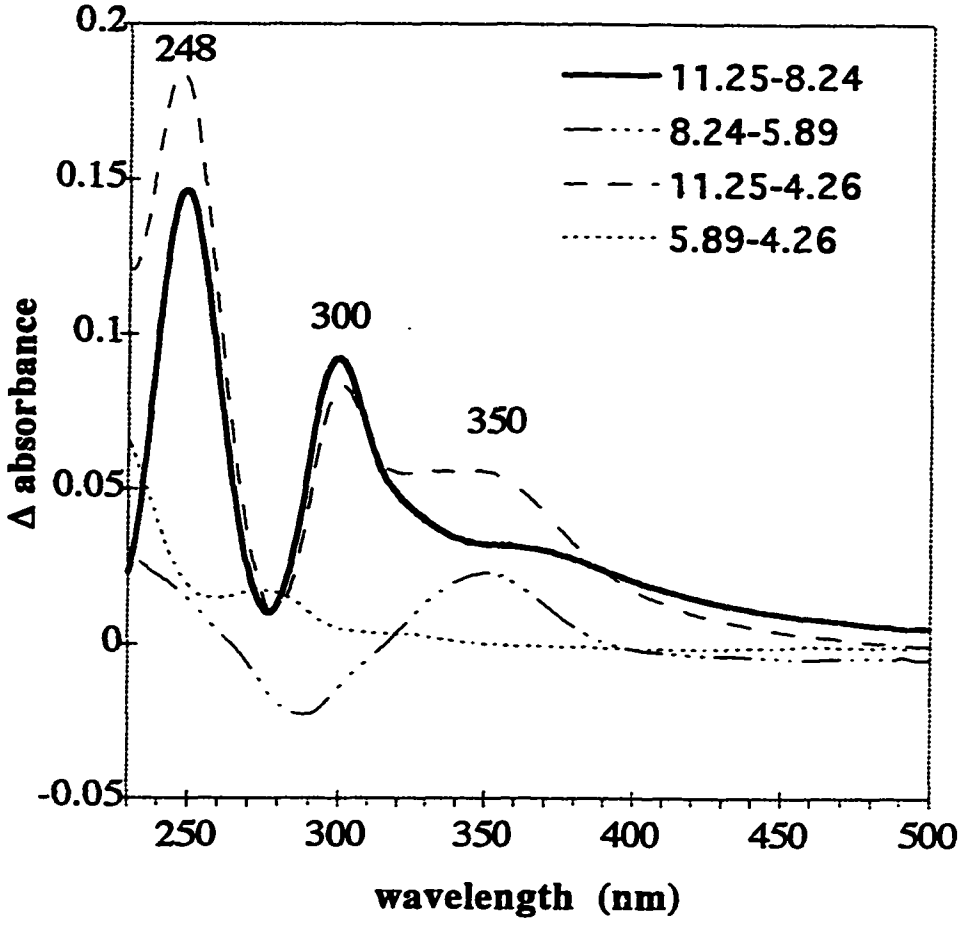

Figure 3.9 UV-VIS difference spectra of softwood lignin in 0.1M NaCl solution

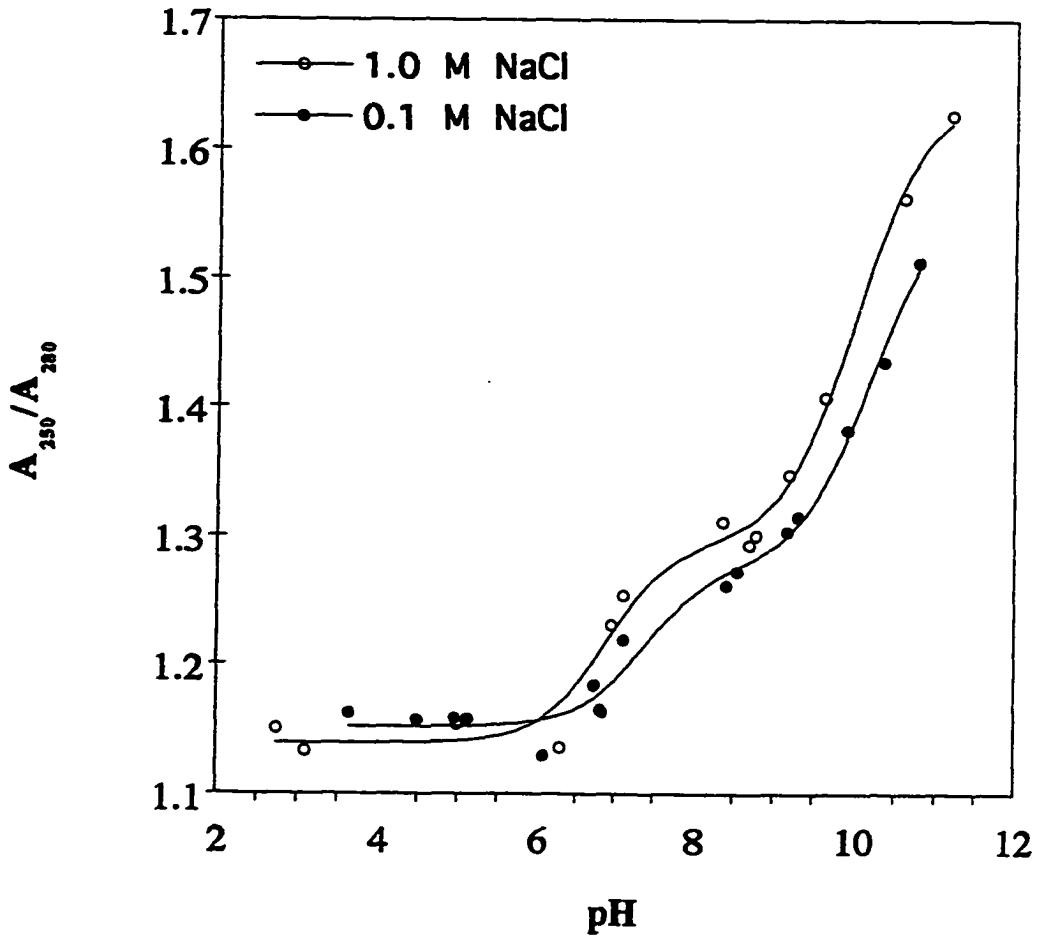

Figure 3.10 The titration curve of softwood lignin in 0.1 M NaCl solution by UV-VIS

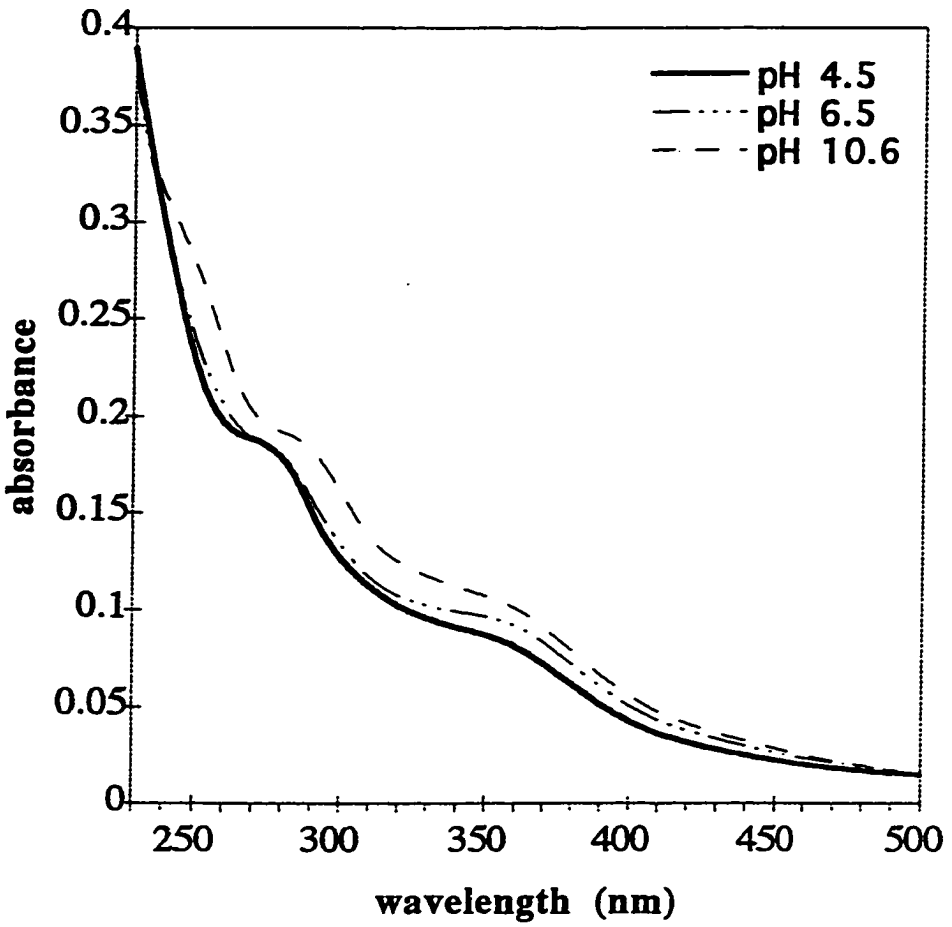

Figure 3.11 UV-VIS spectra of hardwood lignin at different pH values.

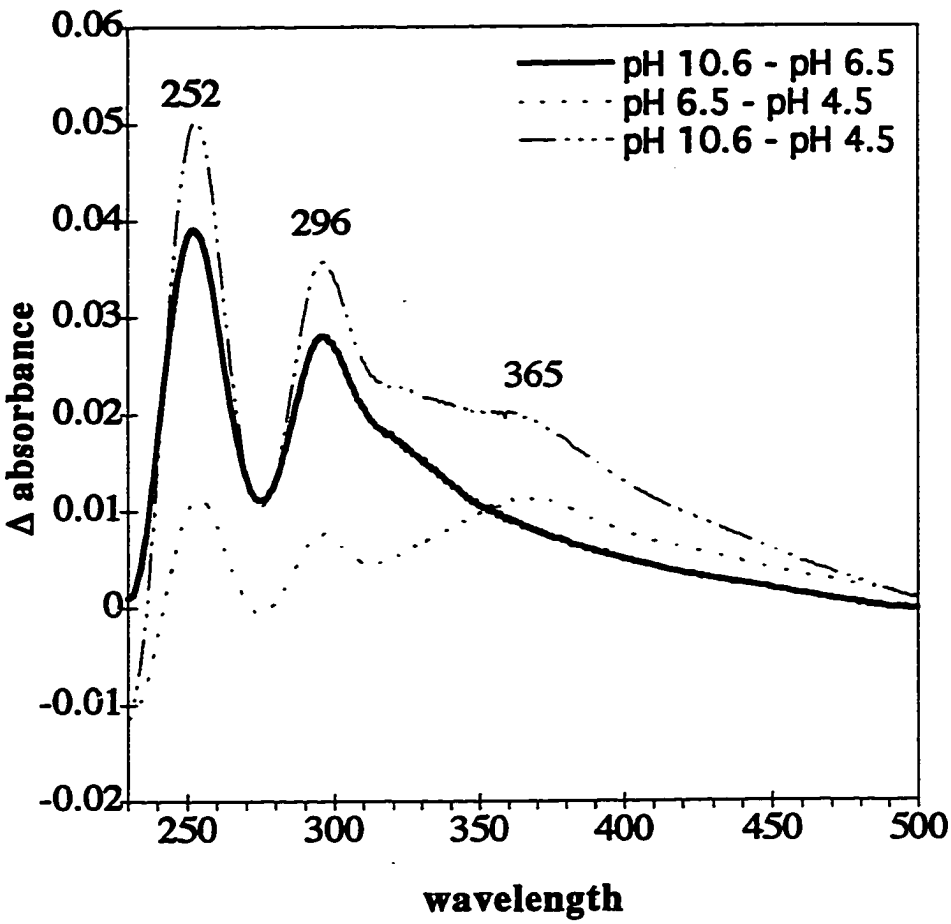

Figure 3.12 UV-VIS difference spectra of kraft hardwood lignin in 0.1 M NaCl solution.

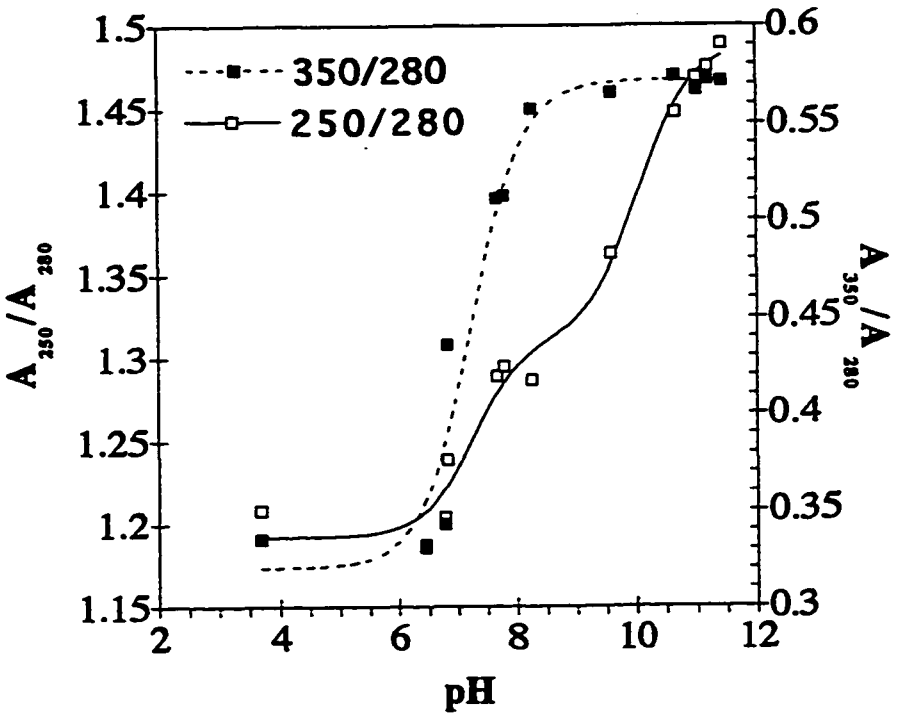

Figure 3.13 The titration curve of kraft hardwood lignin in 0.1M NaCl solution by UV-VIS.

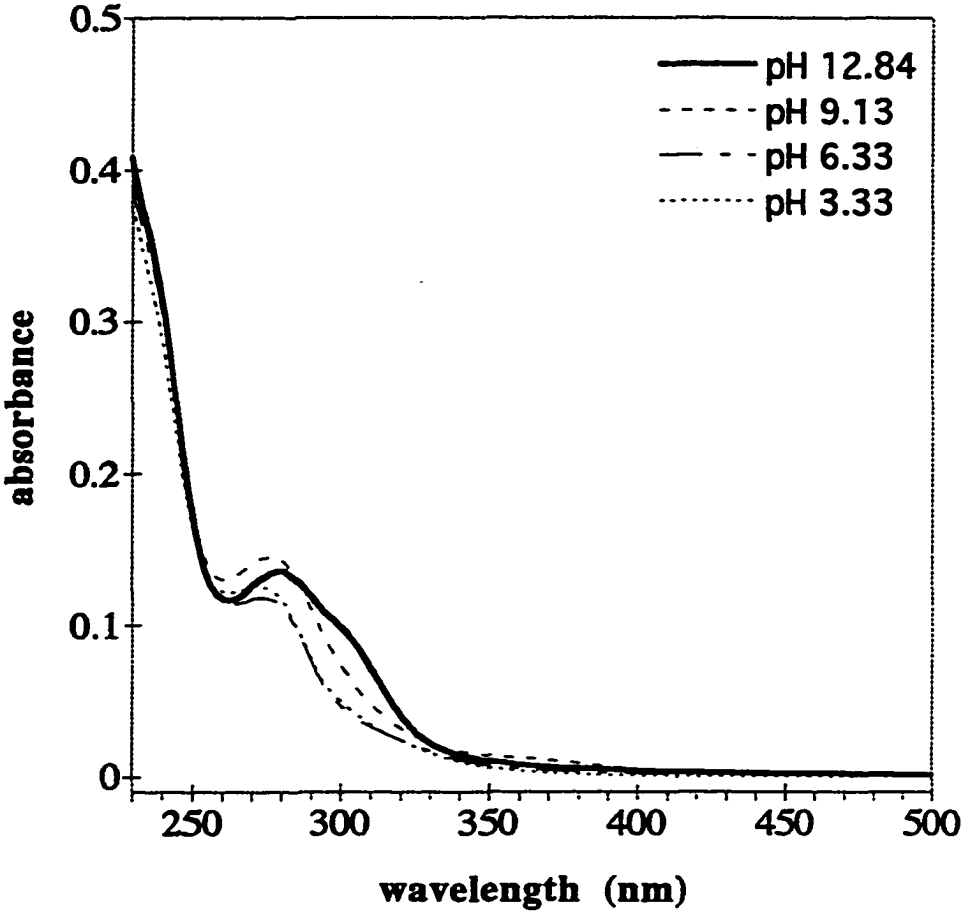

Figure 3.14 UV-VIS spectra of bleached lignin at different pH values.

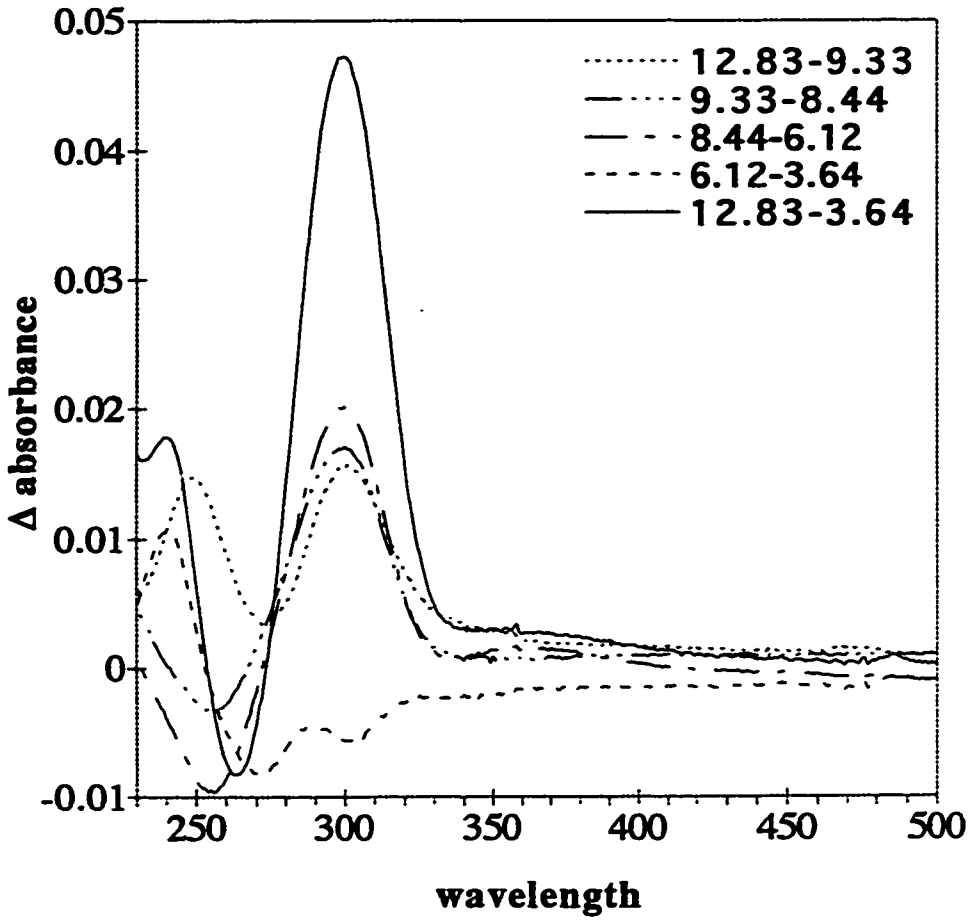

Figure 3.15 UV-VIS difference spectra of bleached lignin in 0.1 M NaCl solution.

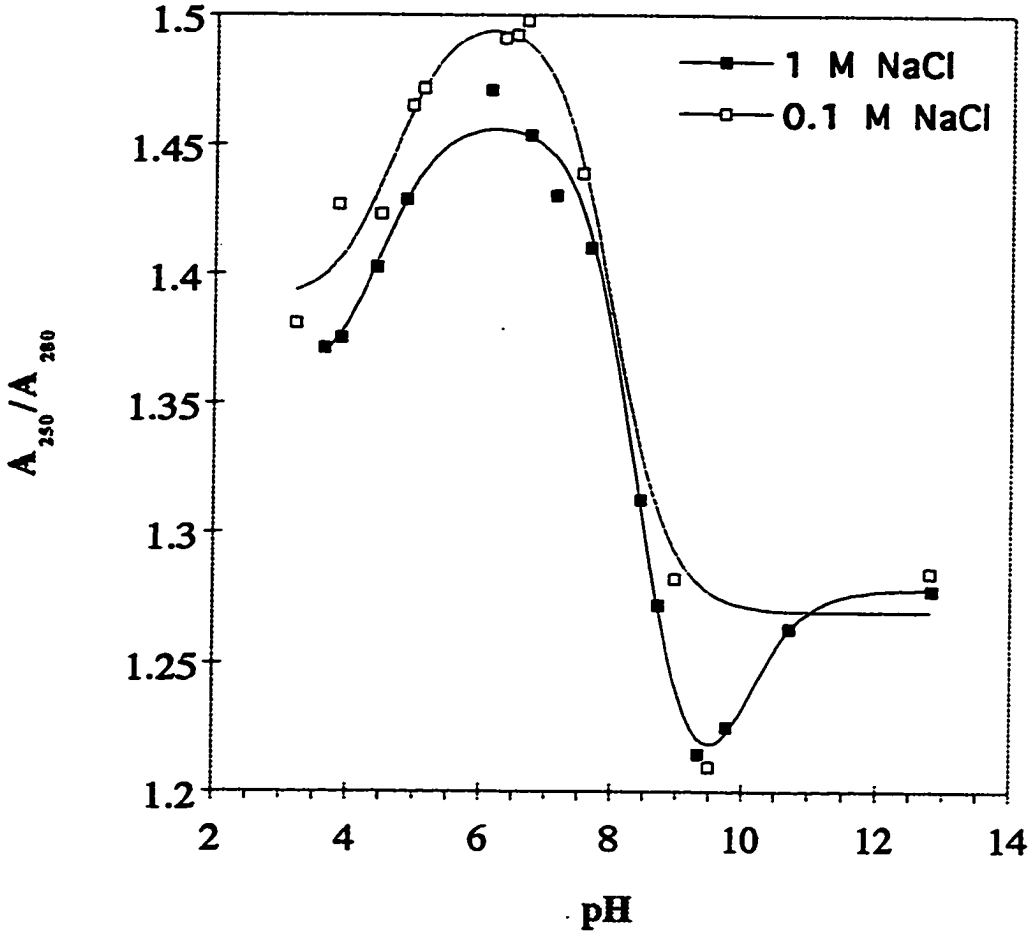

Figure 3.16 The titration curve of bleached lignin in 0.1 M NaCl solution by UV-VIS.

The titration curve shown in Figure 3.10 argues that softwood kraft lignin has two dominate pK_a values that correspond to two main different types of phenol hydroxyl groups (HA and HA') on lignin. One is vanillin type and the other is 4-hydroxy-3-methoxybenzyl alcohol type. Because there are two kinds of phenol hydroxyl in the solution, the absorbance consists of
4 components.

$$A=m1*f[HA] + m2*f[A^-] + m4*f[HA'] + m5*f[A'^-] \quad \text{(Equ.3.6)}$$

Variables f[HA], $f[A^-]$, f[HA'] and $f[A'^-]$ are distribution factors as in equations 3.2 and 3.3.

$$f[HA]=[HA]/([HA]+[A^-])=K_{a1}/([H^+]+K_{a1}) \quad \text{(Equ.3.7)}$$

$$f[A^-]=[A^-]/([HA]+[A^-])=1-K_{a1}/([H^+]+K_{a1}) \quad \text{(Equ.3.8)}$$

$$f[HA']=[HA']/([HA']+[A'^-])=K_{a2}/([H^+]+K_{a2}) \quad \text{(Equ.3.9)}$$

$$f[A'^-]=[A'^-]/([HA']+[A'^-])=1-K_{a2}/([H^+]+K_{a2}) \quad \text{(Equ. 3.10)}$$

Variables m_1, m_2, m_4, m_5 and pK_a1, pK_a2 can be calculated according to eq. 3.6 through fitting titration curves. Table 3.3 and Figure 3.10, 3.13 are the calculated results for softwood and hardwood kraft lignin. Table 3.3 shows the calculated results of m_1, m_2, m_4, m_5 and pK_{a1}, pK_a2 of softwood lignin in 0.1M and 1M NaCl solutions.Table 3.3 indicates that m_1, m_2, m_4, m_5 and pK_{a1}, pK_a2 fluctuate compared with that of model compounds. They have the smallest value in 1 M NaCl solution. These results indicate that lignin has the irregular shape.

The ratios used for the calculation of pK_a values provide better fits to the data than the absorbance values simply corrected for concentration. Shown in Figure 3.13 are the

relative absorbance values for hardwood kraft lignin at 250 nm, and 350 nm with respect to 280 nm. These values plotted are the absorbance values at all pH derived by the absorbance at high pH. The standard deviation of the values at 280 nm is 1% while the standard deviation of values at 250 nm and 350 nm is 7.8% and 13.8%. The absorbance at 250 nm is sensitive to ionization of all phenolic groups. The absorbance at 350 nm is particularly sensitive to ionization of carbonyl conjugated phenolic groups which occurs around 7.

Hardwood kraft lignin has the same properties as softwood kraft lignin. Figure 3.11 is a hardwood lignin spectrum. Figure 3.12 is difference UV-VIS spectrum of hardwood lignin. Figure 3.13 is the titration curve of hardwood lignins at different pH.

Figure 3.14 in the UV spectra of hardwood bleached effluents at different bleaching times (standard condition). Figure 3.16 shows pH difference spectra for peroxide generated effluent. The spectra generated by subtracting the bleaching effluent absorbance at 61 minutes from the absorbance of the effluents at 11 minutes is similar to the pH difference spectrum. This indicates the titration of phenolic groups is important in the bleaching process. The loss of carbonyl groups at 350 nm is also evident by from these difference spectra.

Table 3.3 Hardwood and softwood lignins

	Hardwood 0.1 M NaCl	Hardwood 1M NaCl	Softwood 0.1 M NaCl	Softwood 1M NaCl
m_1	.47657	.46427	.47182	.3949
m_2	.61011	.58461	.5975	.5377
pK_{a1}	7.833	7.2661	7.4037	6.726
m_4	.71218	.7277	.68035	.7405
m_5	.91366	.90414	.96999	1.0669
pK_{a2}	10.244	10.049	10.19	9.833

3.3.3 pKa of peroxide bleached lignin

The bleached hardwood lignin was prepared from the bleaching effluents described in Chapter 2. Figure 3.14 is the UV spectrum of bleached lignin in solution. Figure 3.15 is the pH difference spectrum of bleached lignin. This spectrum shows that its structure has changed after bleaching. From difference spectrum, after bleaching, the 365 nm peak has almost disappeared; the 296 nm peak shifted to 300 nm and intensified greatly; the 252 nm peak shifted to around 245 nm and its intensity reduced.

The bleached lignin has three pK_as from its titration curve. In 0.1 M NaCl solution, its pK_{a1} is 4.64, pK_{a2} is 8.01 and pK_{a3} is 10.01 while in 1M NaCl solution, pK_{a1} is 4.49, pK_{a2} is 8.38 and pK_{a3} is 9.99. From model compound study, pK_{a1} corresponds to muconic acid XIX(pK_a=4.66±0.13); pK_{a2}

corresponds to propiovanillon IX(pK_a=8.05±0.07); pK_{a3} corresponds to vanillyl alcohol(pK_a= 9.76 ±0.03)[3.4].

3.4 Study of Lignin Adsorption to Pulp

3.4.1 Introduction

Lignin removal from pulp has been studied by a lot of researchers [3.19, 3.20, 3.21,3.22]. Goring [3.23] has found that the transfer of lignin from pulp to solution occurs in two distinctly different phases:

1). A rapid phase(seconds) during which dissolved matter is removed from the fibre surface and the lumen

2). A slow phase(hours) during which macromolecules, mainly lignin, diffuse from the fibre wall into the surrounding liquid.

This kind of studies have concluded that the rate of removal of lignin was governed by the diffusion of lignin macromolecules through the fibre wall into the liquid. The diffusion coefficients in this process are in the range of 10^{-17} -10^{-19} m^2 s^{-1}, which is 6-8 magnitude lower than those of free diffusion. All these studies ignored the lignin adsorption to pulp.

There are some studies on the adsorption of synthetic polymers onto pulp [3.24, 3.25]. In our removal and adsorption experiment, the lignin adsorption to pulp is

obvious from our experiments. According to our experiments, it is incomplete without studying the adsorption in the study of lignin removal process.

3.4.2 Experiments

In this experiment, 4 stock solutions were made as follows.

1. Lignin stock solution(A): 50 mg lignin in 1000 ml buffer solution.
2. Pulp stock solution(B): 250g pulp in 1000 ml pH buffer solution.
3. Salt solution(C): 4M NaCl in pH buffer.
4. Buffer solution (D)

pH Buffer solutions

a) 0.05 m potassium hydrogen phthalate, 10.12g $KHC_8H_4O_4$ in 1000 ml distilled water, PH = 4.04(at 20 °C);

b) 0.01 m (borax) sodium bicarbonate, 3.80 g $Na_2B_4O_7.H_2O$ in 1000 ml distilled water, pH = 9.183(at 20 °C);

c) 0.025m sodium bicarbonate + 0.025 M sodium carbonate, pH = 10.014, 2.092g Na_2HCO_3+ 2.640g Na_2CO_3 in 1000 ml distilled water;

d) calcium hydroxide (saturated at 25 °C), pH=12.454;

10 ml stock solution A and 10 ml stock solution B were put in the flask, then different amount stock solutions C and D were put into the same flask. But solution C + D = 20 ml. All the solutions mixed well. These flasks were sealed by parifilm and put in bath (60 °C) for 4 hours.

Before UV measurement, the solution was filtered by 0.45 micron syringe filter in order to remove any interference of the particles. UV spectrometry were obtained by CARY®. The measurement parameters are the same as those used for titration(Chapter 3). The blank has the same ionic strength and pH as that in the sample.

3.4.3 Results and Discussion

The adsorption of lignin to pulp is hard to observe directly because lignin removal from pulp dominates under the some conditions. A simple experiment can be used to show the lignin adsorption to pulp. 2 g pulp and lignin stock solution in pH = 9.1 were put together in a 50 ml flasks(A), 2g pulp in pH (9.1) buffer(B) and the lignin stock solution (C) were put in two 50ml flasks separately. All these three flasks were heated in a 60 °C bath for 4 hours.

If there is no adsorption at all, the UV-VIS absorbance of solution A should be equal to that of solution B plus solution C ($A_A=A_B + A_C$). In fact, from Figure 3.17, $A_A < A_B + A_C$, obviously, this lignin loss is resulted from lignin

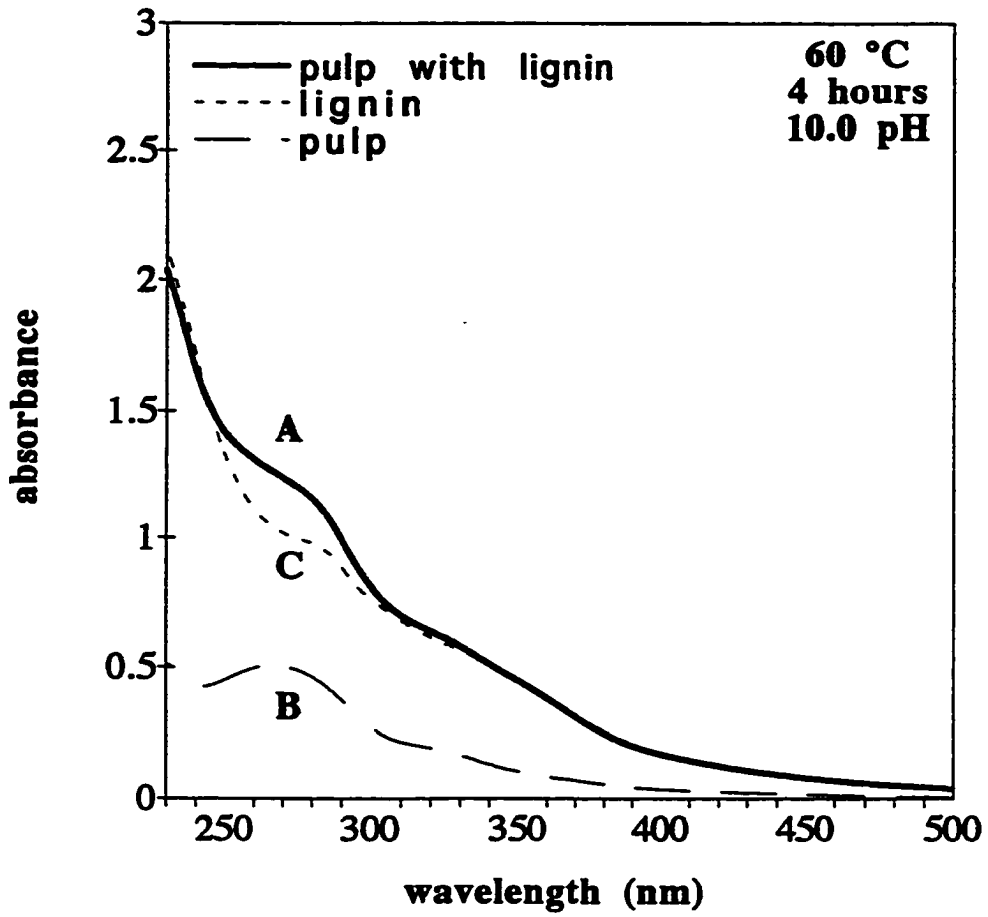

Figure 3.17 UV absorbance of softwood kraft lignin solutions with and without cellulose.

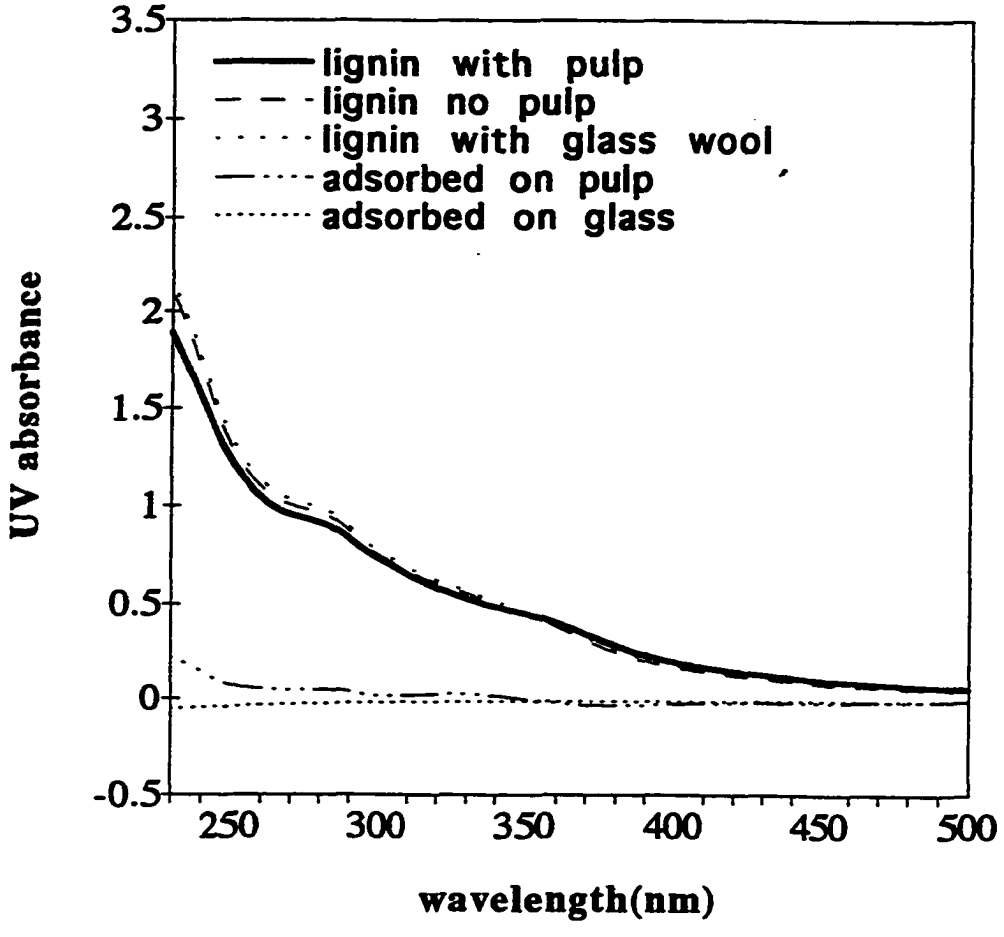

Figure 3.18 UV absorbance of softwood kraft lignin solutions in equilibrium with different solid adsorbants.

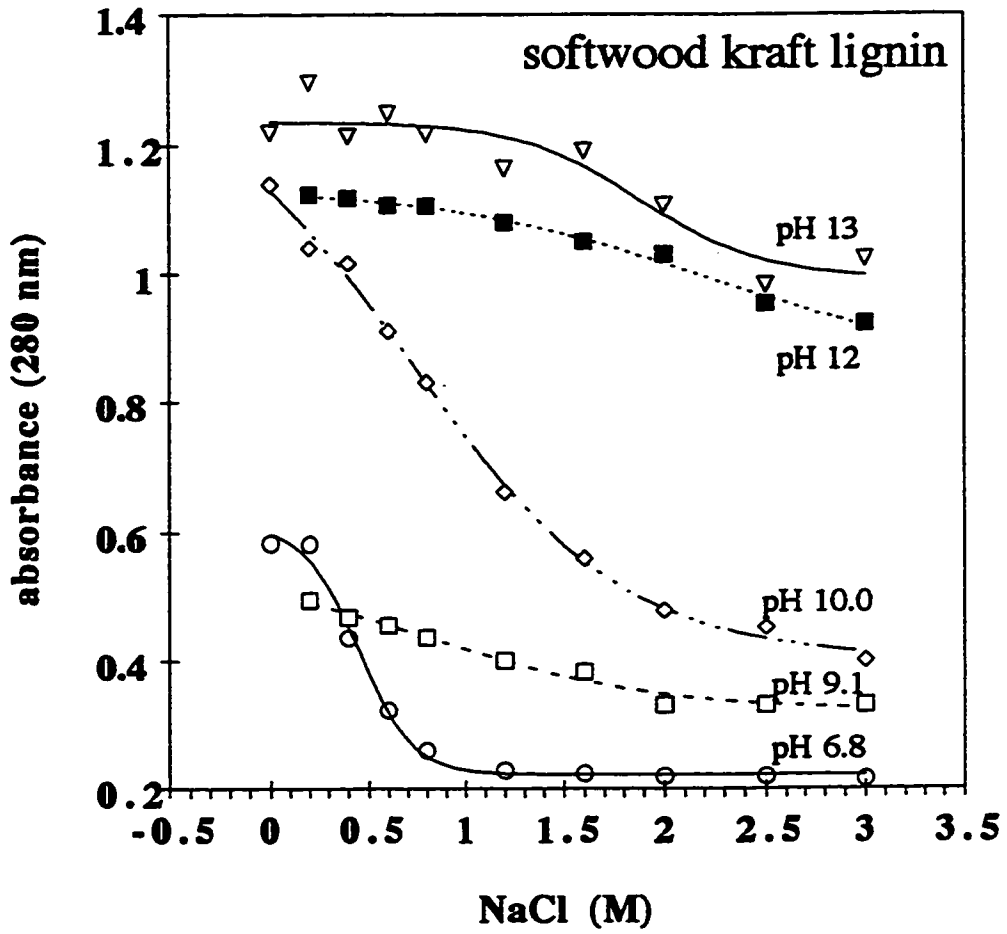

Figure 3.19 UV absorbance of softwood kraft lignin solutions with and cellulose at different pH and ionic strength values.

adsorption to the pulp.

If any other solid material other than pulp is used, for example glass wool, the lignin adsorption is unobservable under these conditions as shown in Figure 3.18. The result shows that the lignin adsorption to the pulp is selective and chemisorption.

All the adsorption at pH 6.8, 9.1, 10, 12, 13 and 0-3M NaCl have been studied. Figure 3.19 is the picture of lignin adsorption to pulp at different ionic strength (NaCl). The adsorption is affected by the ionic strength (NaCl). The biggest jump occurs at pH 9.1.

References

[3.1] D.A.I. Goring Polymer Properties of Lignin and Lignin Derivatives. In Lignin: Occurrence, formation, structure and Reactions; Sarkanen, K.V., Ludwig, C, H., Eds; Wiley-Interscience, New York, 1971.

[3.2] S.Sarkanen; D.C. Teller; E. Abramowski; J.L. McCarthy, Macromolecules 15,1098, 1982.

[3.3] S.Sarkanen; D.C. Teller; E. Abramowski; J.L. McCarthy, Macromolecules 17, 2588, 1985

[3.4] G.F.Zakis Functional Analysis of Lignins and Their Derivatives TAPPI Press, 1994

[3.5] K.Freudenberg, J. Harkin, and H. Werner,Chem. Ber.

97(3):909-920(1964)

[3.6] T. Enkvist, B. Alm and B. Holm,Paperi ja Puu 38(1): 1-8 (1956)

[3.7] J.P. Butler, and T.P. Czepiel, Anal. Chem. 28(9):1468-1472(1956)

[3.8] S. Sarkanen, and C. Schuerch, Anal. Chem. 27(8):1245-1250(1955)

[3.9] F. Gaslini and , L. Z. Nahum,Anal.Chem. 31(6)989-992(1959)

[3.10] F. Gaslini,and L. Z. Nahum, Sven. Papperstidn. 62(15):520-524 (1959)

[3.11] H. Mikawa, K. Sato, C. Takasaki,and K. Ebisawa, Bull. Chem. Soc. Jap. 28(9):653-660(1955)

[3.12] H. Mikawa, K. Sato, C. Takasaki,and K. Ebisawa, Bull. Chem. Soc. Jap. 28(9):649-653(1955)

[3.13] H. Mikawa, K. Sato, C. Takasaki,and K. Ebisawa, Bull. Chem. Soc. Jap. 29(2):245-254(1956)

[3.14] H. Mikawa, K. Sato, C. Takasaki,and K. Ebisawa, Bull. Chem. Soc. Jap. 29(2):254-258(1956)

[3.15] F. Gaslini and L.Z. Nahum, Sven Pappestidn. 62(15) :520-524 (1959)

[3.16] M. Schachter and T.S. Ma, Microchim. Acta (1/2) : 55-62(1966)

[3.17] T.M. Vasilyeva, R.K. Boyardaya, and G.P. Grigoryev, Zh. Prikl.Khim., 41(8):603-608(1968)

[3.18] L. B. Light, J.S.Huebner, and R. A. Vergenz Journal of Chemical Education , Vol 71 No: 2 (1994)

[3.19] Aki Vilpponen, Johan Gullichsen, and Carl-Anders Lindholm TAPPI Journal p134-138 Vol.76, No. 2, (1993)

[3.20]. Allen Joseph Smith, Richard R. Gustafson, and William T. McKean TAPPI Vol. 76, No. 6 Juue (1993)

[3.21]. B.D.Favis and D.A.I. Goring. J. Of Pulp and Paper Science September (1984)

[3.22]. P.M.K.Choi, W.Q.Yean and D. A. I. Goring Transaction of the Technical Section, Vol.2, No.2, June 1976

[3.23] D.A.I. Goring The role of ultrastructure in the removal of lignin during pulp washing Proceedings of XXI EuCePa,Paris, 1984, book 2 p.63

[3.24] J.P.Casey, Ed. Pulp and Paper Chemistry Technology Wiley-Interscience, New York, 1981, 3rd., Vol3.

[3.25] Yutaka Ishimaru, and Tom Lindstrom Journal of Applied Polymer Science Vol.29 1675

Chapter Four

NMR and Pulsed Field Gradient NMR Lignin Study

4.1 Introduction

In 1964, Ludwig [4.1] first employed 1-D NMR technique to lignin chemistry. Since then, NMR has proved to be one of the most powerful tools in lignin chemistry. NMR has been widely applied to quantify the relative frequency of different functional groups[4.2]. ^{13}C NMR has also played an important role in the identification and quantitatively determination of various nuclear centers [4.3] in lignins. More recently, with the technical development in NMR hardware and software, some new methods, such as 2-D NMR[4.4] have been employed to provide additional structural information in lignin chemistry.

One of the major difficulties of lignin characterization is to resolve the structural changes which accompany molecular weight degradation. Previous studies have established that the structure of lignin degradation products varies substantially with molecular mass[4.5]. Furthermore, the size of lignin materials can vary by up to 6 orders of magnitude due to a combination of covalent bonds

and association[4.5]. For this reason, it is important to be able to resolve size-structural variations occurring in lignin derived macromolecules.

Pulsed field gradient NMR is a spin-echo technique that has been used to measure diffusion coefficients(D_0) and resolve molecular size based upon molecular mobility(self-diffusion D_0). This technique has been used widely and achieved great success in polymer science [4.6], biological studies[4.7] and many other areas [4.8,4.9]. Diffusion ordered 2-D NMR(DOSY) technique has been developed and employed to distinguish large unilamellar phospholid vesicles [4.10].

In our research, we attempted to apply pulsed field gradient NMR (PFGNMR) and stimulated echo pulsed field gradient NMR in a high field NMR instrument to measure the diffusion coefficients(D_0) and to distinguish large molecules from small molecules. The goal was to identify the structural features which are clearly size dependent. In order to understand and explain the results obtained by PFG NMR, it is necessary to assign the peaks in the NMR spectrum of softwood and hardwood lignins .

4.2 The Theory of PFG And Stimulated Echo Gradient NMR

In 1946, Felix Bloch proposed the description of magnetic properties of ensembles of nuclei in external magnetic

fields[4.11]. The Bloch equation without diffusion coefficient is expressed in Equation(EQU 4.1).

$$\frac{dM}{dt}=\gamma M\times B-\frac{M_x i'+M_y j'}{T_2}-\frac{M_z-M_o}{T_1}k' \qquad (Equ.\ 4.1)$$

where i', j' and k' are the unit vectors of the laboratory frame of reference. B is the magnetic field, M is the magnetization in the magnetic field. T_1 and T_2 are longitudinal and transverse relaxation times, respectively. M_o is the equilibrium magnetization in the static uniform magnetic field B_{oz}.

PFG NMR is based on the phenomena called *Spin Echoes*, which were first pointed out according to Bloch Equations(EQU. 4.1) and observed by Hahn in 1950[4.12]. *Spin Echoes* are the spontaneous nuclear induction signals which are observed to appear due to the constructive interference of precessing macroscopic moment vector after more than one reference pulses have been applied. Based on *Spin Echoes*, Carr and Purcell[4.13] first developed a method to measure transverse relaxation time(T_2) and the longitudinal relaxation time(T_1) directly. Stejskal and Tanner[4.14] first developed a pulsed field gradient NMR sequence to measure diffusion coefficient(D_0) after adding two pulsed gradients to Hahn's spin echoes sequence. This sequence is the basic and usual PFGNMR sequence. It has a $\pi/2$ -G - π -G sequence

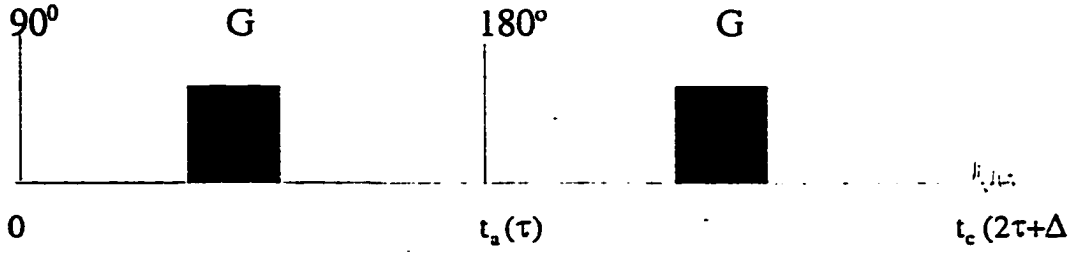

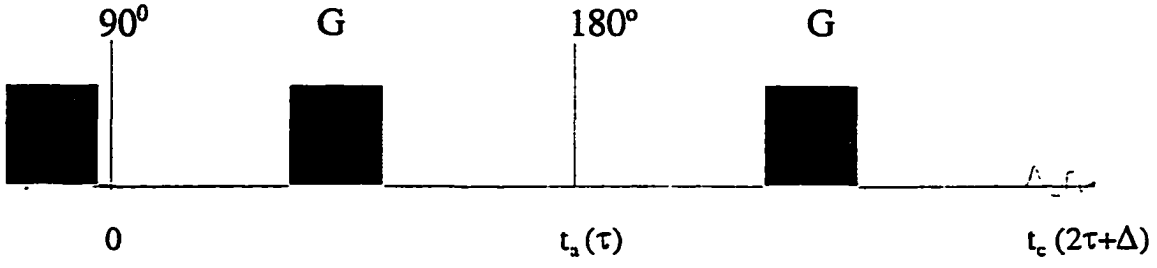

Figure 4.1 PFG sequence with and without prepulse

In PFG NMR, the molecular motion or diffusion coefficient(D_0) must be considered, because it is designed for measurement of diffusion coefficient (D_0). Torrey [4.15] obtained the Bloch equations(EQU. 4.2) after considering self diffusion coefficients(D_0).

$$\frac{dM_x}{dt}=\gamma(M\times B)_x-\frac{M_x}{T_2}+\nabla\cdot D\nabla(M_x-M_{xo})$$
$$\frac{dM_y}{dt}=\gamma(M\times B)_y-\frac{M_y}{T_2}+\nabla\cdot D\nabla(M_y-M_{yo})$$
$$\frac{dM_z}{dt}=\gamma(M\times B)_z+\frac{(M_0-M_z)}{T_1}+\nabla\cdot D\nabla(M_z-M_{zo}) \qquad (EQU.\ 4.2)$$

The echo amplitude, expressed as an echo attenuation, which are expressed in equation (EQU 4.3) for PFGNMR and equation (EQU 4.5) for stimulated echo, can be obtained through solving Bloch equations with the condition for PFGNMR and stimulated echo. The way to obtain the attenuation equations from Bloch Equations can be found in reference[4.16].

(EQU. 4.3)

$$\ln\left[\frac{A(2\tau)}{A_0(2\tau)}\right]=-\gamma^2 D\left(\tfrac{2}{3}G_0^2\tau^3+\delta^2G^2(\Delta-\tfrac{\delta}{3})-\delta G\cdot G_0\left\{\left(t_1^2+t_2^2\right)+\delta(t_1+t_2)+\tfrac{2}{3}\delta^2-2\tau^2\right\}\right)$$

where

- $A_0(2\tau)$= echo amplitude at time t that excludes effects of diffusion, but includes effects of spin-spin relaxation, in practice, it is obtained when power

supply is off;

- A(2τ) = echo amplitude at time t that includes effects of diffusion and effects of spin-spin relaxation;
- γ = magnetogyric ratio of observed species;
- D = diffusion coefficient;
- G_o = background (static) magnetic field gradient;
- G_a = pulsed magnetic field gradient;
- τ_1 = time between 90° rf pulse and field gradient pulse, in PGSE1.AU and PGSE3.AU, it is the first VD;
- δ = length of time the field gradient pulse is applied, in PGSE1.AU and PGSE3.AU, it is p2;
- σ_2= time between field gradient pulse and 180° rf, in PGSE1.AU and PGSE2.AU, it is the second VD;
- Δ = time between start of first field gradient and the start of the second field gradient pulse, Δ=2*VD + P2 + P3;

When $G_a^2\delta^2 \gg G_o^2\tau^3$, the above equation simplifies to

$$\ln\left[\frac{A(2\tau)}{A_o(2\tau)}\right]=-\gamma^2 D\delta^2 G_a^2\left(\Delta-\frac{\delta}{3}\right) \qquad (EQU.4.4)$$

Compared with the other methods, used for measuring diffusion coefficient, such as radioactive and sedimentation method, PFGNMR has a lot of advantages.

First, as a non-invasive technique, PFG NMR allows the observation of the displacements of the individual molecule without any interference with the microdynamic processes within the sample.

Second, the diffusion coefficients(D_o)of various components in the sample can be measured simultaneously.

Third, the measuring temperature and the pressure over the sample may be varied easily.

Fourth, high sensitivity(because of large number of repetition of measurements), the potential for *in situ* measurement and comparatively easy operation, are its additional advantages.

Problems and shortcomings with this method include:

(1). Improper probe design may lead to serious residual gradients, which will make the spin echo attenuation equation (Equation 4.1) very complicated and the measured diffusion coefficient (D_0) smaller than its true value.

(2). A heterogeneous system with $1/T_2$ exceeding $1/T_1$; or the diffusion coefficient, D , being small($D <= 10^{-7} cm^2/s$), may not be determined accurately, because the spin echo signal was stored in the X-axis in PFGNMR.

In order to overcome these difficulties, some new pulse sequences have been developed. The widely used sequence is the pulsed field gradient stimulated echo sequences. The basic gradient stimulated echo sequences and some common

features are shown in Figure 4.2.

The echo amplitude attenuation equation for gradient stimulated echo is expressed by equation(EQU 4.5).

$$\ln\left[\frac{A(t_e)}{A_o(t_e)}\right] = -\gamma^2 D\left(\delta^2\left(\Delta+\tau-\frac{\delta}{3}\right)G_a^2 + \delta\left[2\tau\Delta+2\tau^2-\frac{2\tau^2}{3}-(\delta_1^2+\delta_2^2)-\delta(\delta_1+\delta_2)\right]G_aG_o + \tau^2\left(\Delta+\frac{2\tau}{3}\right)G_o^2\right] \qquad (EQU.\ 4.5)$$

Where A(t), $A(t_0)$,D, G_0 ,G_a,γ, δ have the same meaning as in EQU. 4.4, However, Δ,δ_1 and δ_2 have different meanings:

Δ is the time between the second $\pi/2$ pulse and the third $\pi/2$ pulse. $\Delta=D_2$ in the PGSE3.AU and PGSE4.AU.

δ_1 is time between 90° rf pulse and field gradient pulse, in PGSE2.AU and PGSE4.AU, $\sigma_1=D_3$.

δ_2 time between field gradient pulse and the second 90° rf, in PGSE2.AU and PGSE4.AU, it is the second VD

Compared with equation (EQU.4.4), the effect of the background gradient(G_0) can be reduced greatly through careful selection of τ, σ, σ_1 and σ_2 and EQU. 4.5 could be

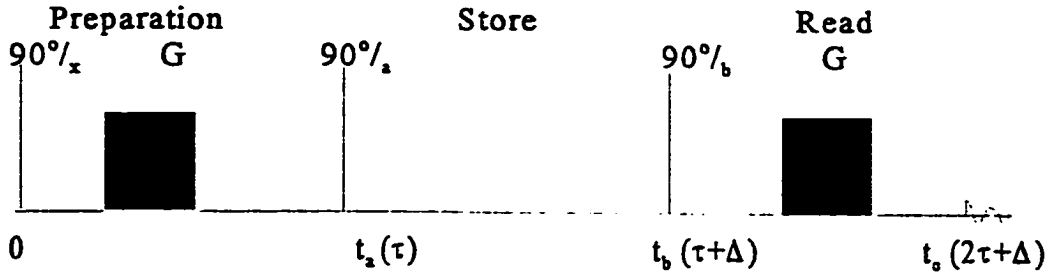

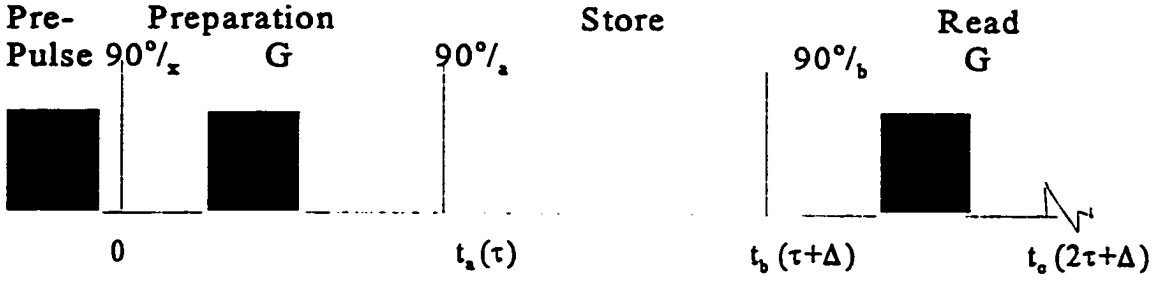

Figure 4.2 Stimulated Echo sequence with and without prepulse

simplified to EQU 4.6.

$$\ln[\frac{A(t_e)}{A_o(t_e)}]=-\gamma^2 D(\delta^2(\Delta+\tau-\frac{\delta}{3})G_z^2 \qquad (EQU.\ 4.6)$$

4.3 Experiments

The Preparation of Lignin Samples

The major lignin preparations used for analysis through this study were isolated directly from a kraft black liquor which was obtained from Avenor Inc in Thunder Bay, Ontario, Canada. The other was isolated from the effluent from the peroxide bleaching of TMP aspen pulp.

The original kraft lignin was isolated from kraft black liquor as follows: 220ml of kraft black liquor (KBL) was diluted to 1000 ml and filtered through a VWR 617 filter before diluting to 1600 ml. The pH of the resulting solution was 12.34. This solution was acidified with 1.0M H_2SO_4 at a rate of 0.4 ml/min to pH 3. A slow precipitation is thought to yield a lignin preparation with less impurities.

After precipitation to pH 3.0 the solution was allowed to stand for 1 hour and the pH was readjusted to 3.0 before centrifugation in polycarbonate bottles on an IEC(International Equipment Company) Centra MP4® at the rate of 3000 rotation/minute for 30 minutes. Subsequent to

precipitation, the lignin was resuspended by vigorous shaking in an aqueous HCl wash at pH 3.0 and recentrifuged. The lignin was washed in this manner three times. The lignin was washed in the same way by water three times. Finally, it was freeze-dried. This dry lignin was used in the following experiments.

The bleached lignin was prepared directly from the bleaching effluents by freeze-drying of the neutralized bleaching effuents.

Acetylation

The acetylation of lignin is used to increase the solubility of lignin in deuterium chloroform(solvent) and to eliminate the exchangeable hydrogen in OH with deuterium in the solvent. The acetylation reaction is occurred as following:

$$R(Ar)\text{-}OH + (CH_3CO)_2O \xrightarrow{pyridine} R(Ar)\text{-}OCOCH_3 + CH_3COOH$$

This acetylation procedure is evolved from reference [4.17]. Impurities and side reactions are our major concerns. High purity reagents and dark and sometimes, nitrogen atmosphere are used in our experiment.

All reagents were doubly distilled; with the first distillation being carried out from a drying agent or, in the case of acetic acid, from an oxidizing agent. In all cases only the portion which was distilled at the boiling point was redistilled. The reported distillation temperature are as follows: pyridine,114.4 °C; acetic acid,117.9 °C;

acetic anhydride, 139.44 °C. Pyridine was distilled from about 4 grams BaO and boiling chips. The portion collected between 114-116 °C was redistilled with boiling chips alone. Acetic acid was first distilled with 14 grams $KMnO_4$ and the above 114 °C portion was redistilled. Acetic anhydride was dried over P_2O_4 24 hours and then decanted before distilling from a 1000 ml flask. The portion collected between 136-139°C was redistilled. The reagents were used immediately for the acetylation [4.18].

The acetylation mixture was mixed as follows: frozen-dried lignin sample of 1-40 mg was dissolved in 0.280 ml double distilled H_2O. Once dissolved the sample was then precipitated with 0.180ml acetic acid. The sample was mixed well and 10 ml pyridine was used to facilitate lignin dissolution. Finally, 6.0 ml of acetic anhydride was added to solution. If the reagents are added in any other than the preceding, the sample will not dissolve completely.

The flask was sealed under nitrogn with parafilm and stirred by magnetic stir in dark for 24-48 hours.

The acetylation mixture was poured into 10 ml pyridine in 140 ml high purity H_2O which was cooled to 0 °C in an ice bath. The mixture was stirred and allowed to stand for about 30 minutes before it was extracted by 40 ml chloroform three times. The 140 ml chloroform was washed five times with 40 ml 1.0M H_2SO_4 and then 40 ml reagent grade water five times. The sample was dried by anhydrous sodium sulfate and decanted into a flask for solvent removal on a rotary

evaporator. The dried sample was further purified by extracting the dry sample on the wall of the flask with hexane, with redissolution in $CHCl_3$ and evaporation between successive evaporation. 99.94% deuterated chloroform($CDCl_3$) from Cambridge Isotope Laboratories was used in our experiments.

NMR Equipment and Parameter

In our experiments, NMR spectrometer is a Bruker AM 200 with a 200 MHZ superconducting magnet and an Aspect 3000 computer. A regular 5 mm ^1H probe is used in this section.

The NMR parameters used in our experiments are as following:

SY=80.13MHz TD=409 SI=8K

T=298K, O1=379 SW=3000Hz

TE=297 NS=1024, RG=8

O2=20,000Hz FW=3800 DW=208.8

SF=200.134MHz DR=12

PFG and Stimulated Echo NMR Experiments

The NMR spectrometer and samples are the same as above. The probe is a 5 mm with a pulsed field gradient generator made by Doty Scientific Inc. 700 Clemson Road Columbia, SC 29223, USA. The probe has a 5mm pulsed Z gradient, inverse RF coils, multi nuclear, for diffusion measurement in Brucker AC-200 (NB 40mm) spectrometer. The parameters of our probe are as following:

Chapter 4 NMR and PFGNMR Studies

A: Highly corrected B_z gradient coils fo efficient generation of linear gradients in the Z direction, including high-order active shielding coils to reduce energy of eddy currents in probe and magnet.

B: 2% gradient linearity over 10 mm diameter sphere

C. Gradient coil resistance 2.4 Ω , inductance ≈ 0.12 mH .

D. Gradient magnitude 40 G Cm^{-1} A^{-1}

E. Continuous operation at 40G/cm , 1% duty cycle @400 G/cm.

F. Switching time 42 μs with Doty gradient driver at 400G/cm, with 14 amp drive in constant current region.

G. Rf shielding between gradient coils and sample region.

H. Supplied with orthogonal saddle receiver coils, for use with 5mm sample tubes, for double resonance experiments. 2 turn (6×6 mm) proton coil on ID of the form, and 4 turn (7×7) obs coil on outside of proton coil.

I. ^{1}H π/2 pulse of 12 μs with <20W @200MHz. This coil double tuned for lock.

J. Multinuclear LF channel via plug in wands.

K. ^{13}C π/2 pulse of 14 μs <100W @40.2MHz.

^{29}Si π/2 pulse of 14 μs with <100W @39.7mHz.

^{14}N pulse of 24 μs with <100W @ 20.2MHz.

N. VT operation over the range of -10 to +60 °C.

The electricity source is a Kepco Bipolar Operation Power Supply Amplifier(model BOP 36-12M) with current control and voltage control. A homemade special switch was used to generate electrical pulses. Its circuit is in Appendix 6. A Philips oscilloscope was used to monitor the pulses and a multimeter was used to measure the voltage from the power supply. The PFGNMR setup was shown in Figure 4.3. The voltage from power supply is changed from 2-9 V.

4.4 Results and Discussions

Sample proton NMR spectra of acetylated softwood and hardwood kraft lignins are shown in Figures 4.4 and 4.5. Overall these spectra are broad and featureless. The following assignments for peaks for lignin structures are shown in Tables 4.1 and 4.2. The primary difference between these two types of lignin is the significantly larger relative amounts of carbonhydrate methoxyl and aromatic acetoxyl groups present in softwood kraft lignin. Few details can be resolved because of the broad peaks.

Setup

contains information concerning neighbouring protons which are responsible for splitting a signal into many peaks according to n+1 rule where n is the number of neighbouring protons. Integration provides a measure of the relative number of protons contributing to a specific peek or group of peaks. Coupling constants obtained by measuring the distance between peaks in a multiplet are used to confirm

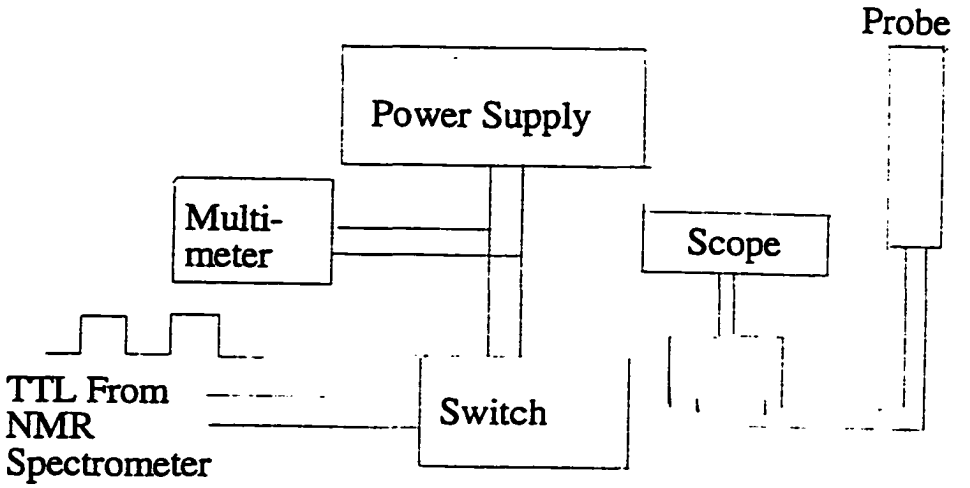

Figure 4.3 PFGNMR and stimulated echo Experiment Setup

assignments and determine configuration.

In lignin, the chemical shift of aldehydic protons occur between 9.8-9.94 ppm, the aromatic region is between 6.4-8.0, methoxyl protons at 3.7-3.94 ppm, aromatic acetoxyl at 2.3 ppm and aliphatic acetoxyl at 2.1 ppm. Vanillic protons between 4.4 - 7.8 ppm may overlap with the aromatic region. The detailed assignments of lignin are listed in Table 4.1 and Table 4.2.

1-D ^{1}H NMR spectrometry contains information regarding chemical shifts, multiplicities, integrations and coupling constants. The chemical shift depends on the electronic environment of the proton. Multiplicity or peak splitting

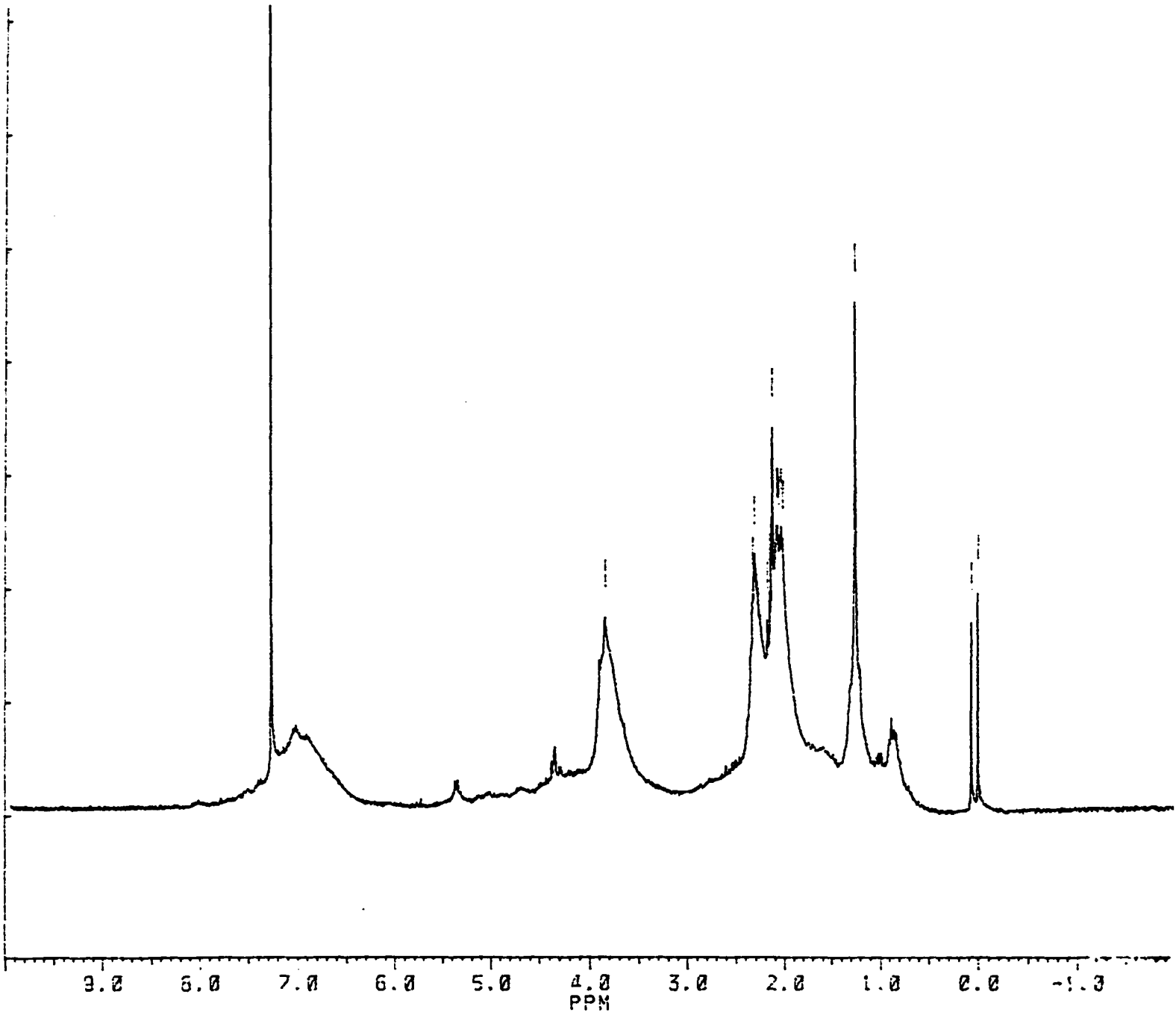

Figure 4.4 NMR spectrum of softwood lignin

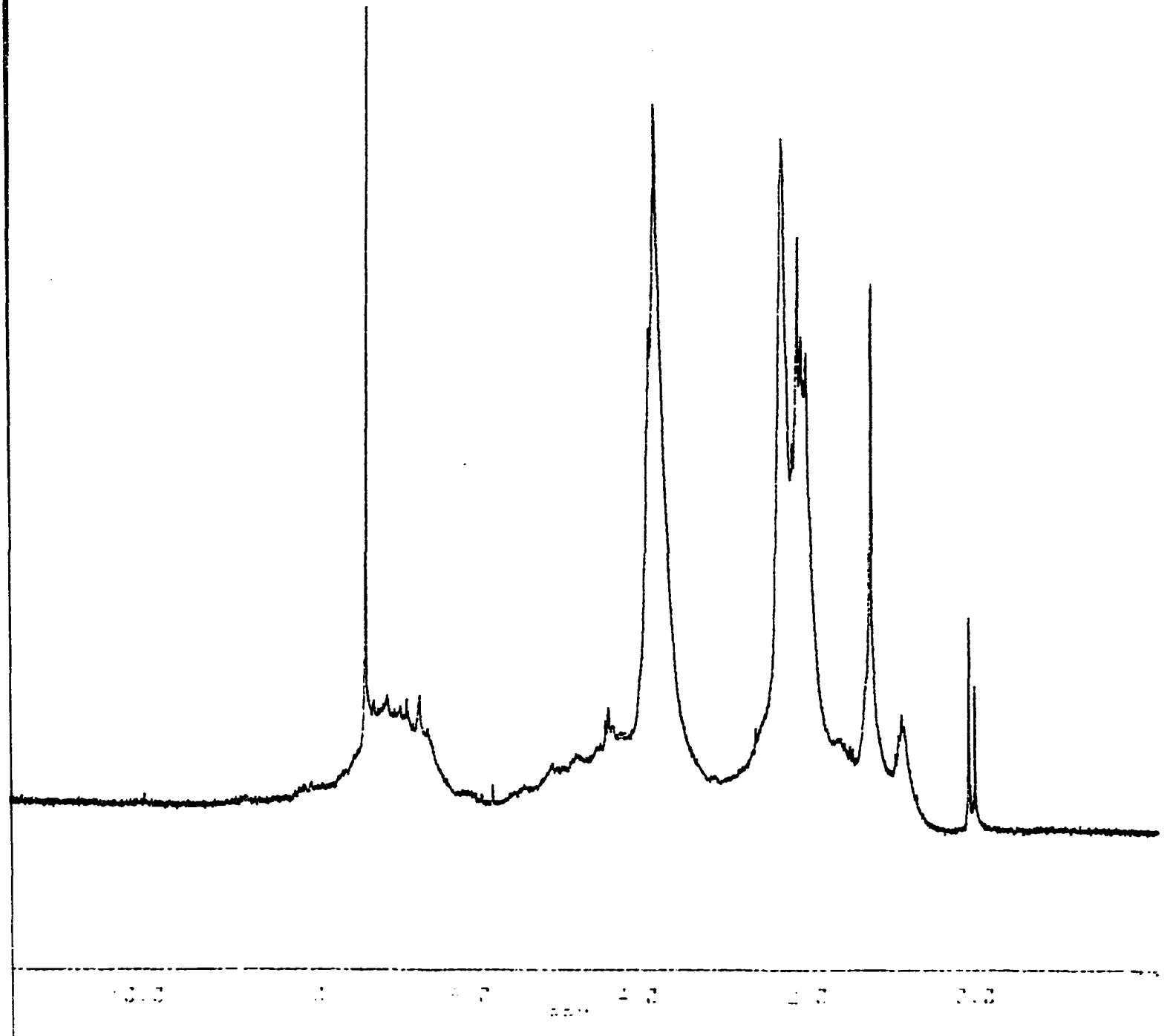

Figure 4.5 NMR spectrum of hardwood lignin

Table 4.1 Assignment of signals in the ^1H NMR spectrum of acetylated spruce kraft lignin(Figure 4.4)

δ	Assignment
1.26	Hydrocarbon contaminant
	Aliphatic acetate
2.28	Aromatic acetate
3.81	Protons in methoxyl groups
4.22-4.44	H_γ in several structures
4.64	H_β in ß-O-4 structures (methylene protons in cinnamyl alcohol units)
5.49	H_α in ß-O-4 structures (H_α in noncyclic benzyl aryl ethers, H_β in 2-aryloxypropiophenones
6.06	H_α in ß-O-4 structures(H_α in ß -1 structures. H_β in cinnamyl alcohol units
6.93	Aromatic protons(certain vinyl protons)
7.29	Chloroform (solvent)
7.40	Aromatic protons in benzaldehyde units and vinyl protons on the carbon atoms adjacent to aromatic rings in cinnamaldehyde units

Table 4.2 Assignment of signals in the ^1H NMR spectrum of acetylated aspen kraft lignin(Figure 4.5)

δ	Assignment
1.26	Hydrocarbon contaminant
3.83	Protons in methoxyl groups
4.0-5.0	H-C on carbohydrate and lignin side chains
6.01	H_α in ß-O-4 structures(H_α in ß -1 structures. H_β in cinnamyl alcohol units
6.60	Aromatic protons in syringyl units(certain vinyl protons)
6.94	Aromatic protons in guaiacyl units
7.29	Chloroform (solvent)
7.43	Aromatic protons in benzaldehyde units

Spin Relaxation and Molecular Size

The nuclear spin relaxation which occurs during the pulsed gradient NMR experiment may affect the results and must be accounted for. In a typical NMR experiment the reorientation correlation time, which may be largely determined by molecular size, is one of the principle factors of the relaxation times. Spin-spin (T_2) relaxation always decreases with increasing correlation time or molecular size. Spin-Lattice (T_1) relaxation times reach a minimum at $\tau_{corr} = 1/\nu$ (ν is frequency). One might be tempted to exploit the molar mass dependence of the relaxation times to simplify spectra. But there is rarely enough variability in the correlation times of dissolved substances to clearly resolve different components. Furthermore, lignin protons are highly coupled by both spin-spin coupling and dipolar coupling, hence quantitative resolution of size-structure relationships is not possible through relaxation techniques alone. Nevertheless, we must account for the differences in relaxation times for various components. T_1 and T_2 signal relaxation for an acetylated aspen kraft lignin sample is shown in Figure 4.6. Relaxation times for different functional groups are given in Table 4. 3. This sample's relaxation times are typical for an acetylated lignin derivative. The T_2 relaxation is significantly faster than the T_1 relaxation. Figure 4.7 shows acetylated aspen kraft lignin spectra at two stages of T_1 relaxation and the corresponding difference spectrum.

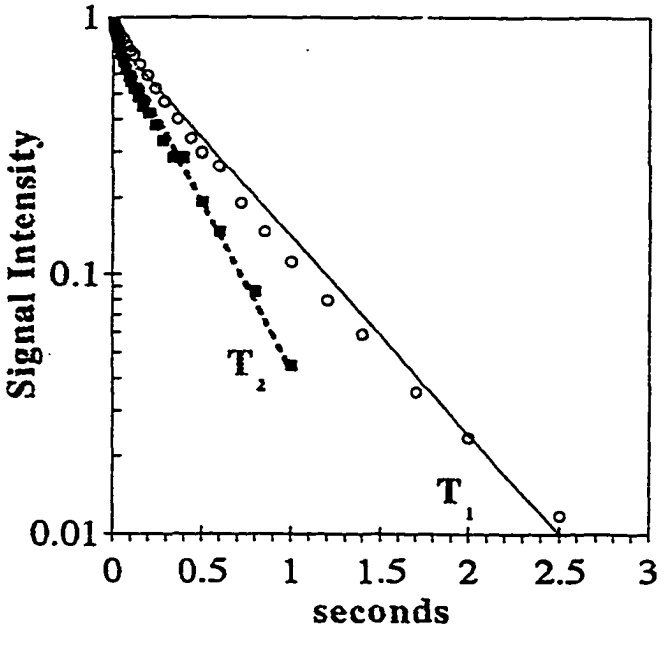

Figure 4.6 T1, and T2 measurements

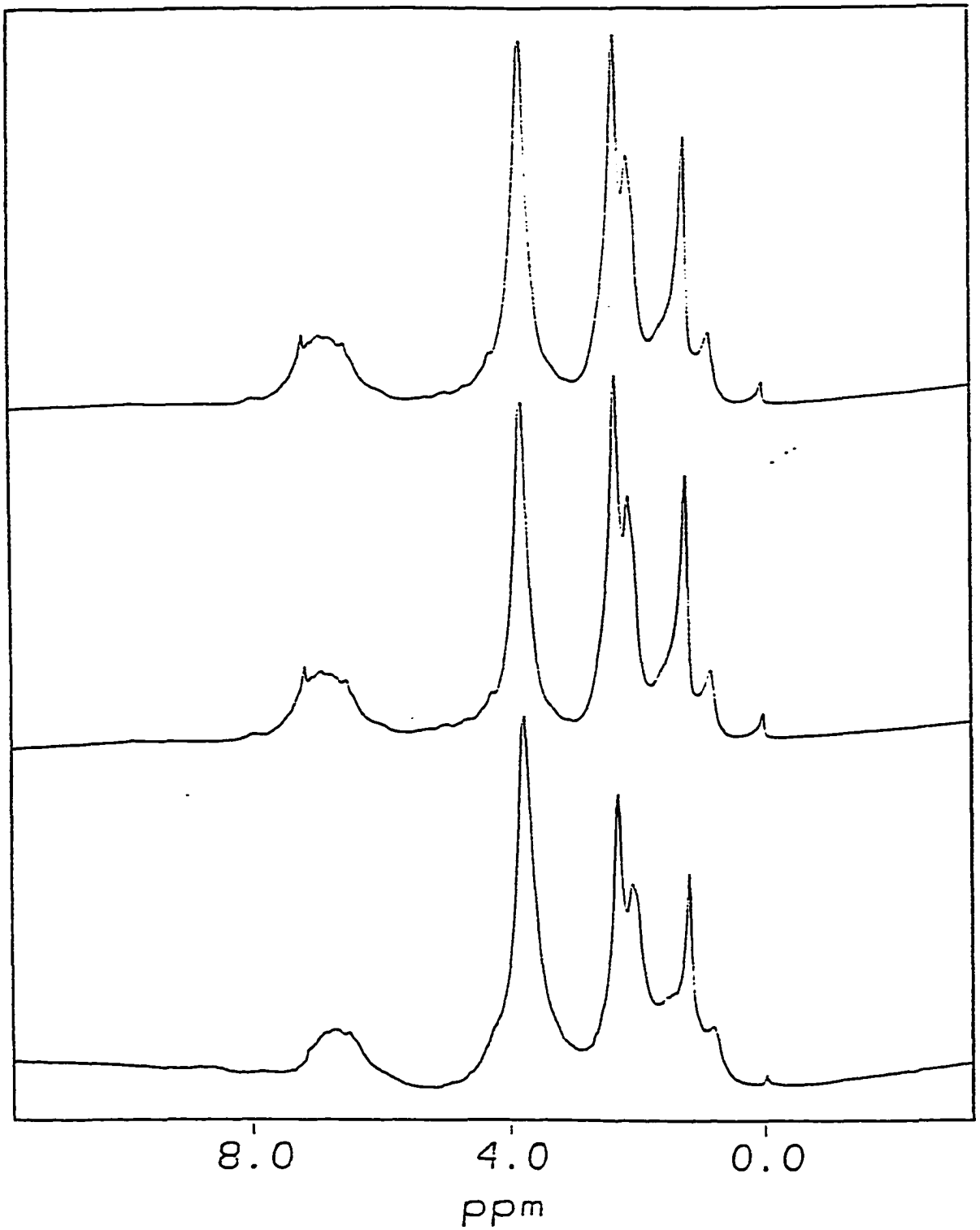

Figure 4.7 spectra at two stages of T_1 relaxation and the corresponding difference spectrum.

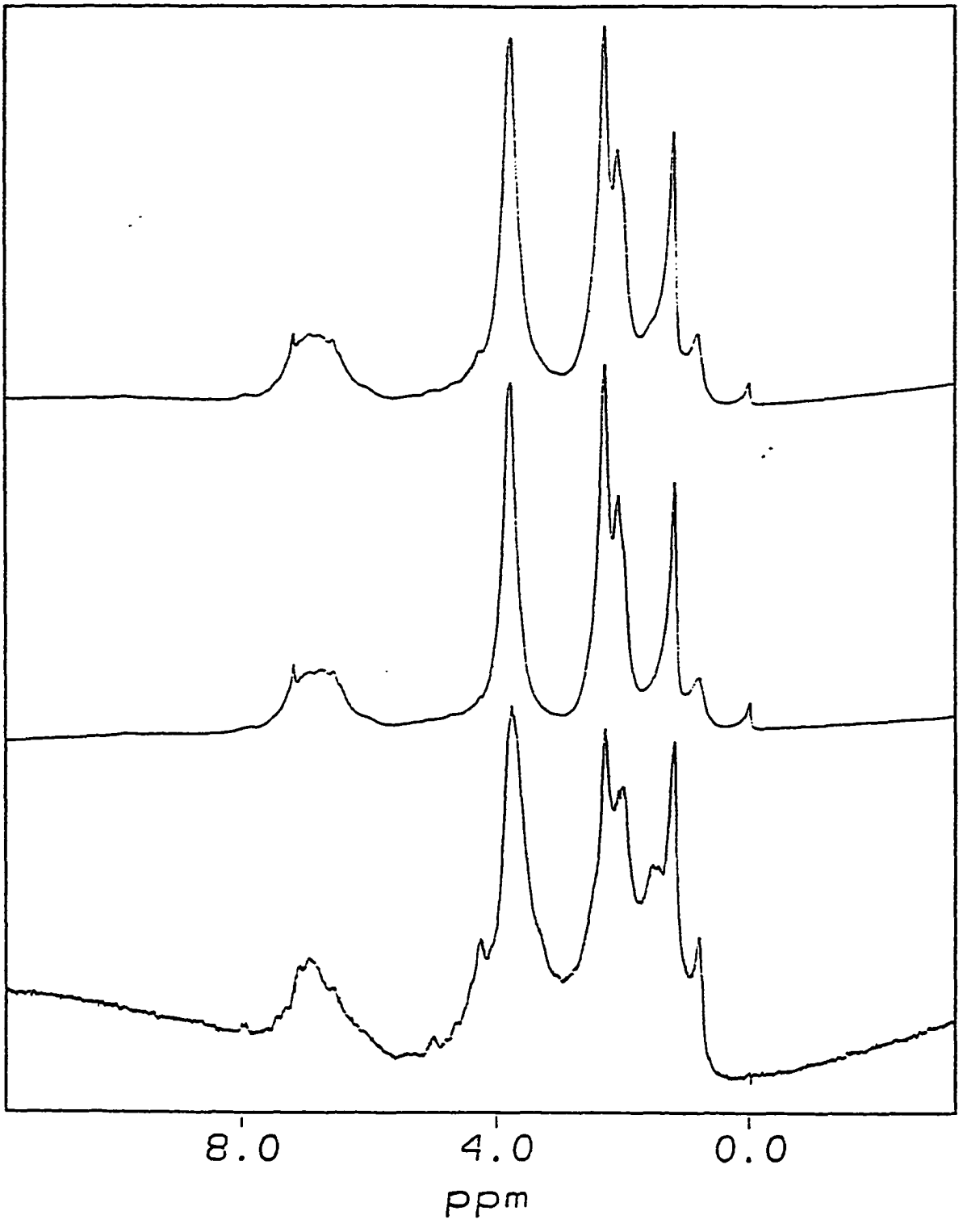

Figure 4.8 Spectra at two stages of T_2 relaxation and the corresponding difference spectrum.

Figure 4.8 shows spectra at two stages of T_2 relaxation and the corresponding difference spectrum. Comparison the spectra of Figures 4.7 with 4.8 show that spin-spin relaxation is much more efficient at differentiating structural features than spin-lattice relaxation. In the pulsed field gradient NMR experiments below the differential effects of T_1 and T_2 relaxation become an important consideration. The signal for small molecules decays slowly for relaxation experiments while pulsed gradients select signal for large molecules. The difficulty lies in resolving molecular size by gradients before significant selection has occurred through relaxation.

Table 4.3. Relaxation times for acetylated kraft aspen lignin.

Proton Type	T_1 (seconds)	T2(seconds)
aromatic	0.865	0.085
methoxyl	0.6	0.172
ArOAc	0.702	0.178
ROAc	0.763	0.194
R (1.2 ppm)	0.662	0.1

The measurement of current in the probe

The current going to the probe was measured by measuring the voltage and resistor according to the Ohm's Law. The relationship between voltage measured across the power supply and the current going to the probe is shown in Figure

4.9. The reproducible results are obtained using the constant voltage mode on the power supply.

The calibration of the probe

The pulse gradient in the probe is very difficult to measure directly. An alternative is to calibrate the probe by a standard sample with a known self diffusion coefficient(D_0). H_2O in D_2O(HDO) is used widely to calibrate the gradient in the probe because its diffusion coefficient has been measured by many researchers and it has a very simple peak. H_2O in D_2O was prepared by putting a little drop of H_2O in D_2O(1%H_2O/D_2O) and a little bit of $CuSO_4$ as the indicator. The standard value of self-diffusion coefficient(D_0) of H_2O in D_2O at 298K used in our experiment is $D= 1.902\times10^{-9}$ m^2 sec^{-1}[4.21]. The magnetogeric ratio of ^1H is 2.6742×10^8 kg^{-1} Sec.

In order to simplify equation 4.2, let

$$y= \ln[A(2\tau)/A_o(2\tau)];$$

$$x=\delta^2(\Delta-\delta/3)$$

$$y = -kx$$

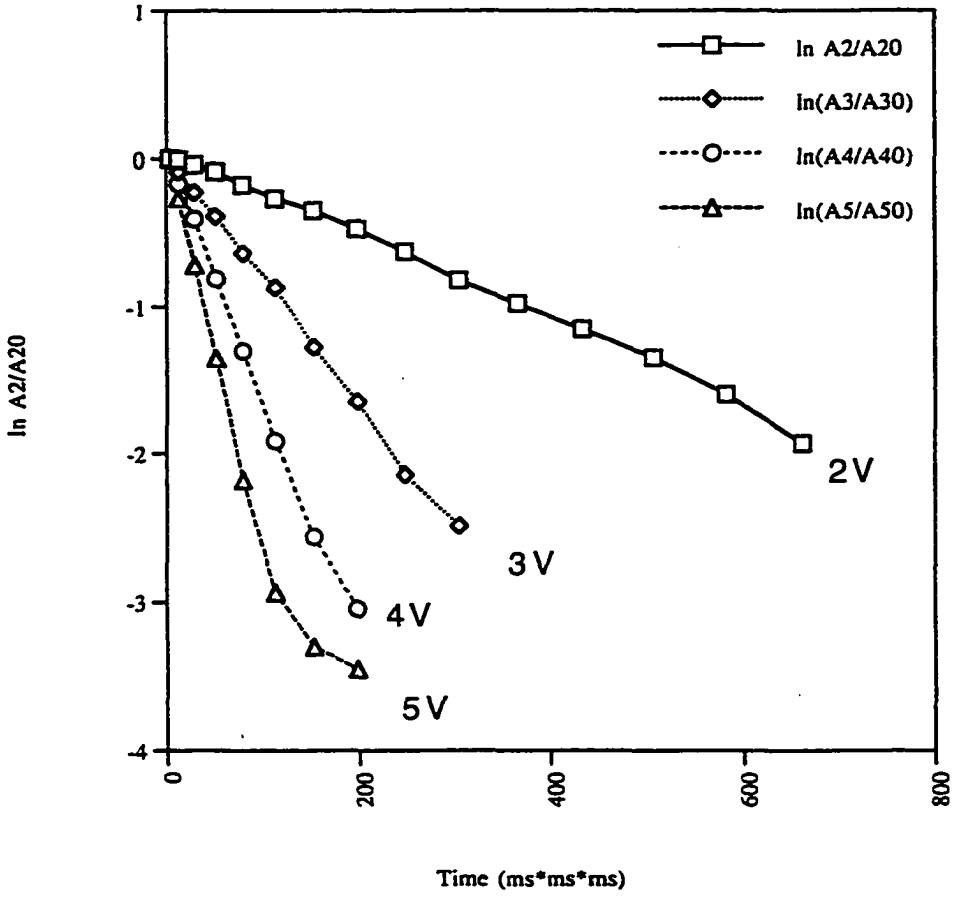

Figure 4.9 The effect of gradient pulse magnitude variation (Current Change)

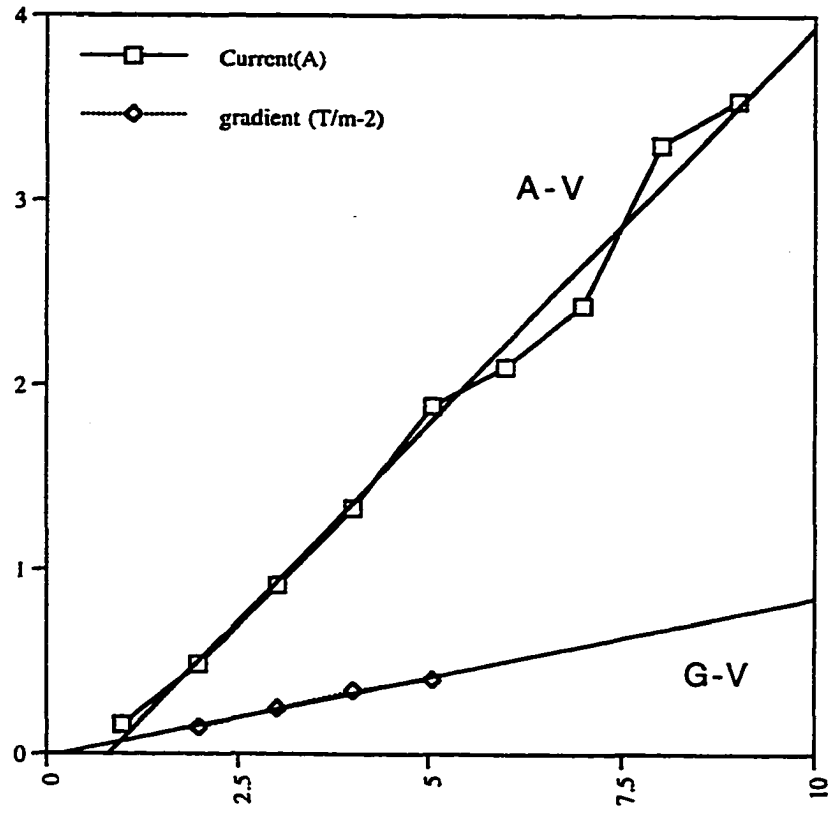

Figure 4.10 Calibration of probe using different voltages

then

$$k = \gamma^2 D G^2 \quad G^2 = k/(\gamma^2 D) \qquad \text{(EQU. 4.7)}$$

In our experiment, k is the slope of the diagram(y vs x).Substituting the values of D and γ, pulsed gradients(G) may be obtained as:

$$G=2.7104k^{1/2}$$

k is solely dependent on the current used to generate gradients. G is measured to be 0.188T/m A

From our experiment, the total resistance of our system is 2.302Ω.

The Measured Diffusion Coefficients (D_o) of Polystyrene and Lignins

The problems in our measured diffusion coefficients(D_o) of the samples are as following:

1) the measured diffusion coefficients(D_o) are 30 - 100 times bigger than the true value;

2) The probe doesn't have enough resolution in term of measured diffusion coefficients(D_o). The measured diffusion coefficients(D_o) of lignin and polystyrenes are close to each other.

3). Although PFG NMR has been applied in many different research areas, almost all researchers use the wide bore(80mm. Our system is a narrow bore(40mm). The narrow bore(40mm) system will result seriously residual gradients and is difficult to shield. This is the fatal drawback in our experiment. The narrow bore and the short T_2 relaxation

times of our samples(lignin) greatly reduce the value of our experiments.

In PFG NMR and stimulated echo experiments, all the problems, except mistakes in calibration of the probe, will result in a greater measured diffusion coefficient(D_o). So it is very easy to obtain a bigger measured value rather than a smaller value of diffusion coefficient (D_o) by PFG NMR or stimulated echo experiments. In our experiments, we found that the residual gradients and the vibrations are the two main problems in our probe.

The residual gradients in the probe

In PFG and stimulated echo PFG NMR experiment measurement of diffusion coefficients(D_o), the residual gradients in the probe are always the major problems. The residual gradients have been studied by Merwall and Kamat[4.19] and Hrovat and Wade [4.20] . In this study, the term residual gradient refers to any additional magnetic field gradients which were observed after the electral current pulse which produces the magnetic pulsed field gradients has die down. Residual gradients are resulted from the application of the pulsed gradient; it may or may not be the result of slowing decaying eddy currents. The residual gradients in the probe can be observed directly by oscilloscope through the observed current to the probe corresponding to the residual. Figure 4.11 is the comparison the residual gradients of the probe in the superconducting magnet(Figure 4.10B) with that outside the superconducting

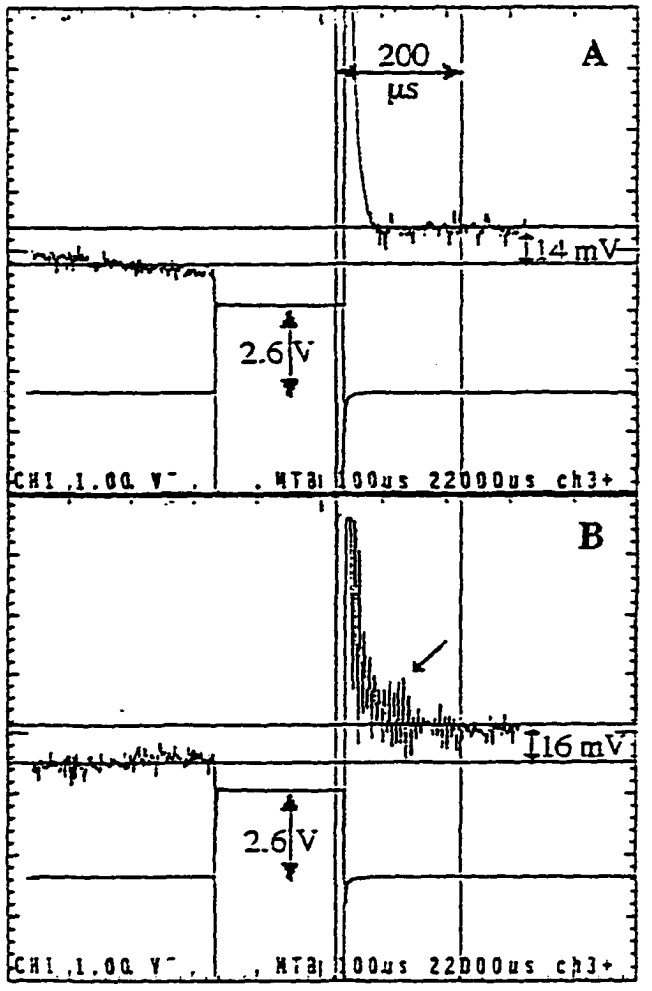

Figure 4.11 Direct Observation of eddy current in the superconducting magnet

magnet(Figure 4.11A). Figure 4.11 shows that the residual gradients of the probe in the superconducting magnet(Figure 4.11B) are much stronger than that outside the magnet(Figure 4.11A).

The residual gradients may be divided into long-term and short-term residual gradients. The long term residual gradients may need hours to decay. Comparatively speaking, long term residual gradient has smaller effects on the measurement of diffusion coefficients. It could be eliminated by a prepulse in PFG NMR or stimulated echo NMR. Figure 4.11 is the effect of prepulse in PFG and stimulated echo experiments. The prepulse resulted about 4% improvement of measured diffusion coefficient(D_0).

The short term residual gradients are responsible for many problems in PFGNMR technique. The major problems resulted from the short term residual gradients are:

1) a decay time is required before a r.f pulse after a gradient pulse in order to avoid the strong residual gradients;

2) Distortions which appear in the Fourier transform of the spin echo;

3) Phase shift which can affect measurement made 'on resonance', this shift can increase the measured value greatly;

4) Errors in the calibration of the probe;

In total, the residual gradients could increase the measured diffusion coefficient(D_0)to 30-100 times greater

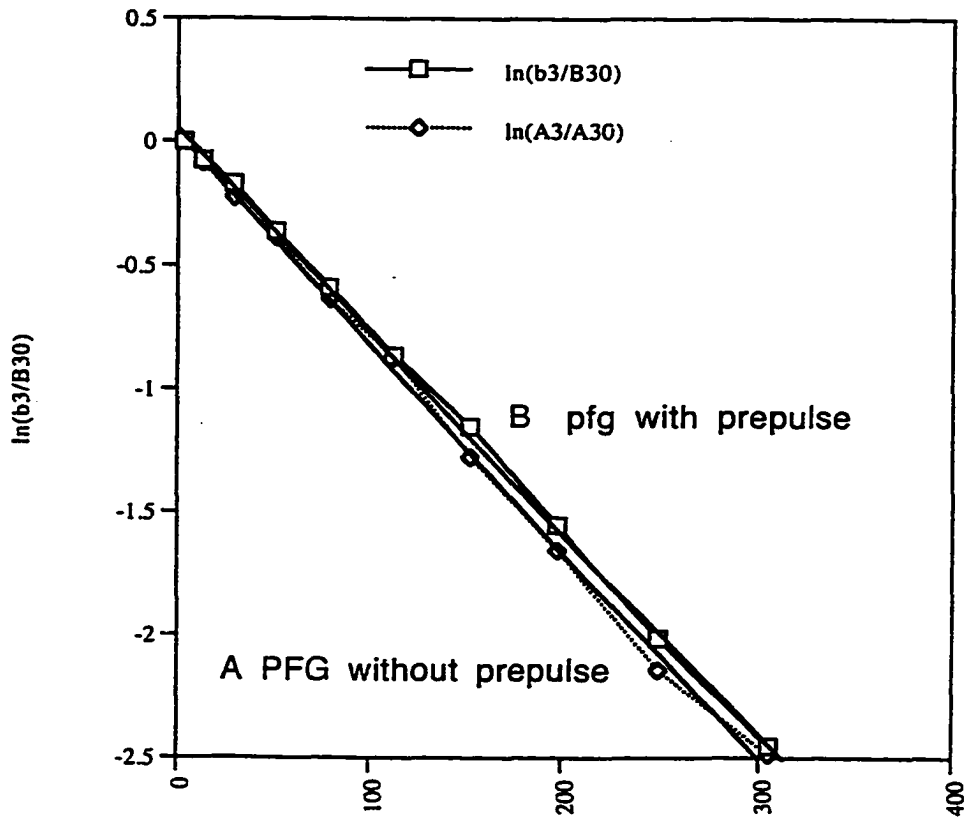

Figure 4.12 A prepulse to compensate the long term residual gradient

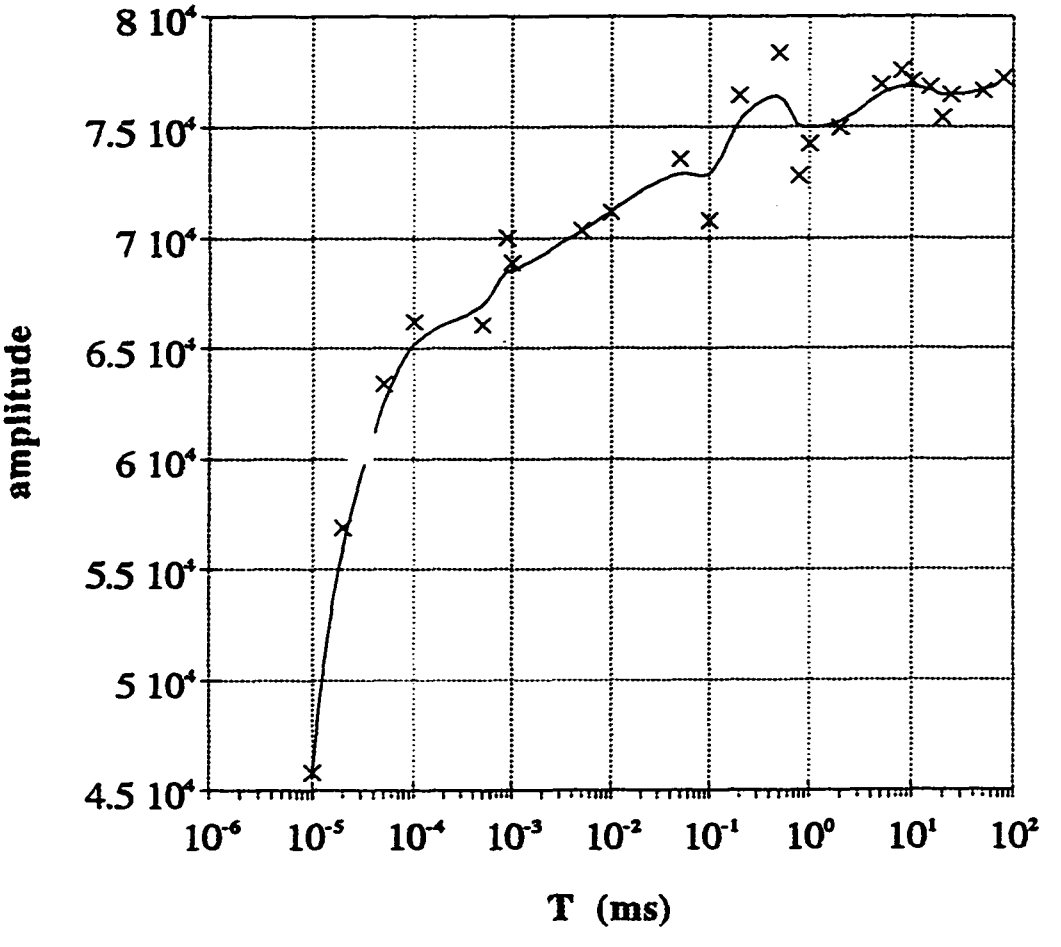

Figure 4.13 H-OD height from a π/2 r.f pulse after a gradient pulse(PGSE1)

than its true value.

In our probe, although it is actively shielded, the residual gradients are still serious. When the pulsed gradients reached to 3A(or 10V), the spin echo attenuation is seriously deformed. This is an evidence of residual gradients.

A very sensitive experiment of detection the residual gradients was employed to observe the short term residual gradients. After a single gradient pulse(3v or 4v, 2ms), a $\pi/2$ r.f pulse was applied at different times to acquire a FID. After Fourier transform, the height of the peak of HDO was plotted verse the time after the gradient. From Figure 4.13, we can find that the height of HDO before 30 ms was extremely unstable. This unstability was an observation of residual gradients. The waiting time after the pulse could not be too long, otherwise, the signals might disappear.

The Interaction Between r.f and Gradient Pulses

Comparing gradient pulses with r.f pulses, r.f pulses are shorter and stronger. The close proximity of the r.f coils with the gradient coils leads to induction of a gradient pulse during r.f pulse. The effective coupling of the r.f and gradient coils may be observed for a pulse sequence with a short time span as shown in Figure 4.11. The gradient generated from the induced current from the r.f pulse will contribute to the deploring which effectively reduces the accurracy of the measurement by misreading the

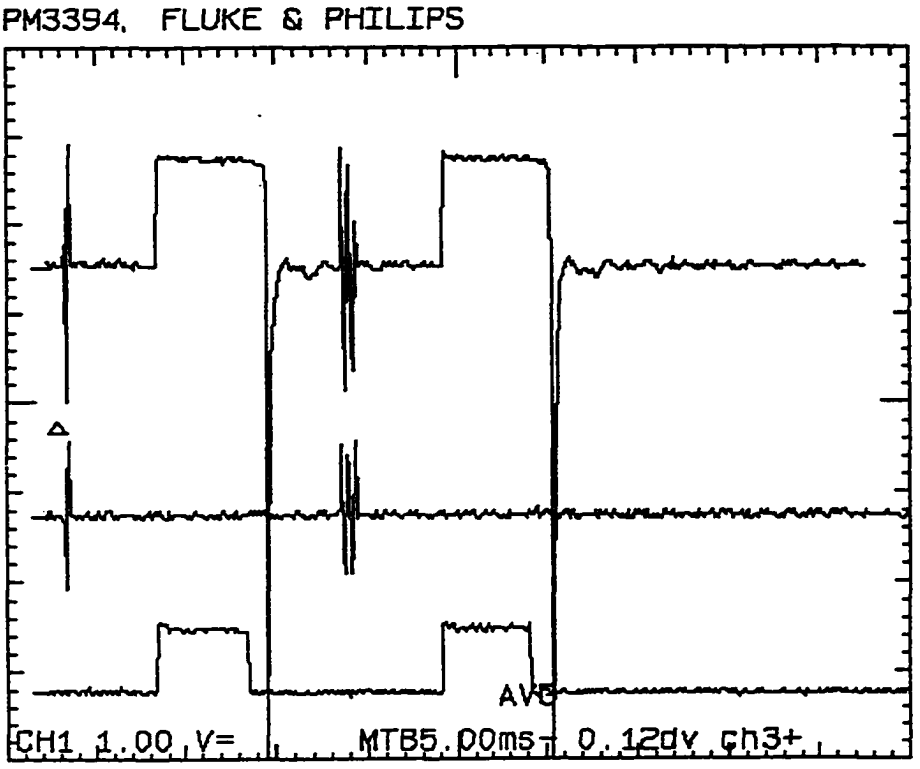

Figure 4.14 The Interaction between gradient pulses and rf pulses.

measured echo attenuation.

The Residual Gradient Reduction Experiments

In order to avoid the residual gradients, every effort has been made to find the cause of residual gradients and the way to elimilate the residual gradients. The most powerful tool to reduce residual gradients is active-shielding. It could reduce the magnitude of the gradient-coil far field by a factor of approximately 20[4.20].

The idea of active shielding is to construct a suitable arrangement of wires at a large radius than the gradient coils, and excite these shielding wires with a current sufficient to cancel out the original gradient fields beyond a specified radius, which is smaller than the inner dimension of the main magnet. The shielding wires may be arranged on a cylindrical format and fed with equal currents if they are appropriately spaced[4.20]. The active-shielding was implemented by the manufacturer.

The stimulated echo PFGNMR can also be used to reduce residual gradients.

The effect of the timing between r.f and gradient pulse is shown in Figure 4.15 - 4.18 for our experiments. In general, a 5 - 10 ms delay between peaks is required.

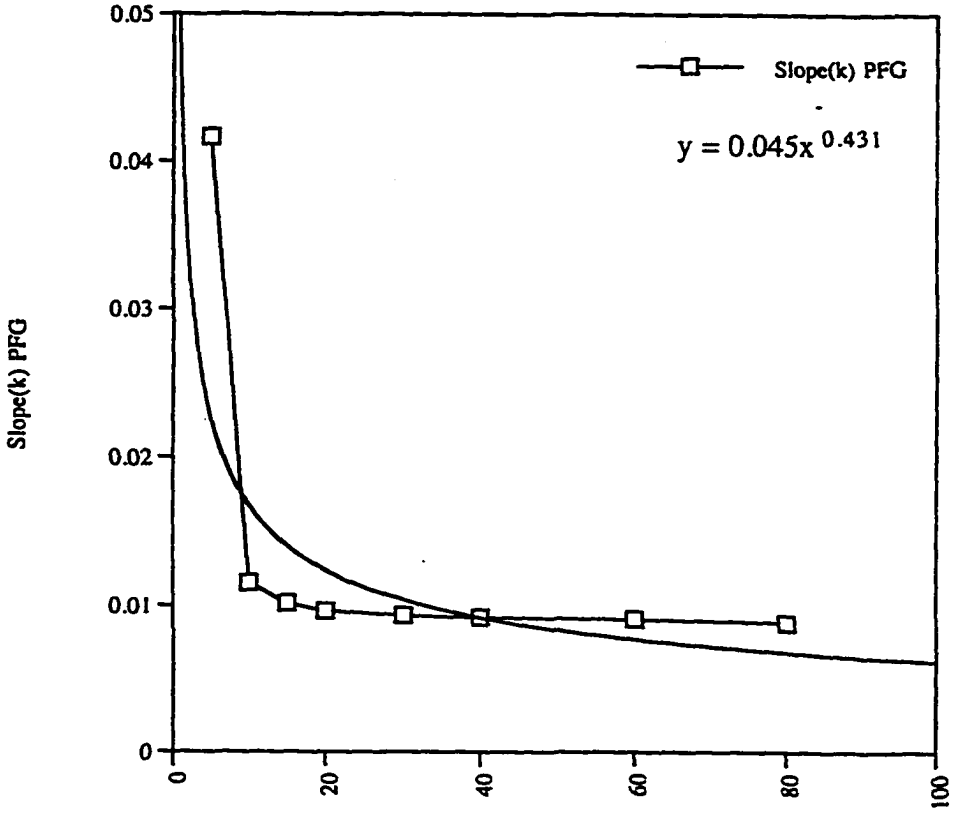

Figure 4.15 The effect of variation of VD in PFG

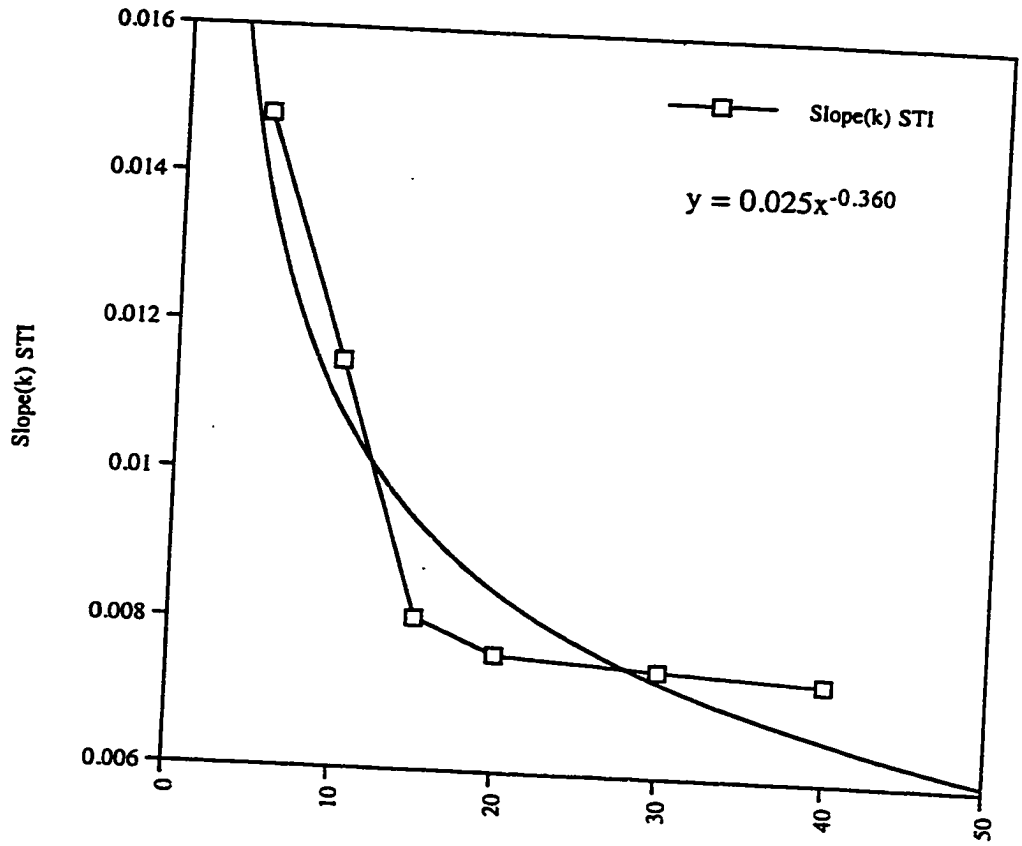

Figure 4.16 The effect of variation of VD in stimulated echo

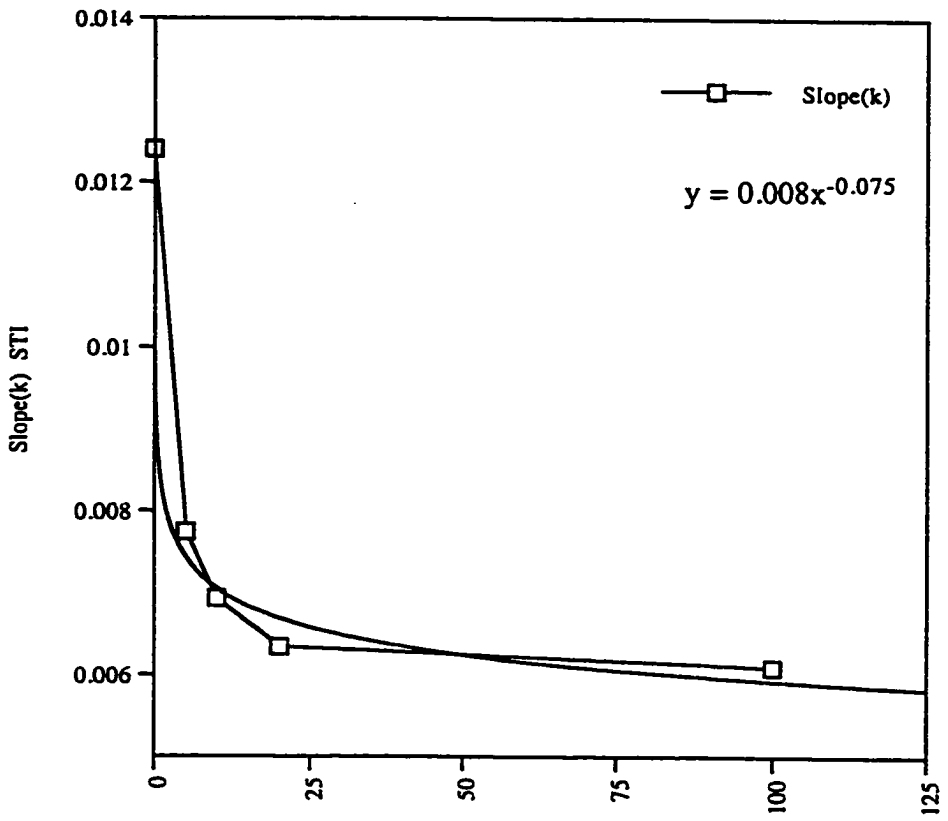

Figure 4.17 The effect of variation of D2 in stimulated echo

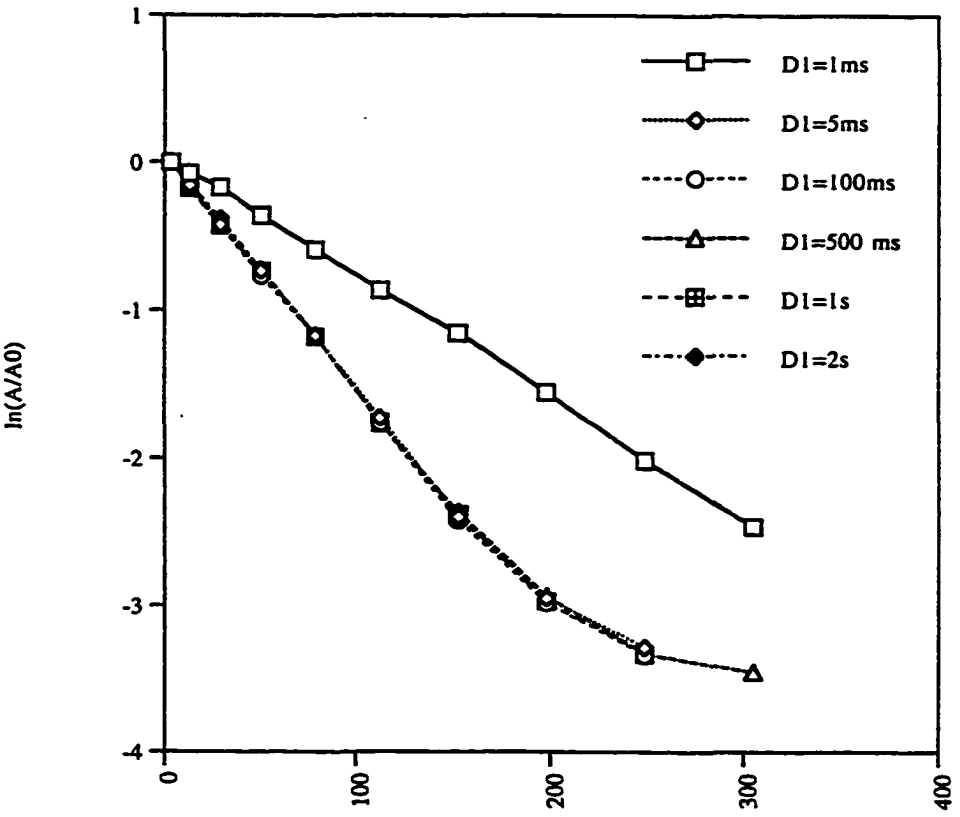

Figure 4.18 The effect of variation of D1 in PFG NMR

The vibrations

In PFG and stimulated echo PFG NMR experiments, there are two kinds of vibrations. One is the vibration of sample tube and probe. The other is the vibration of the magnetic field. These vibrations will result a greater measured diffusion coefficient because the vibration was measured as diffusion.

In order to prevent the tube vibration, we cut the tube to about 4 cm long and sealed it to the probe by a special clip which was added to our probe by L.U machine shop. Even though, VT air and room air on could result in 10% errors respectively. The heater would bring another 10% errors because of extra magnetic field. Interestingly, all these three factors(10%, respectively) are additive and would bring a 30% errors together if all three are on(Figure 4.19).

The other vibration is the one of the pulsed gradient which was resulted from the pulsed electrical current. When the current goes through the coil which was used to generate the pulse magnetic field, the coil will stress. When the current dies out, the coil will relax. This magnetic filed vibration could minimized by sealing the coil to the probe tightly. However, it seems that this vibration is inevitable.

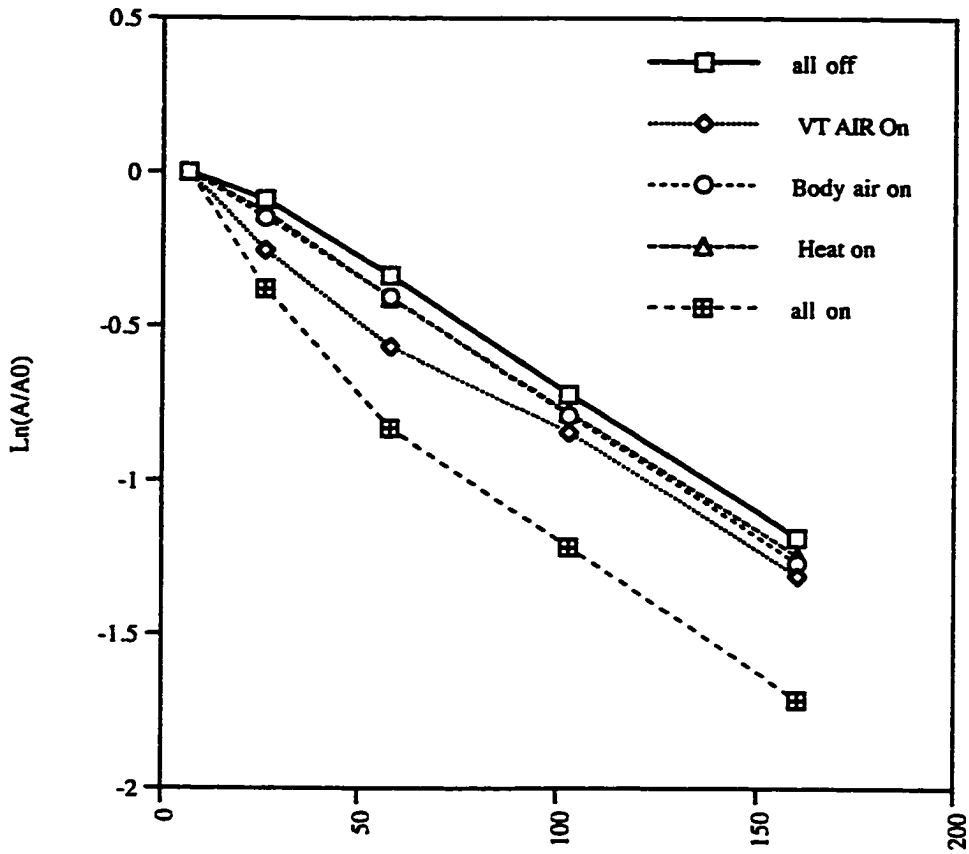

Figure 4.19 The effects of heater, body air and VT air

Difference Spectrum

As described above, the molecular size and structure are important considerations when developing methods for removing and processing effluents. Although our probe has some difficulties to measure the true value of diffusion coefficients(D_0), it may be used to obtain size-resolved spectra and to measure and compare the self diffusion coefficients(D_0) of various functional groups. Also by comparison of the signal with small or no gradient pulses we can identify the large molecular species (residual signal after substantial pulses) and relatively small molecules (by difference with the initial spectra). Spectra obtained from a hardwood kraft lignin which clearly resolve the large molecules from the small molecules are shown in Figure 4.20. Due to residual gradients, we kept our experiment time at 80.4ms. Our gradient pulses were normally between 20 and 40 Gauss cm^{-1} . The high molecular weight material (B) has a much lower frequency of acetylated phenolic hydroxyl group than the low mass material(C). This result corresponds to the molecular mass sequence of ionizable phenolic groups on softwood kraft lignin [4.21] and is expected for lignin generated by kraft processes. In addition, the aromatic region shifts upfield for the higher mass materials.

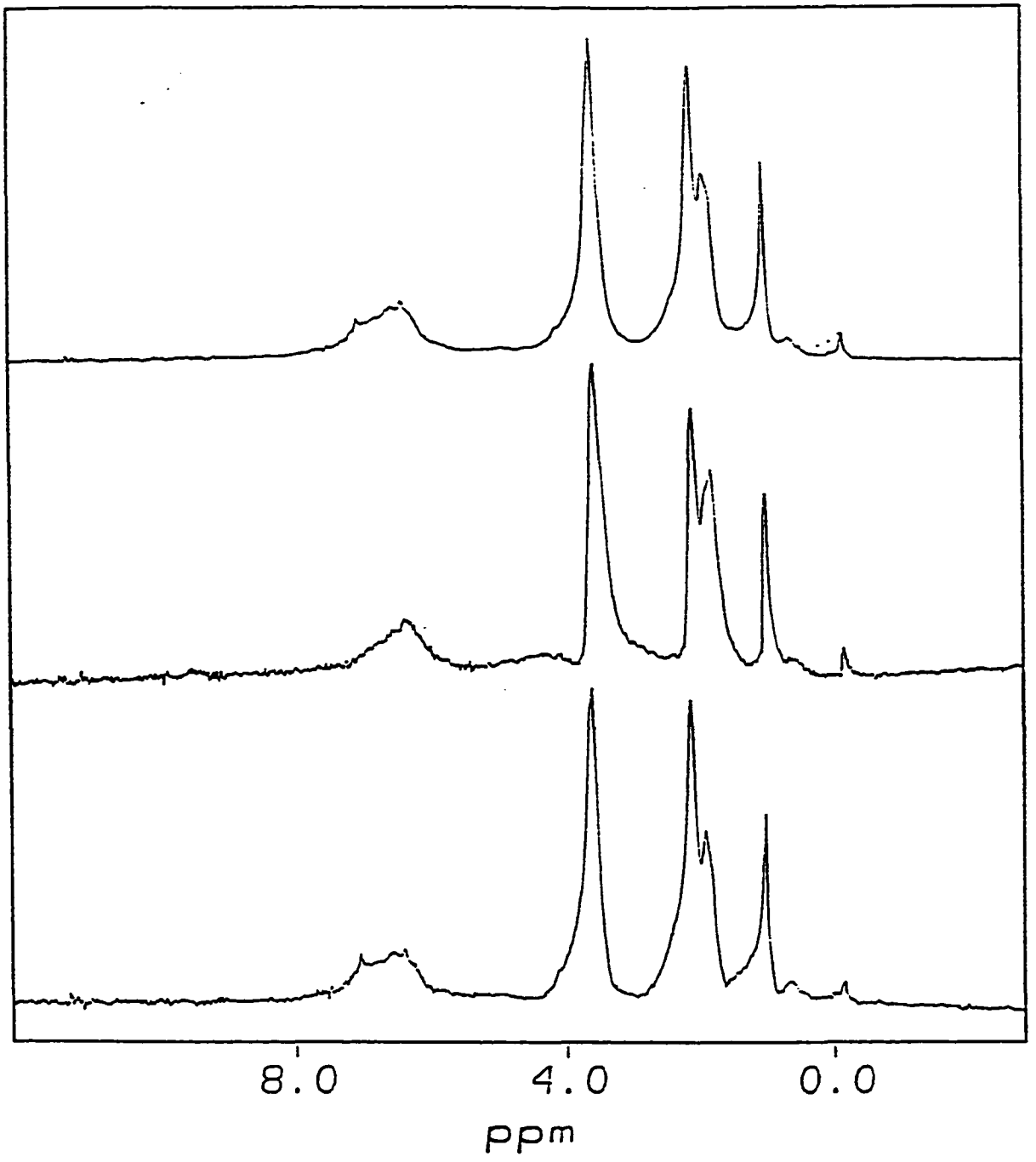

Figure 4.20 Acetylated kraft aspen lignin with pulsed gradient spin echo selection of signal. Top total signal; middle after pulse gradient spin echo (Large mass), Bottom difference(low mass).

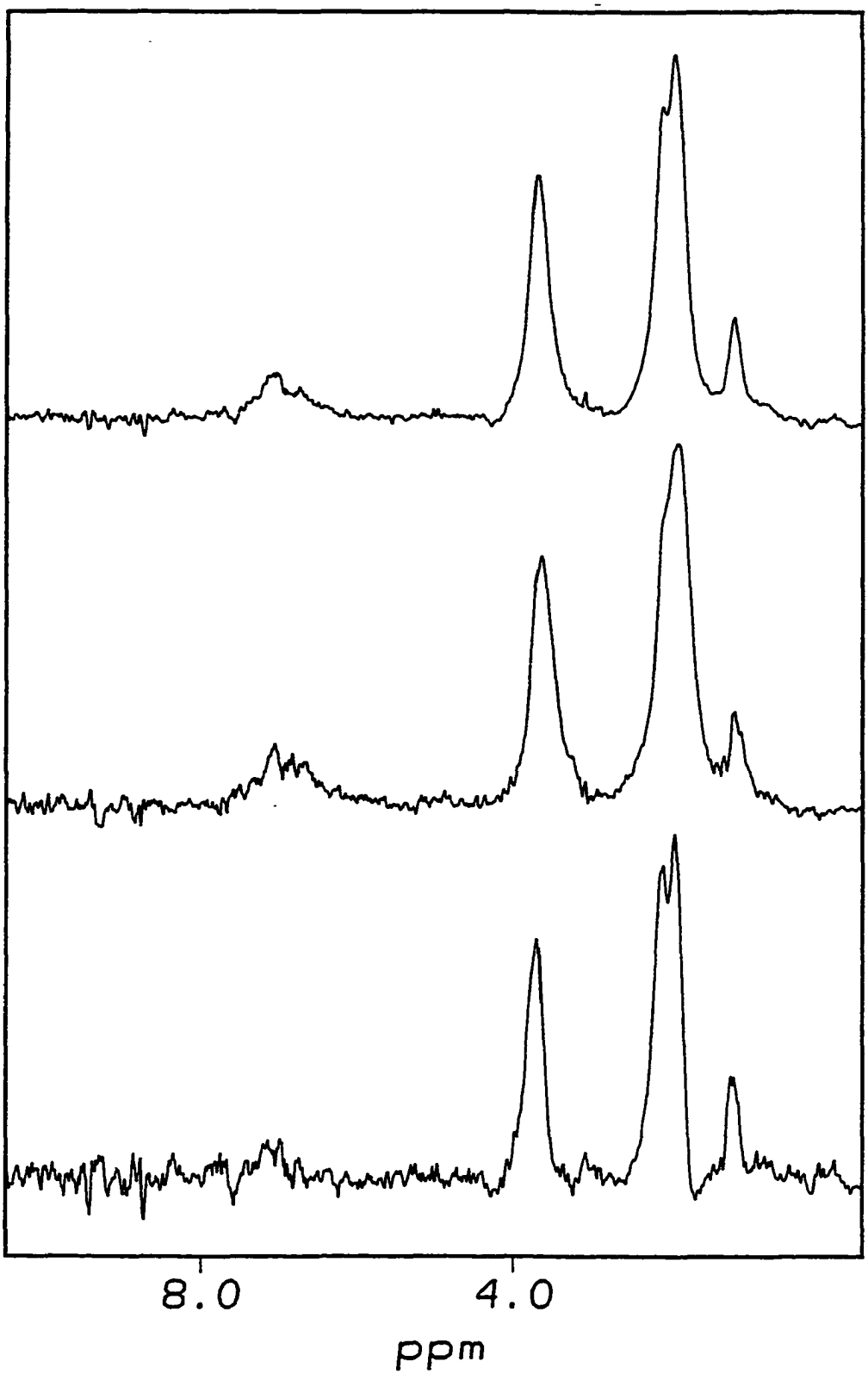

Figure 4.21 Acetylated kraft spruce lignin with pulsed gradient spin echo selection of signal. Top total signal; middle after pulse gradient spin echo (Large mass), Bottom difference(low mass).

Reference

[4.1] C. H. Ludwig,. J. Am. Chem. Soc. 86:1196-1202(1964)

[4.2] R.J Ralph, Magn. Reson. Chem. 31,357(1993)

[4.3] D. Robert, Brunow G, Holzforschung 38:84-90 (1984)

[4.4] K.Lundquist and K. Stern, Nord. Pulp Pap. Research. J. 210(1989)

[4.5] T.M. Jr. Garver, and S. Sarkanen; Holzforschung 40 (supplement) :93-100 (1986)

[4.6] E.D.von Meerwall, Adv. Polymer Sci., 1-29, (1983)

[4.7] G.Fleischer, et al Erop. Biophys. J., 24-30 (1990)

[4.8] J.Krüger, Phys. Rep., 82 229-269, (1982)

[4.9] H.Pfeifer, NMR Basic Princ. Prog., 31, 31-90, (1994)

[4.10] Denise P. Hinton, Charles S. Johnson Jr. J. Phys.Chem. 97,9064-9072, (1993)

[4.11]F. Bloch, Phys. Rev. 70,460 (1946)

[4.12]E. L. Hahn, Phys. Rev. 77, 297(195C)

[4.13]H.Y.Carr and E.M. Purcell, Phys. Rev 94, 630(1944)

[4.14] E.O. Stejskal and J.E. Tanner, J. Chem. Phys. 42,288(1964)

[4.15] H.C.Torrey Phys. Review, 104, 463(1946)

[4.16] R.F.Karlicek Jr. and I.J.Lowe J.Mag.Reson. 37,74-91(1980)

[4.17] Verley, A. And Bolsing, F., Chem. Ber. 34 :3354-3358 (1901)

[4.18] T. M. Garver, Physicochemical Studies of Kraft Lignins, PhD thesis, University of Minnesota, 1988

[4.19] E.D. von Meerwall and Kamat, M.J.Mag.Reson.83, 309-323 (1989)

[4.20] R. Mills, J.Phys.Chem. 77,684-688 (1973)

[4.21] T. M. Garver and P. T. Callaghan; Macromolecules 24, 420-430, 1991

Appendix 1 PGSE1.AU

```
;PGSE1.AU SEQUENCE FOR PULSE GRADIENT NMR
;IT IS USED TO GENERATE HAHN SPIN-ECHO SEQUENCE WITH
;GRADIENT PULSES IN P2
;D1-90° -VD-G-VD-180°-VD-G-VD-FID
1 ZE
2 D1 S1    ;RELAX TO EQUILIBRIUM
3 P1 PH1 ;90 DEG PULSE WITH QP PHASE CONTROL
4 VD      ;PRECESSION OF SHIFT AND J-COUPLING
5 P2:D    ;USE DECOUPLER PULSE FOR GRADIENT TRIGGER
6 LO TO 5 TIMES I; InCREMENT PULSE LENGTH BY P2 MULTIPLE
7 VD
8 P3 PH2 ;180 DEG PULSE, PHASE PROG.PH2
9 VD     ; SET DELTA VD IN VDLIST =P2/2
10 P2:D ; GRADIENT PULSE
11 LO TO 10 TIMES I
12 VD ; REFOCUS SHIFTS BUT NOT J-MODULATIONS
13 GO=2 ;ACQUIRE FID, LOOP TO 2
14 WR #1 ;STORE FID
```

```
15 IF #1; INCREMENT FILE EXTENSION
16 IN=1 ;LOOP FOR NEXT EXPERIMENT, INCREMENT VDLIST
17 EXIT
PH1=A0 A0 A2 a2 A1 A1 A3 A3    ;EXORCYCLE AND Qp
    A2 A2 A0 A0 A3 A3 A1 A1
PH2=A0 A2 A0 A2 A1 A3 A1 A3
    A1 A3 A1 A3 A0 A2 A0 A2
; PROGRAM REQUESTS FILENAME FOR FIDS
;NE DEFINES NO. OF EXPERIMENTS = NO. OF DELAYS IN VDLIST
;CURRENT VDLIST MUST CONTAIN DELAYS (IN SEC) FPR ECHO
;SINGNAL AMPLITUDES DECAY FOR SHORT VD ACCORDING TO EXP(-
;2*VD/T2), FOR LONGER VD DECAY IS MORE RAPID DUE TO
;DIFFUSION
;D1=CA.5*T1 FOT COMPLETE RELAXATION
;P1= 90 DEG PULSE
;P2=GRADIENT PULSE
;P3=180 DEG PULSE
;RD=PW=0, QP PHASE
```

Appendix 2 PGSE2.AU

```
;PGSE2.AU SEQUENCE FOR PULSE GRADIENT NMR
;IT IS USED TO GENERATE STIMULATED ECHO  SEQUENCE WITH
;GRADIENT PULSES IN P2 AND A PREPULSE GRADIENT
;G-D2-90 -D3-G-VD-90-D2-90-90-D3-G-VD-FID
1 ZE
2 D1 S1    ;RELAX TO EQUILIBRIUM
3 P2:D
4 D2
5 P1 PH1 ;90 DEG PULSE WITH QP PHASE CONTROL
6 D3 ;SHORT DELAY BETWEEN 90 RF AND GRADIENT CA 100US
7 P2:D    ;USE DECOUPLER PULSE FOR GRADIENT TRIGGER
8 LO TO 5 TIMES I; InCREMENT PULSE LENGTH BY P2 MULTIPLE
9 VD
10 P1 PH2 ;90 DEG PULSE WITH QP PHASE CONTROL
11 D2      ;PRECESSION OF SHIFT AND J-COUPLING
12 P1 PH3 ;90 DEG PULSE WITH QP PHASE CONTROL
13 D3
14 P2:D    ;USE DECOUPLER PULSE FOR GRADIENT TRIGGER
```

```
15 LO TO 14 TIMES I
16 VD
17 GO=2 PH4 ;ACQUIRE FID, LOOP TO 2
18 WR #1 ;STORE FID
19 IF #1; INCREMENT FILE EXTENSION
20 IN=1 ;LOOP FOR NEXT EXPERIMENT, INCREMENT VDLIST
        ;POINTER
21 EXIT
PH1=A0
PH2=A0 A2 A1 A3
PH3=A0 A0 A2 a2 A1 A1 A3 A3    ;EXORCYCLE AND Qp
    A2 A2 A0 A0 A3 A3 A1 A1
PH4A0 A2 A0 A2 A1 A3 A1 A3
    A1 A3 A1 A3 A0 A2 A0 A2
; PROGRAM REQUESTS FILENAME FOR FIDS
;NE DEFINES NO. OF EXPERIMENTS = NO. OF DELAYS IN VDLIST
;CURRENT VDLIST MUST CONTAIN DELAYS (IN SEC) FPR ECHO
;SINGNAL AMPLITUDES DECAY FOR SHORT VD ACCORDING TO EXP(-
;2*VD/T2), FOR LONGER VD DECAY IS MORE RAPID DUE TO
```

```
;DIFFUSION

;D1=CA.5*T1 FOT COMPLETE RELAXATION

;P1= 90 DEG PULSE

;P2=GRADIENT PULSE

;RD=PW=0, QP PHASE
```

Appendix 3 PGSE3.AU

```
;PGSE3.AU SEQUENCE FOR PULSE GRADIENT NMR
;IT IS USED TO GENERATE HAHN SPIN-ECHO SEQUENCE WITH
;GRADIENT PULSES IN P2 AND PREPULSE GRADIENT
;D1-G-VD-90° -VD-G-VD-180°-VD-G-VD-FID
1 ZE
2 D1 S1    ;RELAX TO EQUILIBRIUM
3 P2:D     ;GRADIENT PREPULSE TO COMPENSATE FOR EDDY
        ;CURRENT
4 VD
5 P1 PH1 ;90 DEG PULSE WITH QP PHASE CONTROL
6 VD      ;PRECESSION OF SHIFT AND J-COUPLING
7 P2:D    ;USE DECOUPLER PULSE FOR GRADIENT TRIGGER
8 LO TO 7 TIMES I; InCREMENT PULSE LENGTH BY P2 MULTIPLE
9 VD
10 P3 PH2 ;180 DEG PULSE, PHASE PROG.PH2
11 VD      ; SET DELTA VD IN VDLIST =P2/2
12 P2:D    ; GRADIENT PULSE
13 LO TO 10 TIMES I
```

```
14 VD ; REFOCUS SHIFTS BUT NOT J-MODULATIONS
15 GO=2 ;ACQUIRE FID, LOOP TO 2
16 WR #1 ;STORE FID
17 IF #1; INCREMENT FILE EXTENSION
18 IN=1 ;LOOP FOR NEXT EXPERIMENT, INCREMENT VDLIST
19 EXIT
PH1=A0 A0 A2 a2 A1 A1 A3 A3    ;EXORCYCLE AND Qp
    A2 A2 A0 A0 A3 A3 A1 A1
PH2=A0 A2 A0 A2 A1 A3 A1 A3
    A1 A3 A1 A3 A0 A2 A0 A2
; PROGRAM REQUESTS FILENAME FOR FIDS
;NE DEFINES NO. OF EXPERIMENTS = NO. OF DELAYS IN VDLIST
;CURRENT VDLIST MUST CONTAIN DELAYS (IN SEC) FPR ECHO
;SINGNAL AMPLITUDES DECAY FOR SHORT VD ACCORDING TO EXP(-
;2*VD/T2), FOR LONGER VD DECAY IS MORE RAPID DUE TO
;DIFFUSION
;D1=CA.5*T1 FOT COMPLETE RELAXATION
;P1= 90 DEG PULSE
;P2=GRADIENT PULSE
```

```
;P3=180 DEG PULSE

;RD=PW=0, QP PHASE
```

Appendix 4 PGSE4.AU

```
;PGSE4.AU SEQUENCE FOR PULSE GRADIENT NMR
;IT IS USED TO GENERATE STIMULATED ECHO  SEQUENCE WITH
;GRADIENT PULSES IN P2 AND 2 PREPULSE GRADIENTS
;D1-G-D2-G-D2-90 -D3-G-VD-90-D2-90-90-D3-G-VD-FID
1 ZE
2 D1 S1    ;RELAX TO EQUILIBRIUM
3 P2:D     ;GRADIENT PREPULSE
4 LO TO 3 TIMES I
5 D2
6 P2:D
7 LO TO 6 TIMES I ;
8 P1 PH1 ;90 DEG PULSE WITH QP PHASE CONTROL
9 D3 ;SHORT DELAY BETWEEN 90 RF AND GRADIENT CA 100US
10 P2:D    ;USE DECOUPLER PULSE FOR GRADIENT TRIGGER
11 LO TO 10 TIMES I; INCREMENT PULSE LENGTH BY P2
                    ;MULTIPLE
12 VD
13 P1 PH2 ;90 DEG PULSE WITH QP PHASE CONTROL
```

```
14 D2      ;PRECESSION OF SHIFT AND J-COUPLING
15 P1 PH3 ;90 DEG PULSE WITH QP PHASE CONTROL
16 D3
17 P2:D   ;USE DECOUPLER PULSE FOR GRADIENT TRIGGER
18 LO TO 14 TIMES I
19 VD
20 GO=2 PH4 ;ACQUIRE FID, LOOP TO 2
21 WR #1 ;STORE FID
22 IF #1; INCREMENT FILE EXTENSION
23 IN=1 ;LOOP FOR NEXT EXPERIMENT, INCREMENT VDLIST
        ;POINTER
24 EXIT
PH1=A0
PH2=A0 A2 A1 A3
PH3=A0 A0 A2 a2 A1 A1 A3 A3    ;EXORCYCLE AND Qp
    A2 A2 A0 A0 A3 A3 A1 A1
PH4A0 A2 A0 A2 A1 A3 A1 A3
    A1 A3 A1 A3 A0 A2 A0 A2
; PROGRAM REQUESTS FILENAME FOR FIDS
```

```
;NE DEFINES NO. OF EXPERIMENTS = NO. OF DELAYS IN VDLIST
;CURRENT VDLIST MUST CONTAIN DELAYS (IN SEC) FPR ECHO
;SINGNAL AMPLITUDES DECAY FOR SHORT VD ACCORDING TO EXP
;(-2*VD/T2), FOR LONGER VD DECAY IS MORE RAPID DUE TO
DIFFUSION
;D1=CA.5*T1 FOT COMPLETE RELAXATION
;P1= 90 DEG PULSE
;P2=GRADIENT PULSE
;RD=PW=0, QP PHASE
```

Gradient Switch

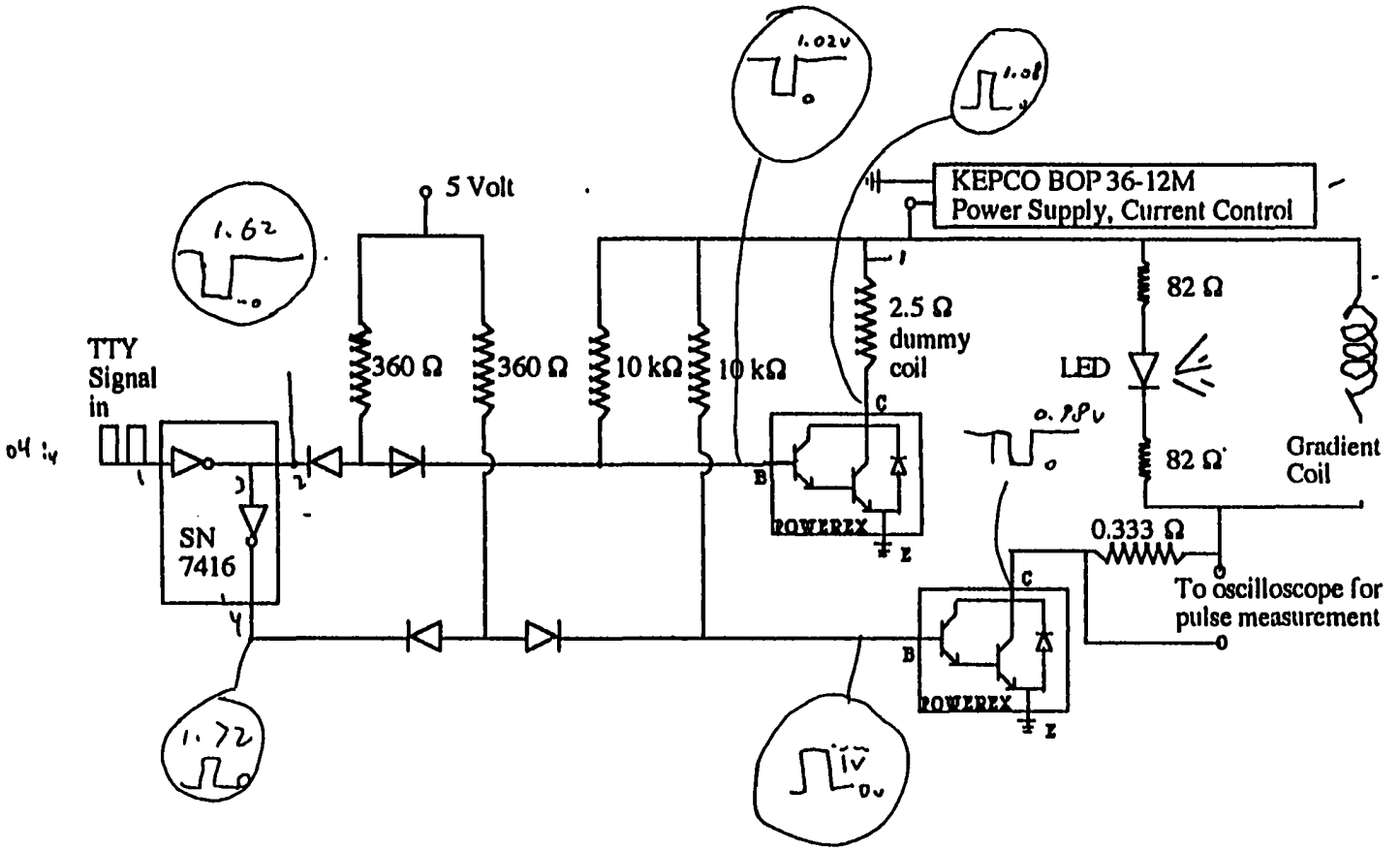

Homemade switch: Design modified from: Callaghan, P. T.; Trotter, C. M.; Jolley, K. W. J. Magn. Reson. 1980, 37, 247.

IMAGE EVALUATION TEST TARGET (QA-3)

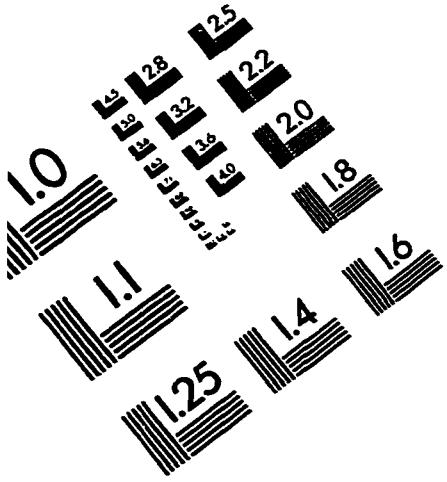

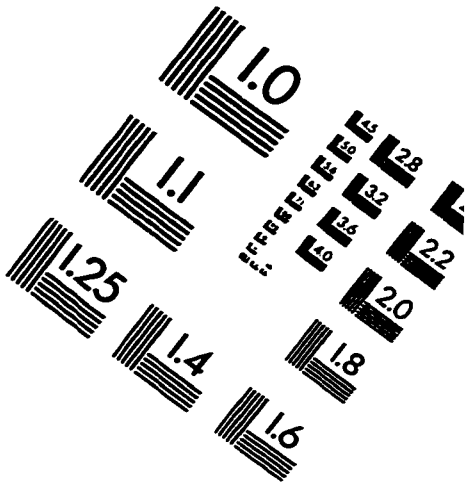

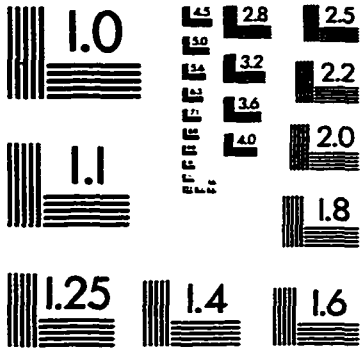

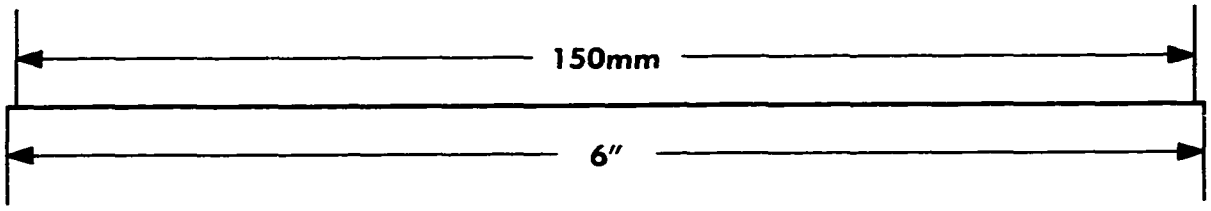

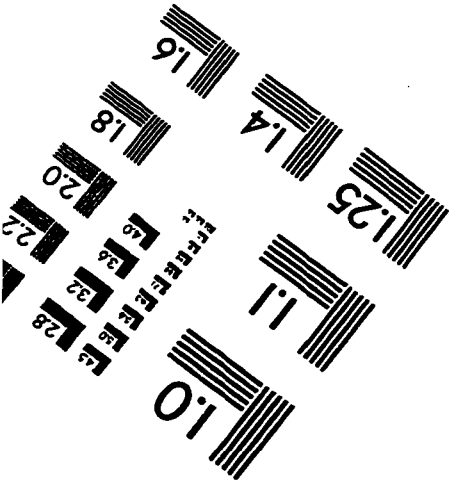

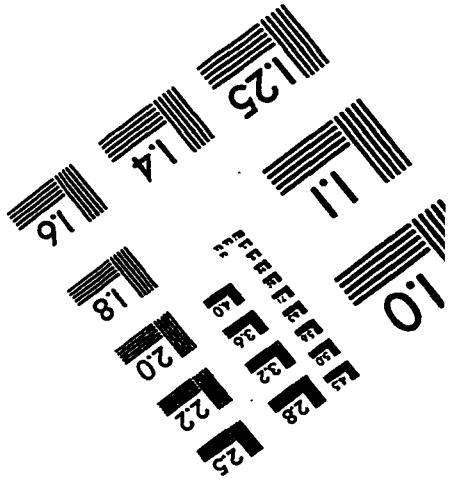

APPLIED IMAGE, Inc
1653 East Main Street
Rochester, NY 14609 USA
Phone: 716/482-0300
Fax: 716/288-5989